PROCESSING-STRUCTURE-PROPERTY RELATIONSHIP OF POLY(ETHER-ETHER-KETONE)-BASED SYSTEMS

A Dissertation

by

ZHIYUAN JIANG

Submitted to the Graduate and Professional School of
Texas A&M University
in partial fulfillment of the requirements for the degree of

DOCTOR OF PHILOSOPHY

Chair of Committee,	Hung-Jue Sue
Committee Members,	Terry Creasy
	Lei Fang
	Svetlana Sukhishvili
Head of Department,	Ibrahim Karaman

December 2021

Major Subject: Materials Science and Engineering

ABSTRACT

PEEK is a high-performance semicrystalline thermoplastic. It exhibits excellent thermo-mechanical properties, enabling its applications in a wide range of fields. For many structural applications such as sealing component, mechanical reinforcement of PEEK is very crucial. Commercially available model PEEK/PBI polymer blend systems were firstly studied but the mechanical reinforcement is limited. Young's modulus and tensile strength are only increased from 3.7 GPa to 5.3 GPa and from 105 MPa to 118 MPa, respectively, with addition of 50 wt.% PBI. PBI is also vulnerable to water, limiting its application in some down-hole scenario where steam or hot wet water are usually presented. Thus, a more efficient reinforcing agent with high resistance to water or other chemicals is needed. MWCNT is a highly efficient reinforcing filler with one of the highest specific modulus and specific strength. Also, MWCNT is not sensitive to water and other chemicals. In this work, we developed a novel and simple solution mixing approach to prepare well-dispersed PEEK/MWCNT nanocomposites. The PEEK/MWCNT nanocomposites exhibit uniform distribution and individual dispersion of MWCNT in PEEK. And the interaction between PEEK and MWCNT is sufficiently strong, resulting in its highly efficient mechanical enhancement. Addition of 10 wt.% MWCNT can significantly improve the Young's modulus and tensile strength to 7.3 GPa and 128 MPa, respectively, outperforming PEEK/PBI system. Another benefit is that PEEK/MWCNT is less vulnerable to water and shows more retarded stress relaxation behaviors than PEEK/PBI, especially under hot and wet condition. This is crucial for some niche applications such as sealing component in down-hole equipment where the retention of modulus is very important.

DEDICATION

To my families and friends.

ACKNOWLEDGEMENTS

In my 6-year life here at Texas A&M, many people have provided me their kind help and support, both scientifically and mentally. A special thank goes to my advisor, Professor Hung-Jue Sue. Throughout my PhD study and research career here, he provided me an excellent training as a graduate student. I really appreciate his training in polymer research. When I look back now, his questions and challenges to me, which really made my life hard in the past, turns to be milestones on my way forward. I was like a brittle polymer resin at the beginning while he was like a rubber and my PhD training process was like a compatibilization process. Throughout my PhD life, he helped me to transform myself from "a brittle polymer" to a super tough one. I would like to thank him for being challenging and supporting.

I would like to thank all members from the Sue group for their helps on some measurements, administrative affairs, and many interesting scientific discussions. A special thank goes to Michael Mullins who gave me many valuable suggestions on scientific writings. Mingzhen Zhao, Zewen Zhu, ChiaYing Tsai and Hengxi Chen helped me with some experimental measurements. I would like to thank them all for their kind helps during this fantastic journey.

I also received many helps from people outside the Sue group. Chenxuan Li, Xiaozhou Ji from the Department of Chemistry, Yufeng Quan, Ruiqing Shen from the Department of Chemical Engineering, Sevketcan Sarikaya from the Department of Aerospace Engineering and Peiran Wei from the Soft Matter Facility helped me with some experimental measurements. I want to thank them all for their helps.

I would also take this chance to thank my good friends, Zhouyang Yin, Guang Hu and Fangqing Xia, for their kind support and encouragement.

Finally, I would like to thank my parents and families for their love, understanding and support.

CONTRIBUTORS AND FUNDING SOURCES

Contributors

This work was supervised by a dissertation committee consisting of Professors Hung-Jue Sue, Terry Creasy and Svetlana Sukhishvili of the Department of Materials Science and Engineering and Professor Lei Fang of the Department of Chemistry at Texas A&M University.

The work conducted in Chapter 2, Chapter 3, and Chapter 4 of the dissertation was completed by the student independently. The work depicted in Chapter 2 and Chapter 3 have been published in 2020 and 2021, respectively.

Funding Sources

This graduate study was supported by the consortium for Advancing Performance Polymers for Energy Applications (APPEAL) at Texas A&M University.

This work was also made possible in part by the Ocean Energy Safety Institute (OESI) under Grant Number E14AC00001. Its contents are solely the responsibility of the authors and do not necessarily represent the official views of the APPEAL consortium and OESI. Special thanks are given to Hoerbiger Corporation of America, Inc., Victrex USA Inc., and Ensinger Special Polymers Inc. for providing some of the physical samples.

NOMENCLATURE

AFM	Atomic force microscopy
CNT	Carbon nanotube
CTE	Coefficient of thermal expansion
DCA	Dichloroacetic acid
DMA	Dynamic mechanical analysis
DSC	Differential scanning calorimetry
K_{IC}	Mode I critical stress intensity factor
MWCNT	Multi-walled carbon nanotube
MWD	Molecular weight distribution
NMP	*N*-methyl-2-pyrrolidone
p-MWCNT	Pristine or unmodified multi-walled carbon nanotube
o-MWCNT	Oxidized multi-walled carbon nanotube
PAEK	Poly(aryl-ether-ketone)
PBI	Polybenzimidazole
PEEK	Poly(ether-ether-ketone)
SEM	Scanning electron microscopy
SWCNT	Sing-walled carbon nanotube
T_g	Glass transition temperature
TGA	Thermal gravimetric analysis
TOM	Transmission optical microscopy
TTS	Time-temperature superposition
WAXS	Wide-angle X-ray scattering

TABLE OF CONTENTS

Page

LIST OF FIGURES

Page

LIST OF TABLES

Page

1. AN INTRODUCTION TO PEEK-BASED MATERIALS: PROPERTIES AND APPLICATIONS

1.1. Introduction

PAEK is a family of synthetic semicrystalline thermoplastics whose backbone chemical structure consists of 1,4-substituted arylene groups linked with alternating ether and ketone functional groups. PAEK family includes: PEKK, PEKEKK, PEK, PEEKK and PEEK. Their chemical structures are depicted in Figure 1-1. And their major differences lie in the ratio of ketone to ether functional groups in their chemical structures because the ketone group is more rigid than the ether group and a backbone consisting of more ketone groups is expected to exhibit higher rigidity. Depending on the ketone/ether ratio, their T_g usually increases with the increasing ketone/ether ratio.[1]

Among PAEK families, PEEK is one of the most important high-performance thermoplastic polymers from the perspective of its overall performances. PEEK was introduced in the early 1980s and soon applied in many high-end applications for its superior properties.

This chapter is going to give a brief introduction to the synthesis and properties of PEEK and then conduct a survey on the applications of PEEK and PEEK-based polymeric materials.

1.2. Synthesis of PEEK

Various routes have been proposed to synthesize PEEK and Devesh et al. have provided a thorough review on the chemistry used to synthesize PEEK.[2] Synthesis of PEEK can be achieved by ring-opening polymerization, electrophilic substitution, and nucleophilic substitution reactions.[3] The disadvantage of ring-opening method lies in its difficult control of polymerization, unattainability of full conversion of monomers, a wide MWD of polymerization

product.[4, 5] For electrophilic substitution method, there are some drawbacks which limit the possible use of this method at the commercial scale. These include the need to use large amounts of catalyst aluminium trichloride and consequently the problem of residual aluminium trichloride removal.[6]

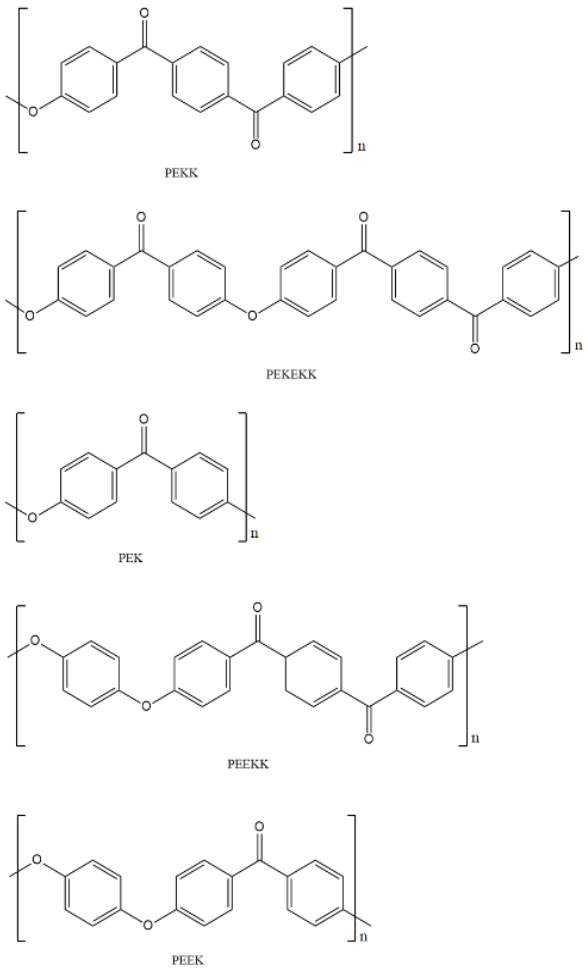

Figure 1-1 Chemical structures of PAEKs.

The nucleophilic substitution reaction is a promising method for the industrial synthesis of PAEKs. Despite the drawbacks like the requirement of high temperature of reaction and removal of impurities such as residual solvent and sodium fluoride salts, synthesis of PEEK by

the nucleophilic substitution reaction possesses advantages including high selectivity and a wide choice of aromatic bisphenols, making it possible to synthesize PAEKs of various structure and properties.[3] In this case, PEEK is usually polymerized by the reaction of difluorobenzophenone with disodium diphenolate salt of hydroquinone. The polymerization requires a very high temperature of about 300 ℃ in a high temperature nonpolar solvent like diphenyl sulfone. This synthesis route is depicted in Figure 1-2.

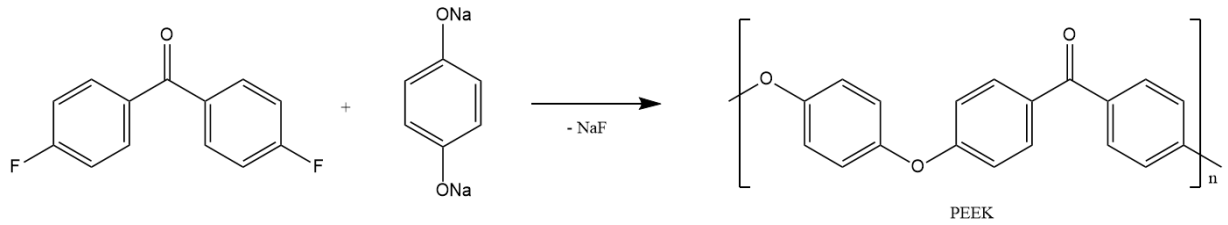

Figure 1-2 Synthesis of PEEK via nucleophilic substitution.

1.3. Properties of PEEK

PEEK has superior thermal and mechanical properties. Its T_g is about 145 ℃ while T_m is about 345 ℃. It is thermally stable and can be continuously used at a temperature as high as 260 ℃. Besides its thermal stability, PEEK also possesses superior mechanical properties. Its Young's modulus is around 3.6 GPa while engineering tensile strength of PEEK can reach 90 to 105 MPa. PEEK is also a super tough polymer and its critical stress intensity factor K_{IC} is about 7 MPa·m$^{1/2}$.[7-9]

PEEK is resistant to many chemicals or solvents. Below 200 ℃, PEEK is usually insoluble in many solvents. It is only soluble in concentrated sulfuric acid at room temperature and in this case, the original chemical structure of PEEK would be destroyed.

PEEK is also a flame retardant polymer without any addition of other flame retardant fillers. It meets the V-0 level of UL-94 (the Standard for Safety of Flammability of Plastic Materials for Parts in Devices and Appliances testing).

PEEK is also well-known for its high resistance to radiation including gamma radiation and X-rays.

As a semicrystalline thermoplastic polymer, PEEK possesses good processibility. It can be easily processed through extrusion, injection molding, compression molding et al.

Due to these superior properties, PEEK is widely used in many structural applications, even including applications in aggressive environments. The following section will be discussing how these superior properties enables PEEK to expand its applications in different fields.

1.4. Applications of PEEK and PEEK-based materials

PEEK is widely used in many high-end applications, including but not limited to oil drilling components such as backup seals, bearings, compressor rings, valve parts, gear pumps, wire packaging of connectors. Its high resistance to radiations also extends its application to aerospace fields. In addition, because of its biological inertness and resistance to biodegradation, PEEK is also used in medical devices to make surgical implants such as artificial hips and dental prosthesis (Figure 1-3[*]).[10]

[*] Reprinted with permission from "Modified PEEK resin-bonded fixed dental prosthesis as an interim restoration after implant placement" by Zoidis, P.; Papathanasiou, L., *J Prosthet Dent* **2016,** *116* (5), 637-641. Copyright 2016 by the Editorial Council for The Journal of Prosthetic Dentistry.

Figure 1-3 Dental prosthesis made of PEEK. Reprinted with permission from "Modified PEEK resin-bonded fixed dental prosthesis as an interim restoration after implant placement" by Zoidis, P. and Papathanasiou, L.

1.4.1. PEEK for biomedical applications

PEEK has been proposed for biomedical application in the late 1990s and Victrex launched PEEK-OPTIMA products for implant applications in 1998.[11] PEEK-based polymeric materials for implant applications may contain various amounts of bioactive substances like tricalcium phosphate and hydroxyapatite. Fillers like carbon fibers sometimes are also added for the mechanical reinforcement of PEEK. For example, carbon fiber reinforced PEEK materials are used for orthopedic implants for its superior mechanical properties and biocompatibility.[12] Unmodified PEEK resin has a young's modulus of 3.6 GPa, which is lower than that of human cortical bone (18.6-20.7 GPa) and human trabecular bone (10.4-14.8 GPa).[13] To be used as implant replacement, it is necessary to reinforce PEEK to make the Young's modulus of PEEK composites match or approach that of human bones. All modifications of PEEK for biomedical applications are aimed to increase its mechanical (or physical) and biological properties.

PEEK is chemically inert and insoluble in almost all kinds of common solvents and its thermal stability make it suitable to be used in human body environment. PEEK is also highly

resistant to wear because of the formation of a transfer layer.[14] On the other hand, PEEK is well known for its resistance to alpha, beta, gamma and X rays.[15] Therefore, PEEK can be processed under gamma sterilization and will not generate secondary radiation originating from absorption of the previous radiation. Bearing such good thermal, chemical and radiation resistance properties, modification of PEEK mainly focused on the improvement of PEEK and PEEK-based materials' mechanical properties and biological properties. The following paragraphs will discuss some recent advances in these aspects.

To improve the mechanical properties of PEEK, chopped carbon fiber reinforced PEEK composites were used for this purpose.[16] It was machined from an injection molded plaque and used for implant material for fracture fixation. With increasing loadings or weight concentrations of carbon fibers, the modulus and tensile strength increases but tensile elongation decreases. For biomedical applications, the modulus of the implant material needs to be close to that of human bones. And it has been reported that 30 wt.% chopped carbon fiber reinforced PEEK composites can reach Young's modulus of 17 GPa, which is close to that of human cortical bone.[13, 16] Besides mechanical reinforcement, carbon fiber reinforced PEEK composites also exhibits very good biocompatibility. The fracture fixation plate made of carbon fiber reinforced PEEK presents a nonspecific foreign body tissue reaction similar to the response observed with ultra-high molecular weight polyethylene (UHMWPE) and is very effective in promoting fracture healing.[16] It is also a promising material that may replace titanium alloy and biological ceramics in orthopaedic surgery.[17]

Similar with carbon fiber reinforced PEEK composites, glass fiber reinforced PEEK composites are also used for biomedical applications. A PEEK composite with 10 wt.% chopped

E-glass fibers is found to support proliferation of human bone cells and provide a favorable environment for the continuous formation of osteocalcin *in vitro*.[18]

To improve the biological properties, particularly the osteo-induction capability, bioactive hydroxyapatite or beta-tricalcium phosphate were added into PEEK.[19, 20] It increases the Young's modulus and compressive strength but decreases the ultimate tensile strength and strain to failure because these two inorganic fillers do not possesses good affinity to PEEK polymer matrix. Adding 40 vol.% hydroxyapatite into PEEK reduces its tensile strength by 50% to 50 MPa, which is still close to that of bony tissue.[20]

Another class of PEEK-based materials for biomedical application is the development of PEEK nanocomposites. Nano-sized silicon dioxide (SiO_2), aluminium oxide (Al_2O_3), titanium dioxide (TiO_2) particles and carbon nano-fibers have been reported to be incorporated into PEEK matrix to make PEEK nanocomposites for biomedical application.[21-23] Generally, they exhibit an increase of Young's modulus and tensile strength but a decrease of elongation.

Besides physical and mechanical properties of PEEK and PEEK-based materials, biological characteristics are also very important, particularly for biomedical applications. PEEK is reported to not cause any chromosome aberrations and it is biologically inert.[24] The biocompatibility of the implant is highly influenced by its surface characteristics, including the surface composition, wettability, and surface roughness etc.[25] PEEK possesses a hydrophobic surface, which does not promote cell adhesion. However, incorporation of bioactive fillers or deposition of bioactive layers on PEEK surface may help improve its biological performance.[25] Cheol-Min Han et al. applied an electron beam deposition method to deposit a titanium layer on PEEK and the result shows enhanced biocompatibility and adhesion to bone tissue. The titanium-coated PEEK exhibits a much higher level of proliferation of cells compared to the non-treated

PEEK.[25] When added into PEEK, nano-sized TiO_2 improves osteoblast cell spreading, promotes cell adhesion and enhances bone regeneration around the implant.[22] PEEK/nano-fluoro-hydroxyapatite bio-composite implants with rough surfaces exhibits cyto-compatibility, good antibacterial activity, and triggers osteogenesis.[26]

By enhancing the mechanical and biological properties of PEEK, PEEK and PEEK-based implants have been widely used in clinical applications[27], including but not limited to:

1) PEEK implants for face and cranial reconstruction.
2) PEEK dental implants for tooth replacement (Figure 1-3).[10]
3) PEEK implants for orthopedic devices like fixation plates and screws.
4) PEEK for cardiac surgery like intra-cardiac pump and heart valves.
5) PEEK implants for femoral bond reconstructions and hip replacement.

1.4.2. PEEK for aerospace applications

The exploration activities of outer space have been gradually increasing since the last century. The harsh environment in the outer space such as high vacuum, atomic oxygen, solar radiations and wide temperature range, limits the choice of certain materials that can be applied.[28] For example, the use of liquid lubricants is restricted in such an aggressive environment. Therefore, self-lubricating solid materials must be used for this purpose. PEEK-based materials have been increasingly employed in aerospace applications for reasons including but not limited to its advanced tribological behaviors, high radiation resistance and superior mechanical properties.

To be used as solid lubricants in outer space equipment, PEEK/molybdenum disulfide (MoS_2) composites have been employed. Geraldine Theiler and Thomas Gradt investigated the

tribological behavior of PEEK composites in vacuum environment.[29] PEEK composites containing 10 vol.% carbon fiber, 10 vol.% PTFE and 10 vol. MoS_2 shows low friction in high vacuum at the low temperature range and at higher loads. However, the tribological performance is limited in ultra-high vacuum environment and at low velocity because of its high static friction and outgassing is observed.

Jiang Wu et al. investigated the dielectric and space charge characteristics of PEEK insulating material to evaluate the insulation issue in the high-voltage system of spacecrafts.[30] They analyzed the electric conduction, trap parameters and space charge characteristics, especially the space charge distribution after 50 keV high-energy electron radiation, of PEEK. PEEK exhibits a low DC conductivity (~10-16 S/cm) and an activation energy of 0.1–0.2 eV. In addition, it shows a deep chemical trap of 2 eV and the space charge accumulations are lower in PEEK than polyimide, and the charge dispersions in the PEEK after irradiation are much faster than those in polyimide. Because the aromatic ring and carbonyl group in the chemical structure of PEEK can introduce deep traps, leading to a higher injection barrier and less space charge accumulation. Therefore, PEEK is believed to be a superior insulating material for applications in outer space because of its excellent dielectric and space charge characteristics.

Though the utilization of thermoplastic PEEK composites is growing, thermoset matrix composites are still the primary one in aerospace applications. The major issue for PEEK composites is their high cost. Michele Iannone and Alberto D'Amore proposed a hybrid semicrystalline-amorphous thermoplastic matrix prepreg consisting of a carbon fiber reinforced PEEK prepreg material sandwiched by two polyethyleneimine (PEI) film layers.[31] Such a hybrid thermoplastic matrix prepreg is cost saving because it can be processed *via* automated lay-up without autoclave cycle.

1.4.3. PEEK for sealing applications

Effective and efficient sealing is very important in almost every modern industrial process where gaseous and liquid substances are being transported. Seals are required wherever the containment of these substances is completed (such as end caps), measured (flowmeters), controlled (valves) or separated from moving parts.[32] Such large application fields demand an equally diverse range of sealing technologies and materials including but not limited to soft and flexible elastomers, various thermoplastic and thermoset polymers, bronzes, and steels.

There are many factors to be considered when one is choosing a suitable sealing material:[32]

1) What the media is to be sealed (for example, aggressive chemicals).
2) What the material of the equipment is to be sealed.
3) Working temperature window.
4) Upper pressure limit.
5) Velocity between the seal and the counter face.

Elastomers have been widely used in many applications because of their resilience and ability to fill space under a compressive stress, making them effective seals. However, when the operating condition becomes aggressive, elastomers become inappropriate in such applications as their resistance to harsh environments is relatively poor.

Another class of sealing materials are thermoplastic polymers. Among them, fluoropolymers exhibit excellent chemical resistance and good temperature resistance while their mechanical properties are relatively poor. Compared to them, PEEK exhibits outstanding mechanical, thermal, and chemical resistance, making it extensively usable in sealing applications across all industries.

In some industries such as the oil and gas sector, the primary use of PEEK is to work as a back-up seal for softer sealing materials, such as elastomers and fluoropolymers. In other fields, PEEK can be used as primary seals depending on the application scenario.

1.4.3.1. PEEK seals for oil and gas applications

One of the most important market for PEEK sealing elements is the oil and gas sector where effective and efficient sealing is highly demanded for safe and stable operation compared to the huge cost of downtime. In oil and gas field, reliable production of oil and gas is quite important, otherwise accident may cause positive influences on the environment or even put petroleum workers' health and safety at risk. In oil and gas industry, PEEK has been used as a back-up ring, primary seal or packing in applications such as valves, compressors, connectors, packers, and blowout preventers (Figure 1-4[*]).[32] In these scenarios, seals are critical for the separation of different media, containment of lubricants and exclusion of contaminants such as rocks and sands.

PEEK is widely used to fabricate the anti-extrusion back-up rings in the seal stack.[32] The elastomer or fluoropolymer is usually used as the primary seal. However, they will eventually extrude under the high temperature and high-pressure conditions because of their low mechanical properties in such aggressive environment and thus the primary seal made of elastomer or fluoropolymer will be damaged. Consequently, PEEK seals as back-up rings find its applications here for its ability to maintain properties at high temperature and high pressure. Seals made of

[*] Reprinted with permission from "Outstanding physical properties make PEEK ideal for sealing applications" by Small, G., *Sealing Technology* **2014,** *2014* (4), 9-12. Copyright 2014 by Elsevier Ltd.

PEEK-based materials fulfill the engineering requirements for the oilfield applications and these requirements include chemical resistance to a wide range of oilfield fluids and hydrocarbons, high resistance to creep at high temperatures and ability to maintain mechanical properties. PEEK seals also fulfill the application requirement in more aggressive underground environment with the presence of sour gas. PEEK is known to be resistant to sour gas.[33] PEEK complies with NORSOK M-710 standard which defines the requirements for critical elastomer sealing, seat and back up materials for permanent subsea use including well completion etc. PEEK has shown its

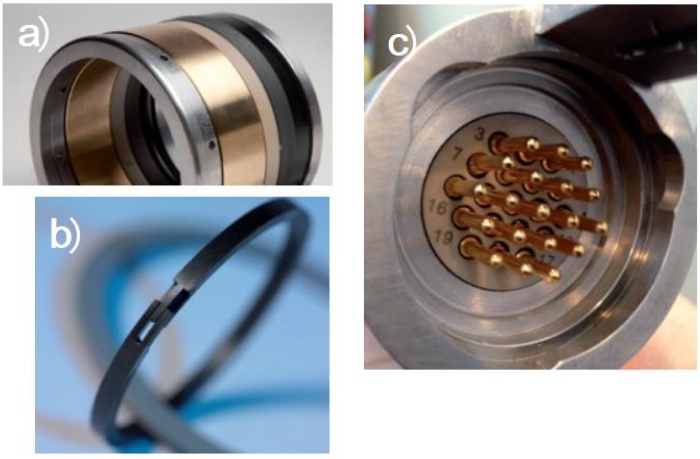

Figure 1-4 a) CDI plunger packing with PEEK seal ring; b) PEEK seal (source: Konzelmann GmbH); c) downhole electric connector with PEEK packaging. Reprinted with permission from "Outstanding physical properties make PEEK ideal for sealing applications" by Small, G.

capability of withstanding higher concentrations of sour gas than the one specified in NORSOK M-710 standard. Apart from these properties, PEEK also possesses low thermal expansion (low CTE), making it a good fit with mating steels.

PEEK can also be used as electrical connectors for downhole applications because of PEEK high mechanical properties, high creep resistance at high temperature and high pressure. Another benefit is that it can be manufactured through injection molding to encapsulate metal

conductors. This manufacturing approach is highly reproducible and most importantly, cost-effective.[32]

1.4.3.2. PEEK seals for automotive applications

In automotive industry, efficient and smooth-shifting transmission is highly demanded to deliver power and to meet the environmental requirement. Therefore, sealing materials for automotive applications require a low coefficient of friction, dimensional stability, and capability of operation at a wide temperature window. Also, the sealing material needs to be resistant to various versions of transmission oils and able to serve in either lubricated condition or temporary non-lubricated condition required by the stop-start system. The specific wear-grade PEEK possesses low coefficient of friction, enabling PEEK seals to work at extreme pressure/velocities under lubricated condition or even temporary non-lubricated condition.[32]

1.5. Conclusion

PEEK exhibits superior properties, including biological inertness, high resistance to solvents or aggressive chemicals like sour gas, high resistance to creep, high resistance to radiation, high resistance to wear, high thermal stability, high mechanical modulus and strength, high electrical insulation, low thermal expansion coefficient and processing easiness. These excellent properties help PEEK find wide applications in biomedical, aerospace, automotive, oil and gas fields etc.

Among these properties, mechanical property is the most critical one. As in oilfield application, PEEK-based seals outperform seals made of elastomers or fluoropolymers in terms of mechanical property at high temperature and high pressure. The maintenance of modulus is very critical in such an aggressive environment, making PEEK outperform seals made of other

materials.[9] Therefore, mechanical reinforcement of PEEK is the key for many engineering applications and is also the focus of this dissertation.

Various routes have been applied to reinforce the mechanical properties of PEEK. Incorporation of fillers and blending with another type of high-performance polymers are two approaches widely utilized to tune the properties of a certain polymer resin. In the following chapters, reinforcing PEEK *via* blending with high-performance polymer PBI to make PEEK/PBI polymer blend and *via* incorporation of MWCNT to make PEEK/MWCNT polymer nanocomposites will be discussed in chapter 2 and chapter 3-4, respectively. Lastly, a comparison of PEEK/PBI polymer blend and PEEK/MWCNT polymer nanocomposite will be analyzed in chapter 5 in terms of their mechanical properties and stress relaxation behaviors at high temperature for the interest of applications of PEEK-based materials in aggressive environments.

2. PAEK/PBI POLYMER BLENDS: AN INVESTIGATION ON THEIR PROCESSING-STRUCTURE-PROPERTY RELATIONSHIP*

2.1. Introduction

Polybenzimidazole (PBI) is a high-performance amorphous polymer possessing one of the highest T_g (436 °C) among known polymers.[34-36] PBI has thermal stability up to 500 °C and mechanical properties retained up to its T_g. Such superior properties make it a promising candidate for high temperature and high pressure applications. Blends of PBI with various polymers, including polyimide (PI), polysulfones (PSF), sulfonated PSF (SPSF), and PEEK, have been reported for fuel cell membranes and high-temperature applications.[37-40] These blends have varying degrees of compatibilities to each other depending on their respective chemical structures and processing routes. The miscible PI/PBI blend exhibits a single T_g and tan δ relaxation peak between those of the two polymers.[39] The PSF/PBI is immiscible but if PSF is sulfonated, depending on the degree of sulfonation, the miscibility of SPSF/PBI blend could be tuned from being partially miscible to fully miscible because of the hydrogen bonding interactions between sulfonated PSF and PBI.[37] In the case of immiscible PEEK/PBI blends, the interfacial strength is found to play an important role in the mechanical properties of the blend.[38, 40] Blending PBI with PAEK has attracted growing interest since this cost-effective solution combines the superior thermal and mechanical properties of PBI and the melt processability of PAEK.

---

* Reprinted with permission from "The influence of processing conditions on the mechanical properties of poly(aryl-ether-ketone)/polybenzimidazole blends" by Jiang, Z. Y.; Liu, P.; Chen, Q. H.; Sue, H. J.; Bremner, T.; DiSano, L. P., *J Appl Polym Sci* **2020,** *137* (33). Copyright 2020 by John Wiley & Sons, Inc.

It is not surprising that mechanical properties of multi-phase polymer blends would be significantly affected by their interfacial characteristics. The interface serves to stabilize immiscible phases and transfer stress between phases to achieve optimized properties from a combination of desired physical and mechanical properties of the blend components. The most frequently used method to improve the interfacial properties of immiscible polymer blends is to introduce coupling agents and compatibilizers.[41-47] Besides these chemical approaches, it has been reported that the processing conditions could also influence the interfacial properties, and thus the mechanical properties of the polymer blends.[41, 43, 44, 48-51] Cimmino et al. found that ternary nylon-6/rubber/modified rubber blend prepared by a two-step mixing procedure where rubber and modified rubber are pre-mixed before final mixing with nylon-6 exhibits fine particle dispersion and better impact resistance than the blend prepared by a one-step blending of three components at the same time.[50] The two-step mixing method was believed to enhance the phase stability and the interfacial strength of the ternary blend. The intensity of mixing, represented by the mixing roller speed, is another important processing parameter and a critical mixing speed was found for the ethylene-propylene random copolymer toughened polybutylene terephthalate (PBT). Below this critical mixing speed, increasing the mixing speed would result in a better interfacial mixing. However, if the speed is further increased above the critical value, the mechanical degradation of PBT melt would reduce the interfacial bonding between rubber particles and PBT matrix, resulting in a worse impact resistance, instead.[48] Thus, the interfacial properties and mechanical properties of immiscible polymer blends can be highly dependent on the processing conditions.

The characterization tools that can be used to investigate the interfacial properties of polymer blends are still limited. DMA has been shown to be an effective way to indirectly study

the interfacial phenomena of polymer blends. It is believed that a good compatibility between the two phases will lead to a shift of their mutual T_g values toward each other.[48] Recently, Peng et al. used AFM PeakForce quantitative nanomechanical mapping (AFM PF-QNM) to study interfacial properties of an immiscible PEEK/PBI blend and found that the measured elastic modulus shows a sharp change between PEEK and PBI phases in dry state, but the interface becomes broadened upon moisture exposure.[40] The elastic modulus mapping makes it possible to directly estimate the thickness of the interface. It has also been reported that for polypropylene/polyamide blends, a thicker interface would improve the stability of particle dispersion and interfacial adhesion.[52] If the interface is thicker, polymer chains can penetrate deeper into each other to have better molecular intermixing and form more physical entanglements and other interactions.

In the present work, the effect of processing conditions on the interfacial and mechanical properties of PAEK/PBI blends is investigated, which includes the pre-mixing methods (physical powder-mixing or melt blending), molding types (compression molding or injection molding) and matrix polymers (PEEK or PEKK). TGA, DSC, and WAXS were used to characterize the thermal stabilities, crystallinities, non-isothermal crystallization behaviors and crystalline structures of these blends, respectively. Tensile properties and fracture toughness values (K_{IC}) were also determined. The interfacial characteristics were further investigated by DMA and AFM PF-QNM to gain fundamental insight on a molecular scale. Correlation between the mechanical properties and interfacial properties and matrix crystallinities of the PAEK/PBI model blends prepared from different processing conditions will be made. Efforts were made to

build a processing-structure-property relationship for PAEK/PBI blends to help optimize their properties for demanding applications.

2.2. Experimental

2.2.1. Materials

Victrex PEEK 150G (M_n=10 kg/mol; M_w=26 kg/mol)[53], Arylmax PEKK K7500 and Celazole PBI U-60 were used for the present study. PBI powders were fine particles with an average size of about 50 μm. All blends to be molded have the same composition of 50/50 by weight percent. All samples were dried in vacuum oven at 110 °C for 12 hours before any tests.

Four PAEK/PBI model blends investigated in this study were prepared in different processing conditions and designated as "P-C PEEK/PBI", "M-C PEEK/PBI", "M-I PEEK/PBI" and "M-I PEKK/PBI", respectively, to differentiate them in terms of pre-mixing methods (powder mixing vs. melt compounding), molding methods (compression molding vs. injection molding) and matrix polymers (PEEK vs. PEKK). They were listed in Table 2-1 and the detailed processing conditions are provided as follows: powder mixing means mechanically mixing PEEK and PBI fine powders at room temperature while melt compounding means that the powders were further melt compounded in a twin-screw extruder. The injection molding temperature was set at 385 °C in the cylinder end while it was 425 °C at the middle, front and nozzle of the cylinder. The screw speed was 120 rpm.

The pellets were then ground into fine powders (≤100 μm) for molding use. The compounded powders were compression molded under a pressure of 100 MPa at 420 °C for 20 minutes. The pressure was re-applied several times while the mold was cooled. For injection molding, the compounded powders were melted at 420 °C for 20 minutes and then injection molded under a pressure of 200 MPa. The mold temperature was set at 200 °C. The neat systems

including PEEK, PEKK and PBI were also included in this study as references although their processing conditions may vary.

Table 2-1 A summary of designation, and processing conditions of PAEK/PBI blends and neat resins.

Designation	Pre-mixing method	Molding method	Matrix polymer
P-C PEEK/PBI	Powder mixing	Compression molding	PEEK
M-C PEEK/PBI	Melt compounding	Compression molding	PEEK
M-I PEEK/PBI	Melt compounding	Injection molding	PEEK
M-I PEKK/PBI	Melt compounding	Injection molding	PEKK
PEEK	-	Injection molding	PEEK
PEKK	-	Injection molding	PEKK
PBI	-	Compression molding	PBI

2.2.2. Characterization

2.2.2.1. TGA

TGA measurements were carried out using a TGA Q500 (TA Instruments, Inc., DE, USA). About 10 mg specimen was placed in an aluminium oxide (Al_2O_3) pan and heated from 40 °C to 800 °C with a heating rate of 20 °C/min. Nitrogen was used as the balance gas with a rate of 40 mL/min while air was used as the sample gas with a rate of 60 mL/min. The temperature at which it reaches a 5% weight loss was recorded as the degradation temperature, $T_{d,\,5\%}$.

2.2.2.2. DSC

DSC measurements were conducted using a DSC-Q20 (TA Instruments, Inc., DE, USA). A typical three-run test was performed. Specimens with a mass of around 6 mg were prepared

and DSC measurements were conducted at a ramping rate of 20 °C/min from 100 °C to 400 °C in N_2 purge protection. The ratio of enthalpy of fusion of specimen, integral of the heating thermal curve, to that of an ideal 100% crystalline PEEK or PEKK, which is 130 J/g, is used for the calculation of the degree of crystallinity.[9, 54] The samples were then thermally equilibrated at 400 °C for 10 mins to remove the prior thermal history before studying their non-isothermal crystallization behaviors. It is well-known that polymer crystals can retain their ordered structures even when melted, which will affect the crystallization process. In this work, it was found that thermal equilibrium at 400 °C for 10 mins is adequate to eliminate this effect (Figure 2-1 and Table 2-2). After this, it was cooled from 400 °C to 100 °C at a constant rate of 20 °C/min. The crystallization enthalpy from these cooling scans were also utilized to calculate crystallinities. Once normalized by these overall crystallinities, the relative crystallinity growth *vs* temperature during cooling can be derived using the following equation:

$$X_T = \frac{\int_{T_i}^{T}(dH/dT)dT}{\int_{T_i}^{T_e}(dH/dT)dT} \quad (1)$$

where X_T is the relative crystallinity as a function of cooling temperature, whose value is between 0 and 1; T_i and T_e are temperatures where crystallization initiates and ends, respectively.

Lastly, the samples were re-heated to 400 °C with a rate of 20 °C /min after holding at 100 °C for 10 minutes. Similarly, the degree of crystallinity was calculated *via* the integral method mentioned above. Summarized results are listed in Table 2-3 while the second heating scans are plotted in Figure 2-2.

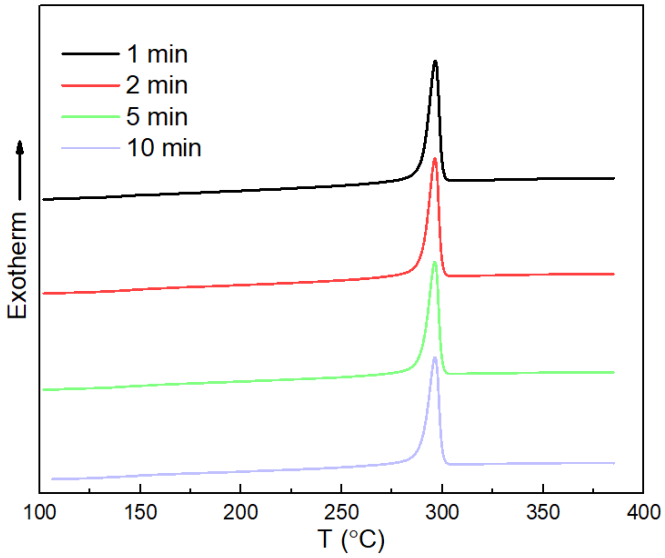

Figure 2-1 DSC cooling scans of neat PEEK 150G after thermal equilibrium at 400 °C for 1 min, 2 min, 5 min and 10 min, respectively.

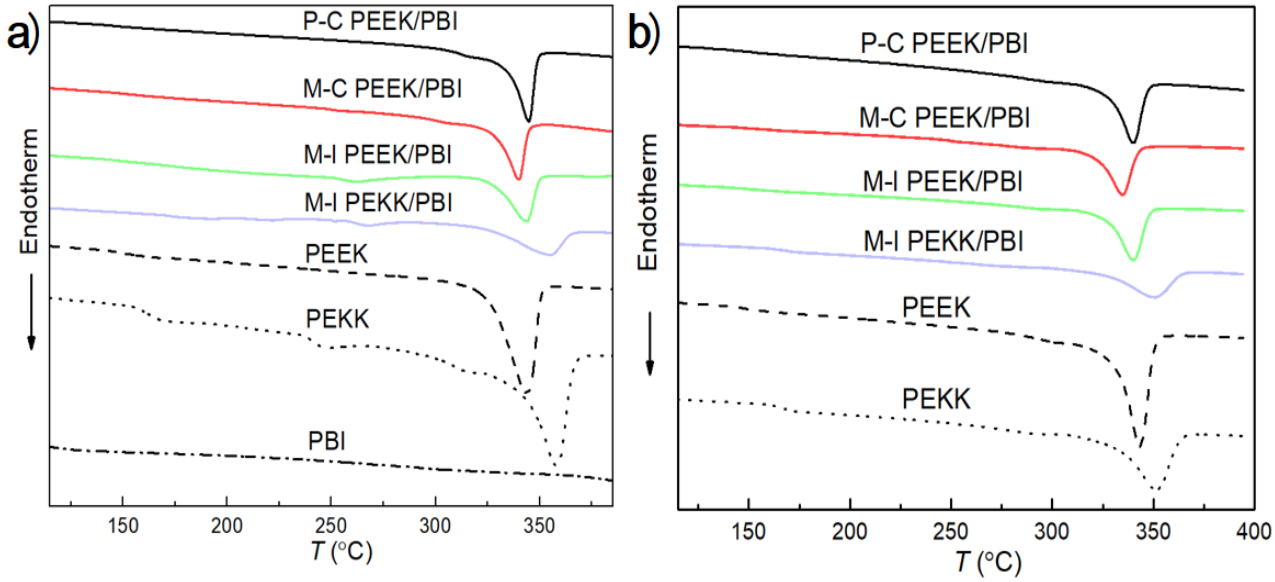

Figure 2-2 The first (a) and second (b) DSC heating scans of PAEK/PBI blends and neat PEEK, PEKK.

Table 2-2 The crystallization peak temperature and crystallinity of cooling scans of neat PEEK 150G after thermal equilibrium at 400 °C for different time.

Equilibrium time at 400 °C	T_c / °C	Crystallinity
1 min	296	42.3%
2 min	296	41.7%
5 min	296	40.6%
10 min	296	40.5%

2.2.2.3. WAXS

The WAXS was measured over the 2θ range of 10-35° on a Bruker D8 ADVANCE X-ray powder diffractometer using Cu K-alpha radiation (λ=1.5406 Å). Specimens were cut from the mid-section of the flex bars and polished into thin films for testing.

2.2.2.4. Tensile test

The uniaxial tensile tests were conducted according to ASTM D638-08 at room temperature. The tensile specimens with a gauge length of 25.4 mm were tested at a crosshead displacement rate of 5 mm/min. For each group, at least three specimens were tested and the average values of Young's modulus, E, strength at break, σ, and strain at break, ε, were reported.

2.2.2.5. Fracture toughness measurements

The single-edge-notch three-point-bending (SEN-3PB) tests were carried out according to ASTM D5045-14. The typical dimension of the specimen for fracture toughness measurement is 30.0 mm × 6.40 mm × 3.20 mm. A V-shaped notch was firstly prepared by using a milling machine and a sharp pre-crack was further prepared by tapping a razor blade with caution to

open the V-notch. The ratio of initial pre-crack length (a_0) to specimen width (W), a_0/W, was controlled to be between 0.4 and 0.6 in accordance with ASTM D5045-14. The pre-cracked specimen was then tested at a crosshead rate of 5.0 mm/min at room temperature. For each group, at least four specimens were tested and the average value of K_{IC} was reported.

The double-notch four-point-bending (DN-4PB) specimens were also prepared for studying the damage mechanism near the crack tip region.[40] Two nearly identical pre-cracks were prepared on one specimen and once tested, one of the pre-cracks failed while the other one survived and was used for analysis. The damage zone near the survived crack tip was carefully polished into thin film (~ 30 μm thick) and the morphology of this damage zone was examined using an Olympus BX 60 optical microscope.

2.2.2.6. DMA

The dynamic mechanical properties were measured using the ARES-G2 rheometer (TA Instruments, Inc., DE, USA). The temperature was increased from 25 °C to 300 °C at a heating rate of 3 °C/min with a constant frequency of 1 Hz and the strain amplitude of 0.05%.

2.2.2.7. AFM

A Bruker dimension icon atomic force microscope with peak force quantitative nanomechanical mode was used to map the elastic modulus across the PAEK/PBI interface at nanoscale resolution. The bulk sample was cut in the middle position and then polished using a microtome to produce a smooth surface for observation. A Bruker AFM probe with the spring constant of 42 N/m was used and the scan rate is 0.3 Hz and 256 points per line.

2.3. Results and discussion

2.3.1. Thermal stability

TGA plots of PAEK/PBI blends and neat resins are presented in Figure 2-3 and the corresponding degradation temperatures are listed in Table 2-3. Among the neat resins, PBI shows the highest degradation temperature, $T_{d,\,5\%}$, suggesting that it is the most thermally stable component. A careful investigation of TGA plot of PEKK shows a continuous small weight loss starting from a much lower temperature and its $T_{d,\,5\%}$ is 521 °C, much lower than that of PEEK (583 °C), indicating a lower thermal stability of PEKK than PEEK. On the other hand, the degradation temperatures of PAEK/PBI blends are similar.

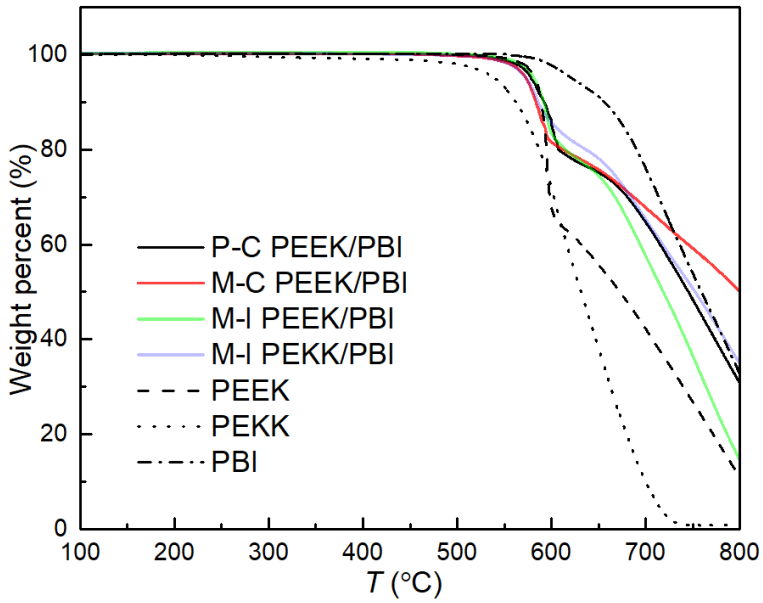

Figure 2-3 TGA plots of PAEK/PBI blends and neat resins in air.

2.3.2. Crystallinity and crystalline structure

The blend components, PEEK and PEKK, are semi-crystalline polymers and their crystallinities measured by DSC are listed in the Table 2-3. The degrees of crystallinity calculated from heating scans and normalized by the weight fraction of PEEK or PEKK are

reported, and the heating scans are also presented in Figure 2-2. The P-C PEEK/PBI appears to have the highest degree of crystallinity, 41.2%, which is almost the same as that of the neat Victrex PEEK 150G reported in our previous work.[9] This suggests that the crystallization of PEEK matrix is not significantly affected by the dispersed PBI particles in P-C PEEK/PBI even though PBI accounts for 50% by weight. The crystallinities of M-C PEEK/PBI and M-I PEEK/PBI are much lower (Table 2-3), suggesting that PBI phase hinders the crystallization of PEEK in melt pre-mixed blends. In this work, the normalized crystallinity of P-C PEEK/PBI almost equals that of neat PEEK resin, indicating that PBI particles and PEEK matrix do not molecularly interact with each other at the interface and thus the crystallinity of PEEK is not influenced by the presence of PBI. Although both are compression molded, the M-C PEEK/PBI has a much lower crystallinity than P-C PEEK, implying a better wetting of PEEK on PBI particles and restricted crystallization of PEEK molecules near their interface.

The M-I PEEK/PBI exhibits an even lower crystallinity than M-C PEEK/PBI and this can be explained by the fact that the cooling rate for injection molding is much higher than that of the compression molding, thus less crystallinity is observed. In the case of PEKK/PBI system, the degree of crystallinity is the lowest among all four blends, which is due to the fact that the crystallization rate of PEKK is much lower than that of PEEK.[55] It should be noted that both M-I PEEK/PBI and M-I PEKK/PBI show a small endothermic peak near 265 °C, whose origin is explained with different interpretations.[56]

2.3.3. Non-isothermal crystallization behaviors

The DSC findings suggest that different processing conditions result in different interfacial characteristics, which are known to play a role in the crystallization of immiscible

polymer blends. The non-isothermal crystallization behaviors of PAEK/PBI blends were compared to neat PEEK and PEKK, hoping to shed some lights on the influence of processing conditions on the interfacial properties indirectly. It should be noted that the prior thermal histories of blends and neat PEEK were removed before the non-isothermal crystallization started (Figure 2-1 and Table 2-2). The cooling scans are shown in Figure 2-4 and the peak temperature is reported as crystallization temperature, T_c, listed in Table 2-3. T_c of all PAEK/PBI blends are lower than those of neat PEEK and PEKK, respectively, indicating that the incorporation of PBI particles retards the crystallization of PEEK and PEKK. According to the literature, the effect of interfacial compatibility on the crystallization of poly(L-lactic acid) (PLLA) has been investigated and found that the enhanced compatibility retards the nucleation process and the overall crystallinity is lowered although spherulite growth rate is increased.[57] Therefore, the crystallization temperature T_c will likely become lower if the interfacial interaction between the phases becomes stronger. For better visual assessment of the non-isothermal crystallization behaviors, the relative crystallinity as a function of cooling temperature is shown in Figure 2-4. A similar conclusion can also be drawn based on the degree of crystallinity calculated from the cooling scans since a better mixing at interface would usually result in more retarded crystallization and a relatively lower crystallinity. Interestingly, the crystallinity calculated from the cooling scan of M-C PEEK almost equals that of M-I PEEK/PBI although its T_c is lower than that of the latter, indicating the interfacial characteristics of M-I PEEK/PBI is comparable to that of M-C PEEK/PBI. The results suggest that the extent of interfacial interaction follows the trend: M-C PEEK/PBI $\approx$ M-I PEEK/PBI > P-C PEEK/PBI.

Table 2-3 The thermal properties of PAEK/PBI blends and neat resins. T_m is the melting temperature; T_c is the crystallization temperature; χ_c is the degree of crystallinity; $T_{d,\,5\%}$ is the degradation temperature at which there is 5% weight loss.

Sample	DSC 1st heating		DSC 1st cooling		DSC 2nd heating		TGA results
	T_m / °C	χ_c	T_c / °C	χ_c	T_m / °C	χ_c	$T_{d,\,5\%}$ / °C
P-C PEEK/PBI	340	41.2%	293	38.8%	340	38.3%	578
M-C PEEK/PBI	344	36.4%	277	36.5%	335	36.4%	573
M-I PEEK/PBI	345	32.9%	285	36.6%	340	36.7%	580
M-I PEKK/PBI	355	30.9%	270	29.4%	351	28.5%	573
PEEK	344	41.1%	296	40.4%	343	41.8%	583
PEKK	358	33.3%	285	32.1%	352	32.4%	521
PBI	-	-	-	-	-	-	620

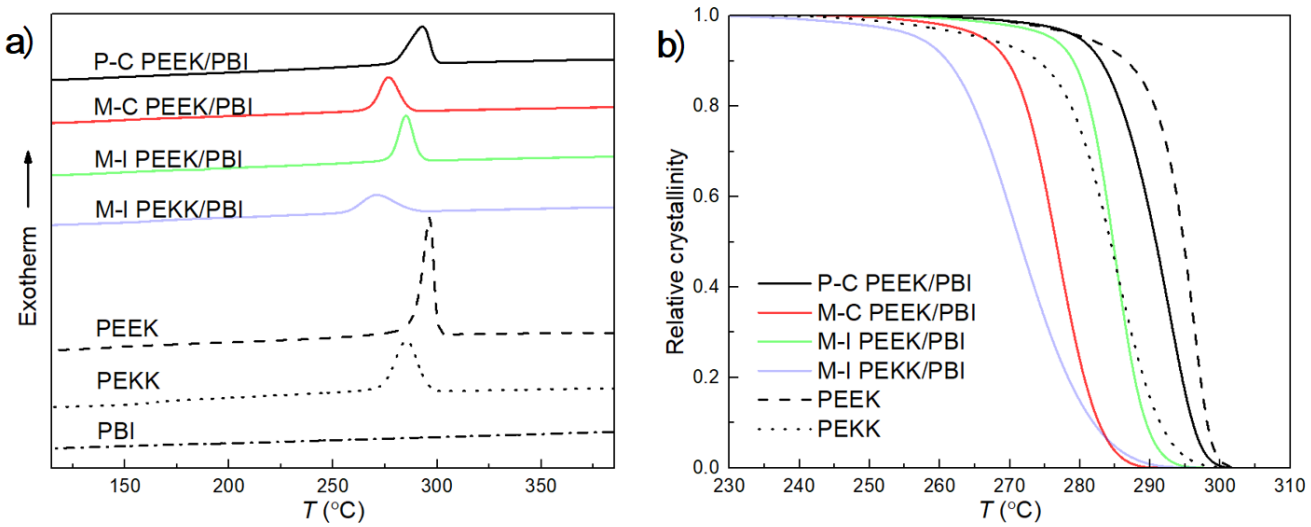

Figure 2-4 a) first DSC cooling scans after equilibrium at 400 °C for 10 mins; b) relative crystallinity as a function of temperature during cooling.

The crystalline structure of the samples investigated by WAXS is shown in Figure 2-5. Consistent with the literature, all PEEK/PBI samples only show Type-I crystalline form while PEKK/PBI also displays the thermodynamically stable type-I form only.[58, 59] This is not

surprising since form-II of PEKK is typically induced by solvent-induced crystallization or cold crystallization, which is not the case for the M-I PEKK/PBI blend prepared in this work.[59] Both crystalline structures of PEEK and PEKK are orthorhombic and their unit cell dimensions are calculated and listed in Table 2-4. The most significant difference between PEEK and PEKK is their unit cell dimension in *b*-axis. For PEEK, the polymer chains are inclined along the *b*-axis to the lamellar normal by 38.1°.[59] When one of the ether groups in PEEK is replaced by ketone group, the dimension of unit cell along *b*-axis is enlarged due to the higher rigidity of ketone group, resulting in a slightly larger value of *b*.

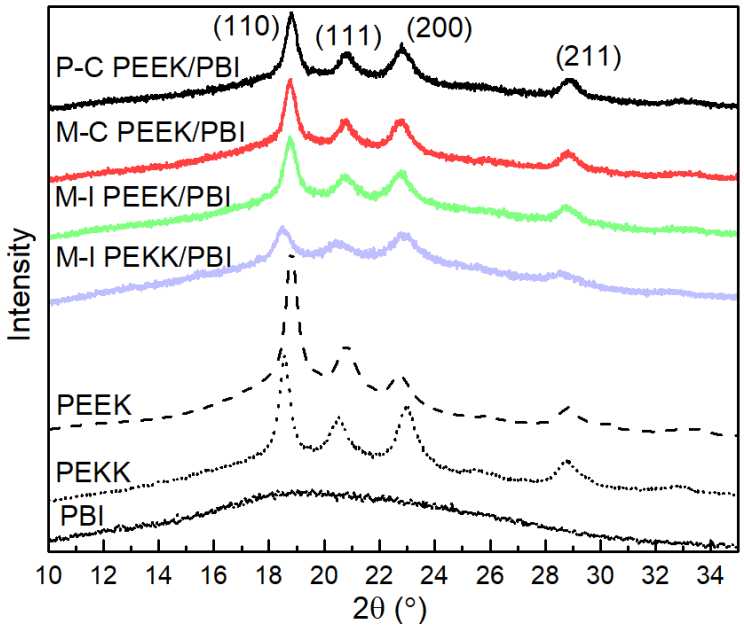

Figure 2-5 WAXS spectra of PAEK/PBI blends and neat resins

Table 2-4 Lattice parameters of crystalline structures in neat resins and PAEK/PBI blends.

Sample	*a* / Å	*b* / Å	*c* / Å
P-C PEEK/PBI	7.79	5.92	10.10
M-C PEEK/PBI	7.79	5.94	10.04
M-I PEEK/PBI	7.81	5.94	10.04
M-I PEKK/PBI	7.76	6.10	10.00
PEEK	7.82	5.91	10.02
PEKK	7.74	6.08	10.11
PBI	-	-	-

2.3.4. Interfacial characteristics

To determine how the different processing conditions may influence interfacial bonding between PAEK and PBI, DMA and AFM PF-QNM were carried out. The DMA results of the PAEK/PBI blends are shown in Figure 2-6 and the corresponding T_g are listed in Table 2-5. The

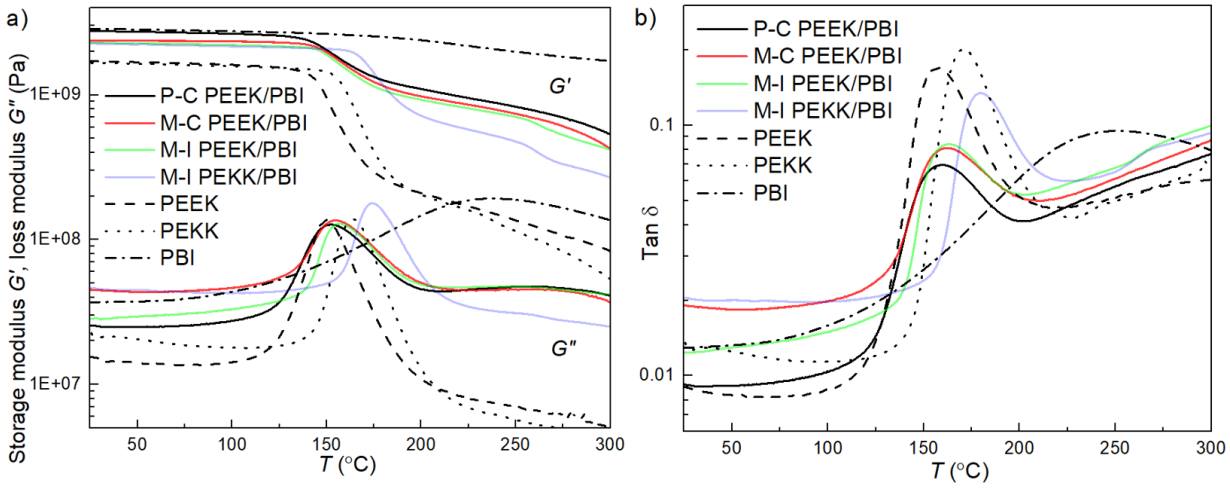

Figure 2-6 a) Storage modulus G', loss modulus G" and b) Tan δ as a function of temperature for all model PAEK/PBI blends and neat resins.

incorporation of PBI particles into the PEEK and PEKK matrix causes the T_g of PEEK and PEKK matrix to increase to varying degrees, respectively, and the glass transition (*G"*) is broadened compared to neat PEEK and PEKK. P-C PEEK/PBI exhibits the lowest PEEK T_g due to its poor interfacial mixing among four model blends. Based on the non-isothermal crystallization studies, it is expected that M-C PEEK/PBI should have a higher PEEK T_g than that of the PEEK in M-I PEEK/PBI if the former has a stronger interfacial adhesion. However, the T_g values of the two blends turn out to be very close to each other. Therefore, it is believed that the extents of interfacial interaction may be different for these two, but the difference is too small to be detected by DMA.

AFM PF-QNM was also utilized to evaluate the interfacial thickness of PAEK/PBI blends. A schematic is presented in Figure 2-8 and Figure 2-7 to show how the average interfacial thickness is determined. It should be noted that the interfacial interaction across the interface is not uniform and may be very different depending on the curvature of the interface.

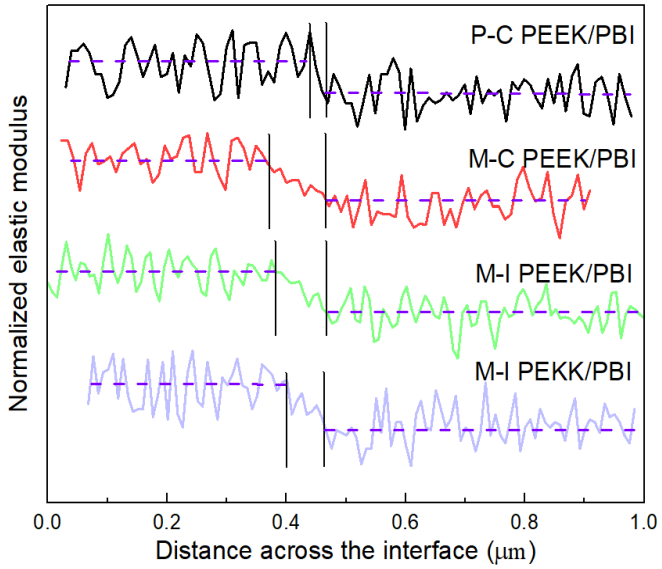

Figure 2-7 AFM mapping of elastic modulus at the interface of PAEK/PBI blends. The normalized elastic modulus curves have been shifted vertically for clarity.

Therefore, to improve the reliability of the data, straight boundary interfaces are randomly chosen and evenly spaced cross bars (white lines in Figure 2-8) perpendicular to the interface were selected. The corresponding modulus *vs.* distance is used to determine the interfacial thickness in a manner shown in Figure 2-7. More than 20 points from each interfacial region were measured for each sample and the average value is reported (Table 2-5).

Table 2-5 T_g of PAEK/PBI blends and the interfacial thickness measured by AFM PF-QNM.

Sample	**T_g / °C**	**Interfacial thickness / nm**
P-C PEEK/PBI	159.9	42 ± 19
M-C PEEK/PBI	162.7	79 ± 29
M-I PEEK/PBI	163.0	77 ± 26
M-I PEKK/PBI	179.8	66 ± 32

As discussed above, the large standard deviation is due to the intrinsic nature of the non-uniformity of the interfacial region. However, the averaged value is still meaningful if the criteria above are fully met. Typical results of elastic modulus change at the interface mapped by AFM PF-QNM are presented in Figure 2-7 and it can be found that the modulus of P-C PEEK/PBI changes suddenly at the interface while other melt pre-mixed blends show more gradual changes. Thus, the interface for P-C PEEK/PBI is the narrowest, consistent with the notion that the powder pre-mixed blend has a much weaker interfacial strength than the melt pre-mixed ones. The interfacial thickness of M-C PEEK/PBI almost equals that of M-I PEEK/PBI. This can be explained by the fact that both M-C PEEK/PBI and M-I PEEK/PBI were melt compounded in the same manner and the interfacial wetting between PEEK and PBI should be the same for these

two blends. The subsequent different molding processes do not affect their wetting significantly and thus their interfacial thicknesses turn out to be almost equal. This finding is consistent with the DMA results and the non-isothermal crystallization studies.

On the other hand, the interfacial thickness of M-I PEKK/PBI is slightly smaller than that of M-I PEEK/PBI, which can be explained by the lower molecular mobility of PEKK than PEEK due to its higher ketone/ether ratio when all other processing conditions are the same and only different matrix polymers are involved. At the same compounding temperature, both PEEK and PEKK are in molten state but chain mobility of PEKK may be more restricted than PEEK due to their higher ketone/ether ratio, making the extent of interfacial mixing of M-I PEKK/PBI slightly lower than that of M-I PEEK/PBI. Therefore, the interface of M-I PEKK/PBI is slightly thinner. A schematic is shown in Figure 2-9 to elucidate how the interfacial interaction is related to the

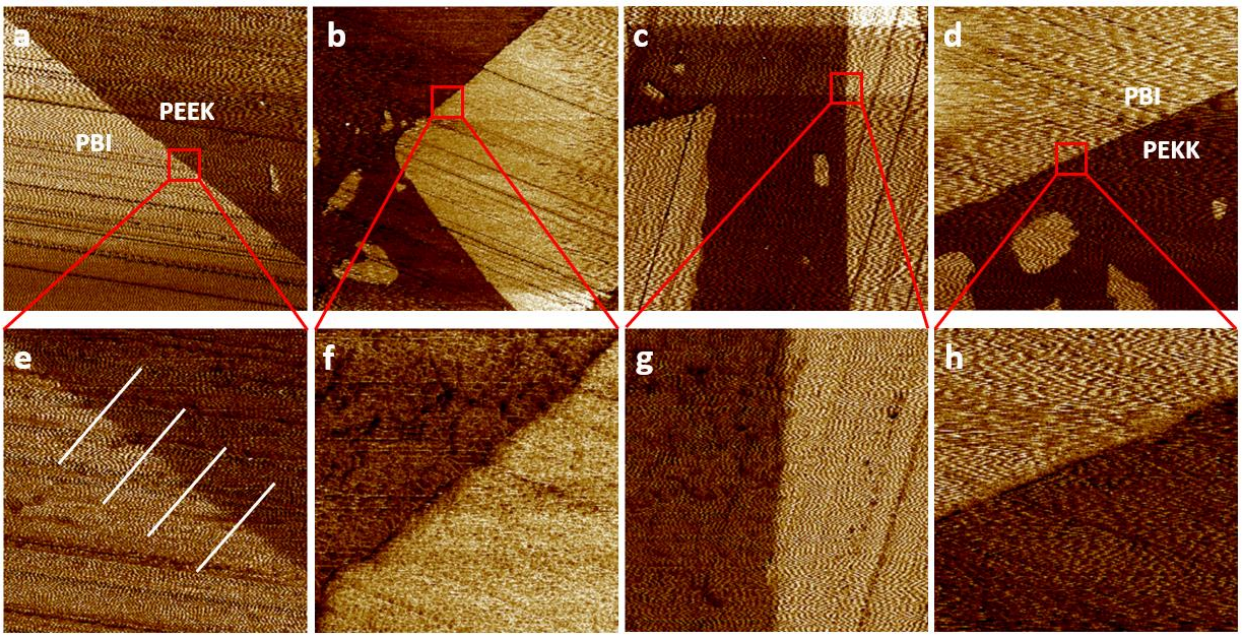

Figure 2-8 AFM PF-QNM mapping of PAEK/PBI blends: P-C PEEK/PBI (a, e), M-C PEEK/PBI (b, f), M-I PEEK/PBI (c, g), M-I PEKK/PBI (d, h). Figures 6e-h are the amplifications of the selected areas in Figures 7a-d, respectively. The size of Figures 6a-d is 10 μm × 10 μm and the size of Figures 7e-h is 2 μm × 2 μm.

interfacial thickness from a molecular scale perspective.

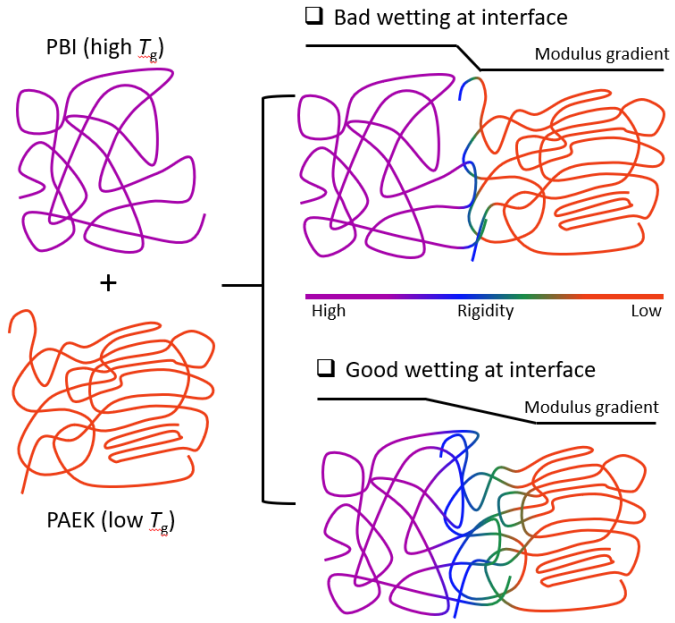

Figure 2-9 A schematic of the relationship between interfacial thickness and the extent of interfacial wetting.

2.3.5. Mechanical properties

The influence of different processing conditions on the mechanical properties of PAEK/PBI blends is investigated and their tensile and fracture toughness properties are listed in Table 2-6. While the Young's modulus exhibits slight differences, the tensile strength appears to be strongly affected by the processing conditions, especially for the P-C PEEK/PBI blend. There appear to be more or larger defects in the physically pre-mixed blend compared to other melt pre-mixed blends. This may be attributed to its very weak interfacial adhesion between PEEK matrix and PBI particles. Among the other three melt pre-mixed blends, the tensile strengths of M-C PEEK/PBI and M-I PEEK/PBI blends are comparable while that of M-I PEKK/PBI appears to exhibit about 10% lower tensile strength than them. Compared to the neat PEKK, there are negligible improvements in the tensile strength of M-I PEKK/PBI. That indicates that the

enhancement effect of PBI particles is not effective in M-I PEKK/PBI, which can be supported by its narrower interfacial thickness compared to M-C PEEK/PBI and M-I PEEK/PBI. In addition, the tensile strength of M-I PEKK/PBI may be limited by the inherent brittleness of the PEKK matrix, which explains that its tensile strength value almost equals that of neat PEKK.

The fracture toughness values are also greatly influenced by the processing conditions (Table 2-6). As expected, the physically pre-mixed P-C PEEK/PBI shows the lowest fracture toughness. M-I PEEK/PBI displays the highest fracture toughness among the four blends while the K_{IC} value of M-C PEEK/PBI is slightly lower than that of M-I PEKK/PBI. These findings are discussed as follow.

It has been reported that the fracture mechanisms of dry and steam-treated PEEK/PBI blends are quite different. For the steam-treated one, crack will propagate through PEEK matrix and PBI particles in a straight fashion.[40] For all the four blends studied in dry condition here, the crack propagates along the interfacial region in a tortuous pathway fashion, rather than breaking through the PBI particles (Figure 2-10). This suggests that the interfacial strengths among the blends are generally weaker than the cohesive strength of PBI particles in dry state and the contribution of PBI phase itself to the fracture toughness of blends is believed to be insignificant since the cracks do not pass through the PBI particles. On the other hand, since crack propagates through PAEK matrix and along the interfaces, the fracture toughness of the matrix itself and the interfacial strength should play a more significant role here. It is expected that a tougher matrix should result in a tougher blend. Also, for systems with a better wetting and stronger interfacial strength between PAEK matrix and PBI particles, more fracture energy is required to break through the interface, resulting in a higher fracture toughness value.

Table 2-6 Summary of tensile properties and fracture toughness of PAEK/PBI blends and resins.

Sample	E / GPa	σ / MPa	ε / %	K_{IC} / (MPa·m$^{1/2}$)
P-C PEEK/PBI	5.2 ± 0.3	77 ± 5	1.5 ± 0.1	1.73 ± 0.17
M-C PEEK/PBI	5.4 ± 0.2	122 ± 15	2.9 ± 0.3	2.78 ± 0.18
M-I PEEK/PBI	5.3 ± 0.3	118 ± 12	3.1 ± 0.4	3.46 ± 0.26
M-I PEKK/PBI	5.4 ± 0.3	107 ± 7	2.3 ± 0.2	3.06 ± 0.17
PEEK	4.1 ± 0.2	105 ± 8	29 ± 4	6.78 ± 0.41
PEKK	4.4 ± 0.3	104 ± 8	10 ± 1	1.92 ± 0.05
PBI	7.1 ± 0.1	150 ± 7	2.3 ± 0.1	3.53 ± 0.25

The most notable finding is the lowest fracture toughness of P-C PEEK/PBI, which is consistent with the previous explanation that the interfacial adhesion in the powder-mixed blend is poor when compared with the melt pre-mixed ones and it also suffers from a very high degree of crystallinity. According to the literature, the mode I fracture toughness of neat PEEK decreases with increasing crystallinity.[60] Interestingly, M-I PEEK/PBI shows the highest fracture toughness value (K_{IC}) among the four blends. As mentioned above, M-C PEEK/PBI and M-I PEEK/PBI have comparable level of interfacial interaction. Therefore, the higher fracture toughness of the latter can be explained by the contribution from the lower matrix crystallinity of M-I PEEK/PBI.[60]

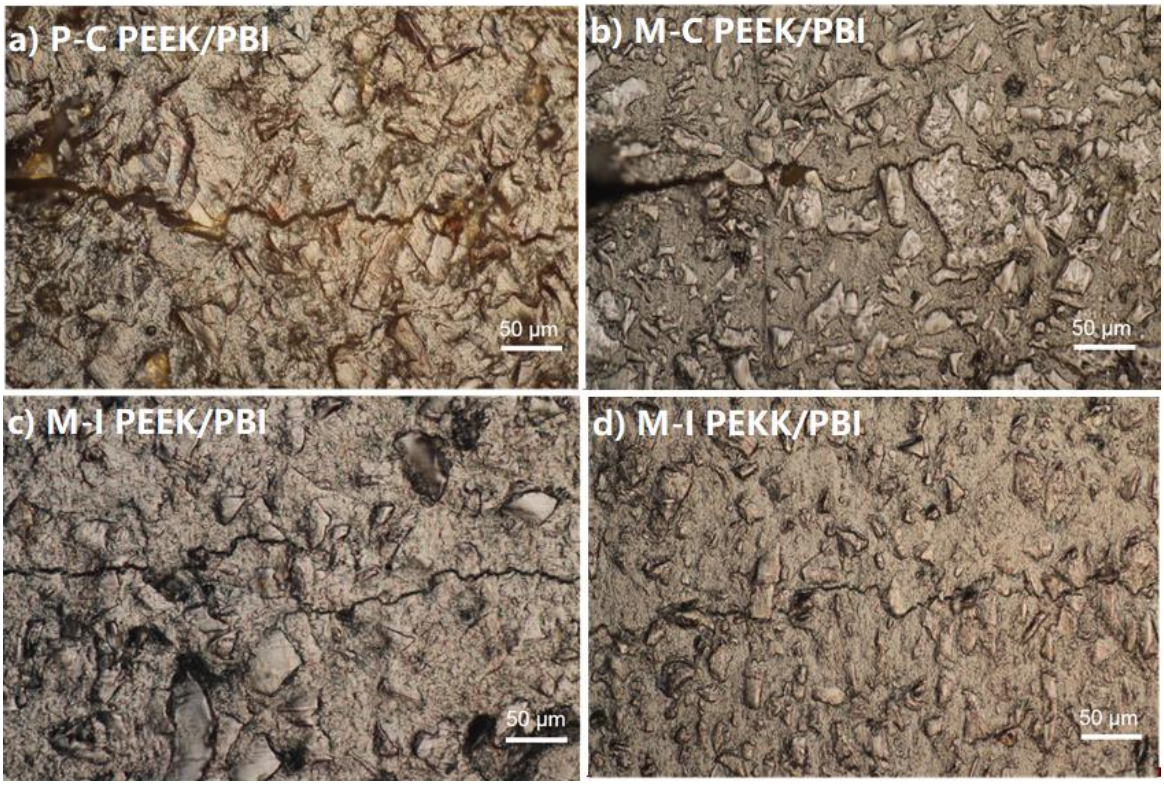

Figure 2-10 Crack propagation in dry condition: a) P-C PEEK/PBI; b) M-C PEEK/PBI; c) M-I PEEK/PBI and d) M-I PEKK PBI.

When comparing the fracture toughness of M-I PEEK/PBI and M-I PEKK/PBI, besides matrix crystallinity and interfacial thickness, another factor that needs to be considered is the compatibility difference of PEEK and PEKK with PBI. Although PEEK and PEKK have similar chemical structures, the different ketone/ether ratio between them may result in their different affinities to PBI. The solubility parameter is widely used to predict the compatibility between two polymers.[61] The solubility parameters for PEEK, PEKK and PBI are listed in Table 2-7, showing that the solubility parameter of PEKK is closer to that of PBI than PEEK.[62-64] This suggests that PEKK has a higher affinity to PBI than PEEK. M-I PEKK/PBI also has the lowest crystallinity among all the blends. The reason why M-I PEKK/PBI has a lower fracture

toughness than that of M-I PEEK/PBI may be due to the inherent brittleness of PEKK over PEEK. Even though M-I PEKK/PBI benefits from a higher affinity of PEKK to PBI but its interfacial thickness is still slightly narrower than M-I PEEK/PBI. It is difficult to decouple the influences of compatibility and interfacial thickness to determine the interfacial strength differences between PEEK and PEKK with PBI quantitatively.

Table 2-7 Solubility parameters of PEEK, PEKK and PBI.

Sample	**δ / MPa$^{1/2}$**
PEEK	22.2[61]
PEKK	23.1[62]
PBI	31.1, 33.7[63]

Finally, besides matrix crystallinity and interfacial strength, the fracture toughness values of M-I PEEK/PBI and M-I PEKK/PBI can also be affected by the inherent properties of matrix polymer, which determines the fracture toughness of matrix itself and influences the interfacial adhesion with dispersed particles at the same time.

The present work shows the significance of processing conditions on the mechanical properties of immiscible PAEK/PBI blends. Different processing conditions could result in different matrix crystallinities and interfacial strengths, which then affect the mechanical properties significantly. The powder-mixing at room temperature leads to extremely weak interfacial strength, thus exhibiting the lowest tensile strength and fracture toughness among all the blends. On the other hand, the interfacial strength is significantly enhanced if blends are melt-compounded. The two melt pre-mixed blends, M-C PEEK/PBI and M-I PEEK/PBI, show

similar interfacial characteristics while they also possess comparable tensile properties. Their most notable difference is the higher fracture toughness of M-I PEEK/PBI due to its lower matrix crystallinity.

Finally, the intrinsic properties of the polymer matrix play a significant role in determining the mechanical properties of the blend. The tensile strength of M-I PEEK/PBI is improved by 12% from neat PEEK resin while the improvement for M-I PEKK/PBI compared to neat PEKK is negligible. The fracture toughness of M-I PEKK/PBI is improved by nearly 60% compared to neat PEKK but still lower than that of M-I PEEK/PBI. The neat PEEK and PEKK resins have similar tensile strength, but the latter shows much lower facture toughness. This explains why the fracture toughness of M-I PEKK/PBI is lower than that of M-I PEEK/PBI.

2.4. Conclusion

The effect of different processing conditions, including pre-mixing methods, molding methods, and matrix polymers, on the mechanical properties of PAEK/PBI blends was investigated. The mechanical properties are highly influenced by the inherent matrix properties, matrix crystallinities and interfacial strength. The major findings in this study are highlighted as follows:

1) Powder pre-mixing results in weak interfacial adhesion and low mechanical properties and should be avoided. Melt pre-mixing is necessary and highly recommended since it is a key step in achieving satisfied levels of interfacial adhesion in immiscible polymer blends.
2) Compression molding and injection molding mainly affect the degree of matrix crystallinity. Injection molding results in a lower crystallinity, which impacts little on tensile strength but contributes significantly to the fracture toughness of PEEK/PBI blends.

3) The choice of matrix polymer is important since it may affect fracture toughness, degree of crystallinity and the interfacial strength.

Blending PEEK with PBI does help improve the mechanical properties if a suitable processing condition is applied, especially melt pre-mixing step. However, it should be noted that improvements on Young's modulus and tensile strength are limited, given that such a huge amount of PBI (50 wt.%) are added.

The limited mechanical enhancement by this approach inspired us to find a more efficient way to finish this job. For this purpose, MWCNT was chosen as reinforcing filler to make PEEK/MWCNT nanocomposites. A challenge is how to achieve good dispersion state of MWCNT in PEEK. In the following two chapters, we will start with a low concentration system to elucidate that MWCNT can be well dispersed by a novel solution mixing approach (Chapter 3). However, this low concentration PEEK/MWCNT system shows mild mechanical reinforcement due to low MWCNT loadings. Therefore, in Chapter 4, this novel solution mixing approach was further modified to prepare a high concentration system (10 wt.% MWCNT), which exhibits much more efficient enhancement with its Young's modulus higher than that of 50 wt.% PEEK/PBI blend.

3. DEVELOPMENT OF WELL-DISPERSED PEEK/MWCNT NANOCOMPOSITES*

3.1. Introduction

Chapter 2 discussed the mechanical reinforcement of PAEK by blending with high-performance polymer PBI particles. Although the Young's modulus and tensile strength can be increased to around 5.4 GPa and 120 MPa, respectively, these improvements are still considered to be low and fail to meet the requirement for some applications. Modulus enhancement by blending with PBI is inherently finite because of the classic "rule of mixing". The Young's modulus of PBI, a more rigid component in PEEK/PBI binary blend, is only about 7.1 GPa, which also indicates the theoretical upper limit of modulus it can improve according to the "rule of mixing". Another drawback is the use of a high loading of PBI (50 wt.%), which can impose adversary effects on processing as well as increase the cost because PBI is quite expensive.

Much effort has been dedicated to enhancing the properties of PEEK *via* incorporation of other reinforcing agents like glass fibers, carbon fibers, and MWCNT, etc.[65-68] In addition to blending with PBI, the other options are to add glass fibers or carbon fibers into PEEK matrix. Yuan et al. prepared a PEEK/short glass fiber composite with a loading of 30 wt.% glass fibers and the consequent Young's modulus is increased from 3.6 GPa to 11.8 GPa.[65] It was also reported that addition of 30 wt.% short carbon fiber into PEEK can even improve the Young's modulus to 24 GPa.[69] However, such an achievement results from the high loading of fillers, which usually increases the processing difficulty as the viscosity will be increased. On the other

* Reprinted with permission from "Well-dispersed poly(ether-ether-ketone)/multi-walled carbon nanotube nanocomposites prepared via a simple solution mixing approach" by Jiang, Z. Y.; Chen, Q. H.; Zhu, Z. W.; Tsai, C. Y.; Zhao, M. Z.; Sue, H. J.; Chang, A.; Bremner, T.; DiSano, L. P., *Polym Int* **2021,** *70* (8), 1090-1098. Copyright 2021 by John Wiley & Sons, Inc.

hand, for some applications where mass matters, like aerospace field, high loading of fillers with a higher density may be economically unfavorable since densities of glass fiber (ρ=~2.6 g/cm^3) and carbon fiber (ρ=~1.8 g/cm^3) are higher than that of PEEK (ρ=~1.3 g/cm^3).[9, 70, 71] Consequently, reinforcing PEEK in a more efficient manner, namely with lower loading of fillers to achieve higher modulus, is highly favorable.

MWCNT appears to be a promising reinforcing filler, given that it possesses low density, high strength, and modulus as well as high aspect ratio, enabling it high specific strength and high specific modulus. Such properties make it a good candidate as effective reinforcing filler. Direct melt-mixing of MWCNT in polymer matrix does not lead to significant breakup of the aggregated MWCNT due to their large surface area, strong van der Waals forces, and lack of surface functional groups to interact with the hosting polymer matrix. A good dispersion and strong bonding of MWCNT to the polymer matrix is beneficial for enhancing their mechanical properties. Substantial research has been aimed at improving the dispersion of PEEK/MWCNT nanocomposites.[67, 72] Rong et al. prepared PEEK/MWCNT composites by premixing of PEEK powders with MWCNT solution before melt blending to achieve better dispersion of MWCNT in PEEK;[73] however, some agglomerations of MWCNT still persisted. Another strategy is to improve the compatibility between CNT and PEEK matrix by using compatibilizers or chemical modification of CNT to improve dispersion and interfacial adhesion at the same time. Díez-Pascual et al. used two kinds of polysulfones (PSF), poly(bisphenol-A-ether sulfone) (PES) and poly(1-4-phenylene ether-ether sulfone) (PEES), to wrap SWCNT in solvent, followed by drying, and melt blending with PEEK powders, respectively.[74, 75] Unfortunately, the resulting PEEK/SWCNT composites compatibilized with the two kinds of PSFs still showed bundled SWCNTs and the polysulfone-based compatibilizers also hindered the crystallization of PEEK,

leading to their inferior mechanical properties. Lin et al. synthesized a series of carbazole-based poly(aryl-ethers) with conjugated structure on the backbone and on the side chain as compatibilizers to wrap MWCNT in the preparation of PEEK/MWCNT nanocomposites.[76, 77] But these systems are vulnerable to thermal degradation and lead to insignificant improvement in mechanical properties. Other researchers have also reported the preparation of PEEK/SWCNT nanocomposites *via* the incorporation of hydroxylated PEEK covalently grafted on SWCNT.[78] However, this approach cannot avoid the degradation of hydroxylated PEEK during melt processing, thus destroying the PEEK/SWCNT interfaces since the hydroxylated PEEK has much lower thermal stability.

Solution processing is a widely used technique to prepare polymer nanocomposites to achieve good dispersion.[79] However, it was rarely applied to PEEK since PEEK is well-known for its chemical resistance and is only soluble in limited kinds of solvents at elevated temperatures.[80] Recently, the phase behavior of PEEK in dichloroacetic acid (DCA) solvent was studied and found that PEEK can remain dissolved in DCA even at room temperature for a long period of time at low concentrations.[80, 81] This provides a route for preparing good quality PEEK/MWCNT nanocomposites *via* a solution approach.

In this chapter, we describe a simple solution mixing approach to prepare PEEK/MWCNT nanocomposites. Both p-MWCNT and o-MWCNT were used to prepare PEEK nanocomposites for investigating the effect of surface treatment of MWCNT on their crystallization and mechanical properties. The dispersion state of MWCNT in PEEK, PEEK crystallization behavior, and their thermal and mechanical properties were investigated. CTE was also measured to evaluate their dimensional stabilities for their possible high temperature applications. A PEEK wrapping of MWCNT mechanism is proposed to explain why a good

dispersion could be achieved by this solution mixing approach. The approach presented here is easily scalable and may be applicable for preparation of other high-performance polymer nanocomposite systems.

3.2. Experimental

3.2.1. Materials

Victrex PEEK 150G powders were kindly provided by Hoerbiger Corporation of America, Inc. (Houston, TX). MWCNT (SWeNT SMW 100) was purchased from Sigma-Aldrich (Saint Louis, MO). The content of MWCNT in this grade is > 95% and its outer diameter and length are about 6-9 nm and 5 μm, respectively. DCA (> 99%) and NMP (> 99%) solvents were purchased from VWR International, LLC.

3.2.2. Preparation of o-MWCNT

p-MWCNT (250 mg) was added into a mixture of concentrated sulfuric acid (45 mL) and concentrated nitric acid (15 mL) and ultrasonicated in a sonication bath (Branson 2510) for 2 h at room temperature. Then, 190 mL of deionized water (DI water) was added to hinder further oxidation. The solution was further sonicated for 1 h at room temperature. o-MWCNT was filtered with a polyvinylidine fluoride (PVDF) filter membrane (0.45 μm pore size, Millipore, Durapore). The o-MWCNT was washed with DI water multiple times and then washed with methanol multiple times to remove residual acid. Then, o-MWCNT was collected and re-dispersed in NMP *via* sonication for about 15 minutes. The residual methanol in the solution was removed using a rotary evaporator to obtain o-MWCNT/NMP solution.

3.2.3. Preparation of PEEK/MWCNT nanocomposites and thermal treatment

p-MWCNT was dispersed in NMP solvent *via* sonication for about 15 minutes for later use. PEEK powders at 2 wt.% in DCA solvent were added into a flask and then heated to 185 °C

until PEEK was fully dissolved. The PEEK/DCA solution was subsequently cooled down to room temperature and poured into p-MWCNT/NMP (or o-MWCNT/NMP) solution (~1 mg/mL), immediately followed by shaking manually to mix the two solutions. The resulting suspension was filtered using a PVDF filter membrane and washed with DI water and methanol to remove residual DCA and NMP solvents. The precipitates were dried at 80 °C in a vacuum oven overnight to obtain PEEK/MWCNT dry powders.

The PEEK/MWCNT powders were injection molded into tensile bars (ASTM D638 Type V) and rectangular bars (30 mm × 9 mm × 3 mm) using a Haake MiniJet Pro Piston Injection Molder (Thermo Fisher Scientific, Inc.). The cylinder temperature, mold temperature and injection pressure were set at 400 °C, 180 °C, and 680 bar for the nanocomposites and 390 °C, 180 °C, 600 bar for neat PEEK, respectively. Different cylinder temperatures and injection pressures for neat PEEK and nanocomposites were applied to compensate for their differences in melt viscosities. Nanocomposites with 0.5 wt.%, 1.0 wt.% and 1.5 wt.% of p-MWCNT and o-MWCNT were all prepared as described above.

After injection molding, bulk samples were annealed at 260 °C for 1 h to increase the degree of crystallinity for the subsequent thermal and mechanical tests. For clarity, the composition, thermal treatment condition and sample designation are summarized in Table 3-1.

Table 3-1. Designation, composition**,** and annealing condition of PEEK and PEEK/MWCNT nanocomposites.

Designation	MWCNT content	Annealed at 260 °C for 1h
uPEEK	0	No
PEEK	0	Yes
0.5pCNT	0.5 wt.% p-MWCNT	Yes
1.0pCNT	1.0 wt.% p-MWCNT	Yes
1.5pCNT	1.5 wt.% p-MWCNT	Yes
0.5oCNT	0.5 wt.% o-MWCNT	Yes
1.0oCNT	1.0 wt.% o-MWCNT	Yes
1.5oCNT	1.5 wt.% o-MWCNT	Yes

3.2.4. Characterization

3.2.4.1. TOM

Solid specimens (about 2 mg) were placed between two glass slides and then hot pressed at 400 ℃ to obtain thin films with a thickness of about 50 μm. TOM images of MWCNT dispersion were obtained by observing the thin films under an Olympus BX60 microscope.

3.2.4.2. TEM

TEM images of MWCNT dispersion were obtained by microtoming bulk samples to about 100 nm in thickness and observed using a JEOL 1200 EX TEM operated at 100 keV.

3.2.4.3. SEM

SEM was acquired using a JEOL JSM-7500F field emission scanning electron microscope (FE-SEM), operated at 2.0 kV. The tensile fracture surfaces were observed.

3.2.4.4. TGA

TGA tests were conducted using a TGA Q500 (TA Instruments, Inc., DE, USA). Specimens with a mass of about 6 mg were heated form 30 °C to 900 °C in air at a heating rate

of 30 °C/min. The degradation temperature (T_d) is defined as the temperature at which a weight loss of 3% has reached.

3.2.4.5. DSC

DSC measurements were used to determine crystallinity using a DSC-Q20 (TA Instruments, Inc., DE, USA). Specimens (about 5 mg) were cut from regions away from the surface of the bulk samples. A typical three-scan characterization was conducted under N_2 purge protection (50 mL/min): 1) heating from 100 °C to 400 °C with a rate of 20 °C/min, 2) cooling from 400 °C to 100 °C with a rate of 20 °C/min after being isothermally equilibrated at 400 °C for 10 min, which was shown to be adequate to remove thermal history effect,[82] and 3) heating from 100 °C to 400 °C with a rate of 20 °C/min after being isothermally treated at 100 °C for 10 min.

The first heating scan was used to calculate the degree of crystallinity of the bulk sample while the cooling scan was used to study the non-isothermal crystallization behaviors of neat PEEK and PEEK/MWCNT nanocomposites. The ratio of the measured enthalpy of fusion to that of an ideal 100% crystalline PEEK (130 J/g) was used to calculate the degree of crystallinity.[9] The degree of crystallinity has been normalized by the weight fraction of PEEK for all nanocomposite samples. Each group has been tested for three times and the average value was reported with standard deviation.

3.2.4.6. Tensile test

True stress-true strain testing was used in this study. Tensile tests were conducted on a MTS Insight test fixture with a 30 kN load cell at a loading speed of 2.54 mm/min under ambient test conditions according to ASTM D638-08. A Cannon EOS Rebel T5i camera was used to take videos of the dog-bone shaped tensile bars (ASTM D638 Type V) during uniaxial stretching and

then the videos were analyzed using a digital image correlation software kindly provided by Correlated Solutions, Inc. The resulting true stress-true strain curve was used to calculate Young's modulus (E), ultimate tensile strength (σ_t) and tensile strain (ε_t). E was defined as the slope of the initial linear portion of the true stress-true strain curves. σ_t and ε_t were reported as the maximum true stress and the true strain at break, respectively. At least 5 specimens per sample were tested and their average values were reported.

3.2.4.7. DMA

Dynamic mechanical properties were measured using an ARES-G2 torsional rheometer (TA Instruments, Inc., DE). The dimensions of specimens were about 30 mm × 9 mm × 3 mm. The temperature ramp was conducted from 25 °C to 300 °C at a heating rate of 3 °C/min with a frequency of 1 Hz and a small strain of 0.1%, which is within the linear viscoelastic region.

3.2.4.8. CTE

CTE measurements were conducted using RSA-G2 (TA Instruments, Inc., DE). Thin specimens (30 mm × 4 mm × 0.2 mm) were heated from 30 °C to 200 °C with a ramping rate of 5 °C/min. A small constant tension stress of 50 mg/mm^2 was applied to keep the specimen in shape and measure the length change for the calculation of coefficient of linear thermal expansion using the following equation:

$$\alpha_L = \frac{1}{L}\frac{dL}{dT} \approx \frac{1}{L}\frac{\Delta L}{\Delta T}$$

Where α_L is the coefficient of linear thermal expansion; L is the length of specimen; ΔL is the length change of specimen within a temperature change of ΔT. In this work, length change measurements within two temperature ranges of 30 °C - 110 °C and 165 °C - 200 °C were used to calculate the α_L below and above T_g, respectively.

3.3. Results and discussion

3.3.1. MWCNT dispersion and morphology

TOM and TEM were both used to observe the dispersion states of PEEK/MWCNT nanocomposites at both micro and nano scales, respectively, to confirm that the good dispersion is truly representative of bulk samples. Representative TOM images of 1.5pCNT and 1.5oCNT are shown in Figure 3-1. No microscale aggregation of MWCNT could be found.

TEM images also show a good dispersion of MWCNT in the nanocomposites without any detectable agglomerations (Figure 3-2). The careful examination of TEM images also directly provides useful information regarding the outer diameter of MWCNT in the nanocomposites and the average outer diameter of MWCNT in the nanocomposites is found to be around 9 nm, which matches the value of outer diameter of MWCNT provided by the vendor (6-9 nm). This suggests that MWCNT are well dispersed in PEEK.

The TOM and TEM results strongly supports that a nearly homogeneous distribution of MWCNT in PEEK matrix has been achieved at both micro and nano scales. Such a good

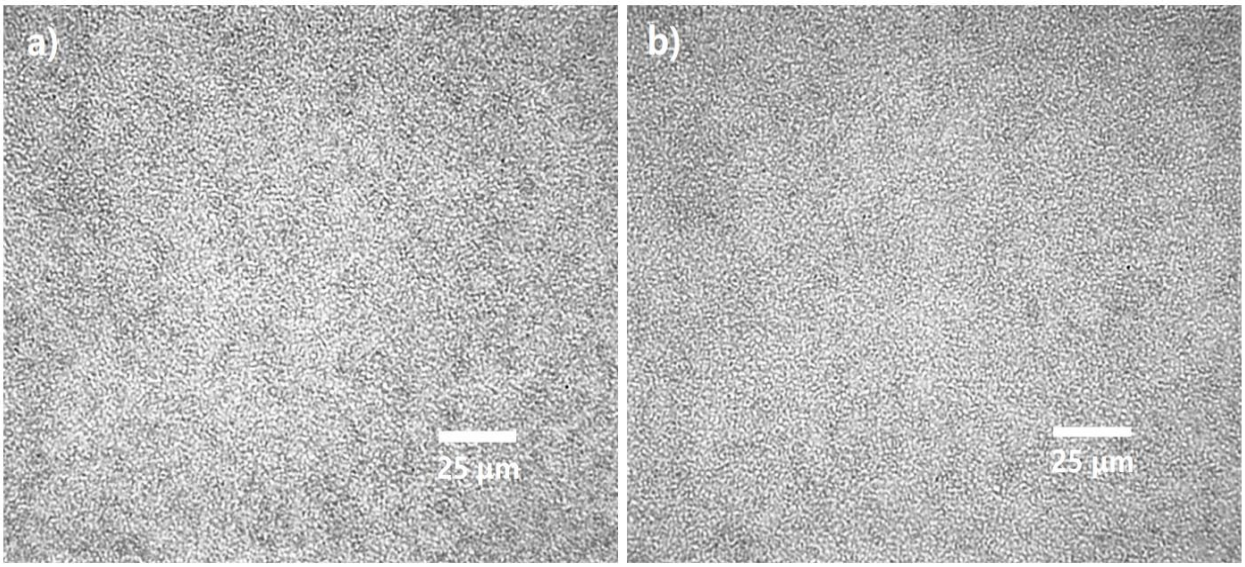

Figure 3-1 Representative TOM images of a) 1.5pCNT and b) 1.5oCNT.

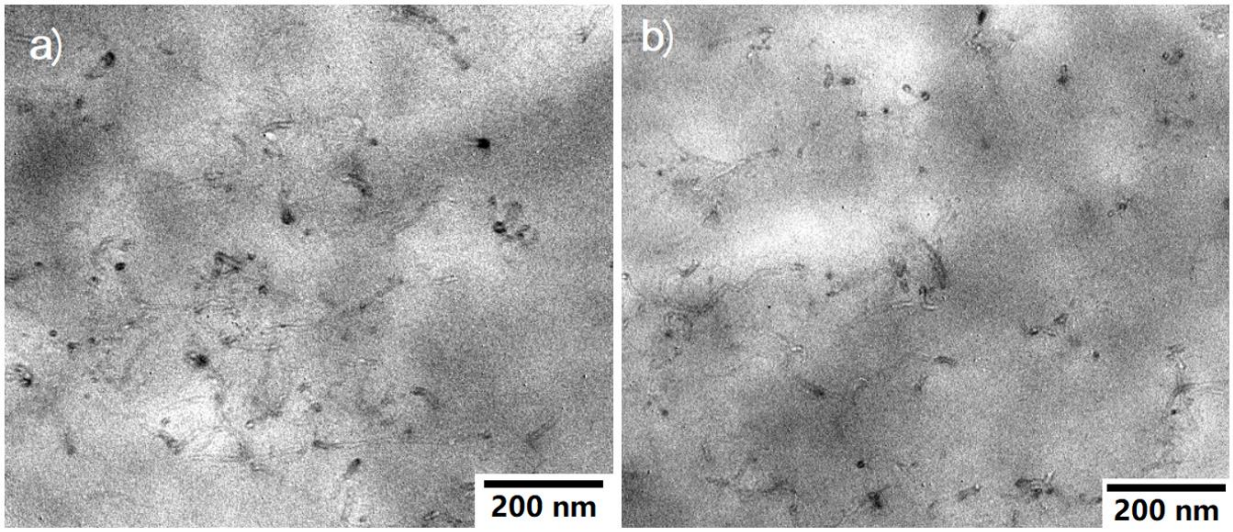

Figure 3-2 Representative TEM images of a) 1.5pCNT and b) 1.5oCNT.

dispersion in PEEK matrix is highly unusual and the cause(s) for such a good quality of dispersion will be discussed in detail later.

3.3.2. Thermal stability

The thermal stability was characterized by TGA. Figure 3-3 reveals that the thermal degradation behaviors of nanocomposites are almost the same with that of neat PEEK and the onset degradation temperatures (T_d) of nanocomposites are not affected Table 3-2. Therefore, addition of MWCNT does not affect their thermal stability. This is expected because this approach does not involve any modification of neat PEEK matrix and no significant mechanical forces were used during processing, minimizing the possibility of thermomechanical degradation. Therefore, the superior thermal stability of PEEK has been preserved and this is extremely important since PEEK is widely used for high temperature applications where an excellent thermal stability is demanded.

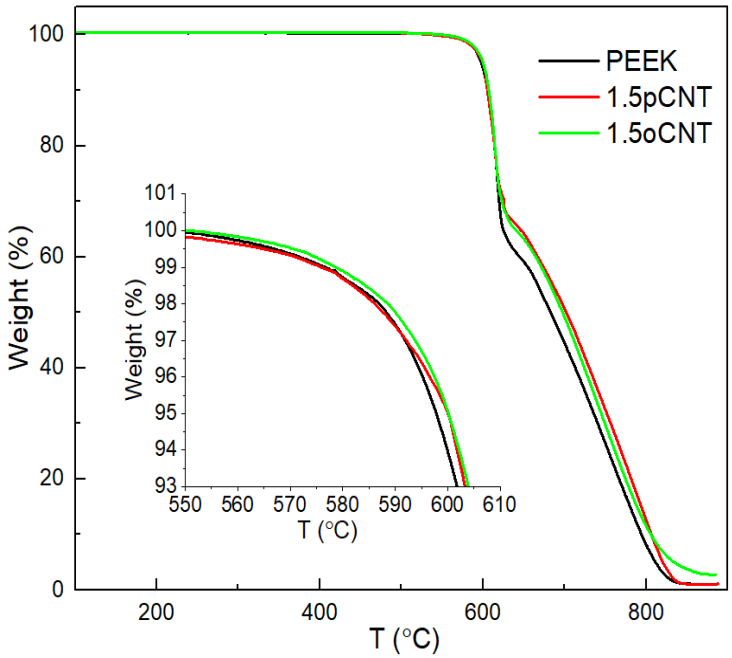

Figure 3-3 Representative TGA curves in air of neat PEEK, 1.5pCNT and 1.5oCNT. Inset shows the enlargement of onset degradation.

Table 3-2 Summary of onset degradation temperatures (T_d). T_d is defined as the degradation temperature at 3% weight loss.

Samples	T_d /°C
PEEK	591.9
0.5pCNT	591.7
1.0pCNT	592.4
1.5pCNT	592.1
0.5oCNT	592.5
1.0oCNT	592.0
1.5oCNT	593.8

3.3.3. Crystallinity and crystallization behaviors

The degrees of crystallinity of the injection molded PEEK/MWCNT nanocomposites are about 33% while that of the neat PEEK is about 37%. To normalize the influence of different

crystallinities on the mechanical properties, it is important to tune the crystallinities of neat PEEK and nanocomposites to be at the same level. Consequently, the PEEK nanocomposites were annealed at 260 °C for 1h to reach the same level of crystallinity with unannealed PEEK before mechanical testing. The first heating scans of DSC are presented in supporting information (Figure 3-4) and were used to calculate the degrees of crystallinity (Table 3-3). Upon annealing, the degrees of crystallinity of PEEK/MWCNT nanocomposites are increased to about 37%, similar with that of unannealed neat PEEK but still lower than that of annealed PEEK ($X_c \approx 40\%$). Among the nanocomposites, the crystallinity appears to be unaffected by the MWCNT loadings. The peak melting temperatures (T_m) of the nanocomposites are around 340 °C, also lower than that of the neat PEEK (T_m=345 °C).

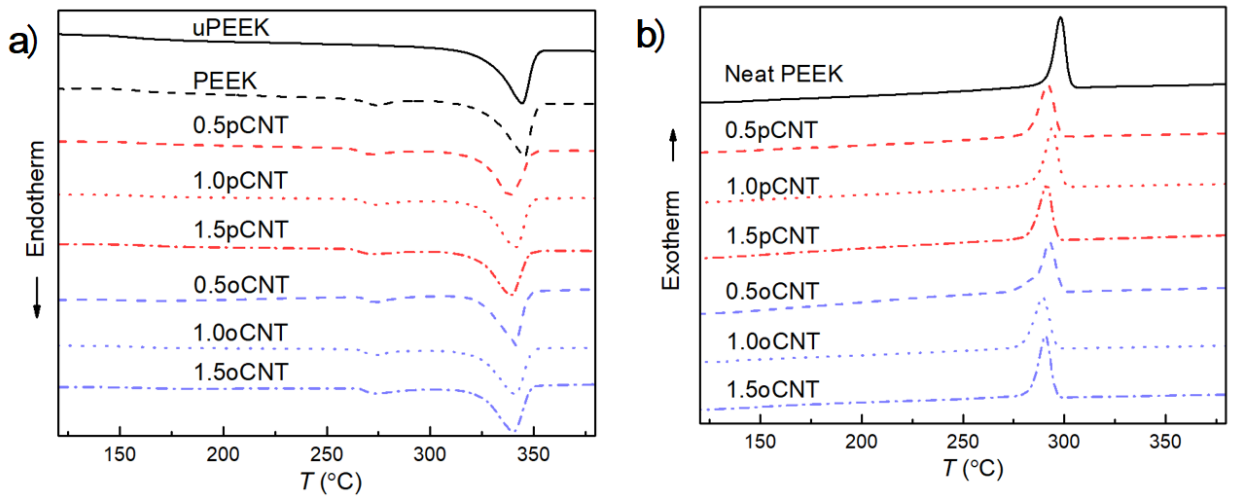

Figure 3-4 a) first heating DSC scan and b) first cooling DSC scan of neat PEEK and nanocomposites.

Table 3-3 Peak melting temperature (T_m), peak crystallization temperature (T_c), onset of crystallization (T_o) and degree of crystallinity (X_c).

Samples	1st heating scan		1st cooling scan		
	T_m /°C	$X_{c,\ normalized}$/%	T_o /°C	T_c /°C	$X_{c,\ normalized}$/%
uPEEK	345 ± 1	37.4 ± 0.2	306 ± 1	298 ± 1	40.0 ± 0.2
PEEK	345 ± 1	40.0 ± 0.2	306 ± 1	297 ± 1	40.2 ± 0.3
0.5pCNT	339 ± 2	37.5 ± 0.3	301 ± 1	292 ± 1	37.4 ± 0.1
1.0pCNT	341 ± 1	37.2 ± 0.2	302 ± 2	293 ± 1	37.6 ± 0.2
1.5pCNT	340 ± 1	36.9 ± 0.1	300 ± 2	292 ± 1	37.1 ± 0.3
0.5oCNT	341 ± 1	36.8 ± 0.2	301 ± 1	292 ± 2	37.8 ± 0.3
1.0oCNT	341 ± 1	36.9 ± 0.1	298 ± 1	289 ± 1	37.7 ± 0.2
1.5oCNT	340 ± 1	37.4 ± 0.2	298 ± 2	291 ± 1	37.2 ± 0.2

To further investigate the crystallization behavior in detail and to explain why different crystallinities are observed, the non-isothermal crystallization behaviors of neat PEEK and PEEK/MWCNT nanocomposites were studied using DSC (Figure 3-4). It should be noted that the incorporation of MWCNT may impact polymer crystallization differently. On one hand, MWCNT surfaces may act as heterogeneous nucleation sites and facilitate PEEK crystallization.[83] On the other hand, the incorporation of MWCNT may hinder molecular mobility significantly and limit the ability of polymer chains to participate in crystal growth, thus impeding PEEK crystallization.[68] How the presence of MWCNT would influence the crystallization of PEEK depends on the relative effectiveness of these two competing factors. In the present work, the addition of MWCNT decreases both the peak crystallization temperature (T_c) and the degree of crystallinity (X_c), compared to the neat PEEK. Apparently, the confinement effect of MWCNT on PEEK crystallization plays a predominant role here, resulting in the decrease of X_c and T_c.[68] Since the MWCNT dispersion in PEEK is good, it is not surprising that the well-dispersed MWCNT can restrict PEEK chain mobility, thus hindering the crystallization of PEEK and causing X_c and T_c to decrease.[68, 84, 85] To account for the unusual

decrease of X_c and T_c observed in PEEK/MWCNT nanocomposites above, a separate control experiment was carried out on PEEK directly mixed with p-MWCNT in methanol. This control system showed a poor dispersion of MWCNT in PEEK (Figure 3-5). A subsequent DSC study shows a higher T_c than that of neat PEEK, indicating that the MWCNT used in the poorly dispersed PEEK can act as a nucleating agent (Figure 3-5). In contrast, when the dispersion of MWCNT becomes good, which is our case, these well dispersed MWCNT will impose significant confinement on PEEK chain mobility to impede PEEK crystallization.

It is noted that the T_c and X_c of PEEK/MWCNT nanocomposites appear to be independent of MWCNT loadings (Table 3-3).[74, 75] This can be attributed to the good dispersion states of MWCNT among all MWCNT loadings investigated in this work. The diffusion of PEEK polymer chains has already been significantly restricted even at a relatively low MWCNT loading of 0.5 wt.% since MWCNT are almost individually dispersed in PEEK. And since the individual dispersion of MWCNT has been achieved and polymer chain diffusion has already been impeded significantly to a critical extent, further addition of more MWCNT (1.0 wt.% and

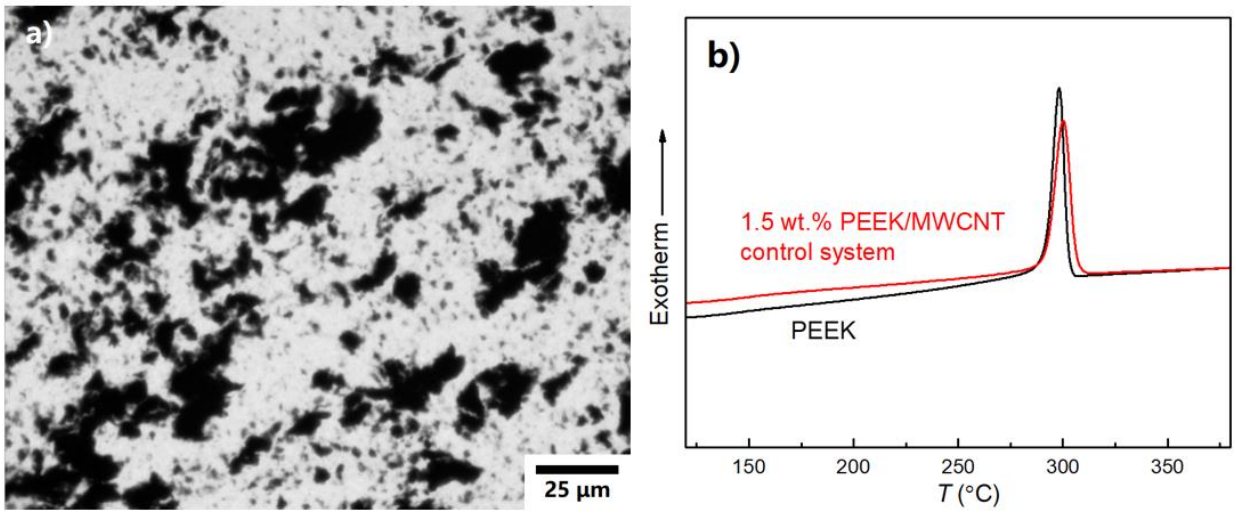

Figure 3-5 a) TOM image and b) DSC cooling scan of 1.5 wt.% PEEK/MWCNT composites prepared from solvent mixing in methanol;

1.5 wt.%) may contribute little to additional confinement effect. Therefore, the addition of well-dispersed MWCNT will decrease both the T_c and X_c of PEEK due to confinement effect while the T_c and X_c of PEEK/MWCNT nanocomposites appear to be independent of MWCNT loadings due to good dispersion of MWCNT.

3.3.4. Dynamic mechanical behavior

Dynamic mechanical properties of neat PEEK and PEEK/MWCNT nanocomposites are investigated (Figure 3-6). It shows that annealing and addition of MWCNT increases the modulus in both glassy and rubbery states. A careful examination of the storage moduli (G') at 30 °C and 230 °C, respectively, shows that with the same level of crystallinity (X_c~37%), addition of 1.5 wt.% MWCNT into PEEK would increase the $G'_{30\,°C}$ by 28% from 1.22 GPa to 1.57 GPa (Table 3-4). While the $G'_{230\,°C}$ shows an increase by nearly 70% with addition of 1.5 wt.% MWCNT. The reason why the increase in storage modulus is more pronounced in the rubbery state can be attributed to the high mobility of the polymer chains above T_g that would be restricted by the presence of MWCNT more significantly. However, in the glassy state, polymer

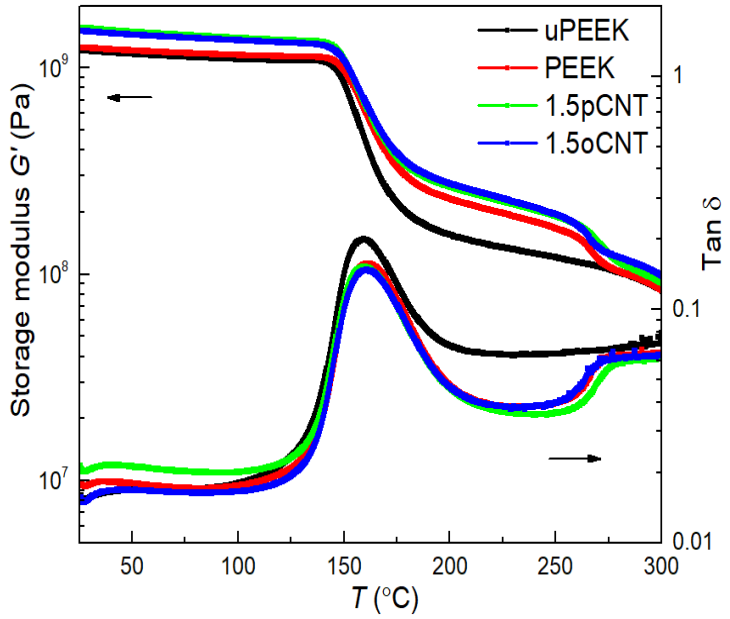

Figure 3-6 Representative storage modulus, G', and tan δ of neat PEEK and nanocomposites.

chains are already immobilized; the addition of MWCNT would only have limited impact on affecting molecular mobility of PEEK chains. There is a slight increase of T_g of neat PEEK due to annealing. However, if all annealed, the PEEK T_g appears to be unaffected by the incorporation of MWCNT (Table 3-4).

Table 3-4 Summary of T_g and storage modulus at 30 °C and 230 °C, respectively. The peak of tan δ is regarded as T_g.

Samples	T_g **/°C**	$G'_{30\,°C}$ **/×10^{9}Pa**	$G'_{230\,°C}$ **/×10^{8}Pa**
uPEEK	158.9	1.22	1.33
PEEK	160.3	1.26	1.90
0.5pCNT	160.6	1.40	1.98
1.0pCNT	160.1	1.50	2.02
1.5pCNT	159.2	1.57	2.21
0.5oCNT	161.7	1.42	2.04
1.0oCNT	160.2	1.50	2.15
1.5oCNT	160.2	1.55	2.25

3.3.5. Tensile Properties

The tensile properties of PEEK are known to be affected by its crystallinity. Thus, to unambiguously determine the effect of MWCNT on the tensile properties of PEEK, PEEK/MWCNT nanocomposites were annealed to reach the same crystallinity as the unannealed neat PEEK. The representative true stress-true strain curves of neat PEEK and PEEK/MWCNT nanocomposites are plotted in Figure 3-7 and their tensile properties are summarized in Table 3-5. At the same level of crystallinity ($X_c \approx 37\%$), the Young's modulus will increase by 22% from 3.7 GPa for neat PEEK to 4.5 GPa for the PEEK/MWCNT nanocomposite containing 1.5 wt.% of MWCNT. Annealing will increase the crystallinity of neat PEEK and thus the Young's modulus, but the modulus of annealed PEEK is still lower than those with the MWCNT

reinforcement. Although the incorporation of MWCNT hinders the crystallization of PEEK and causes a lower crystallinity, it still results in a higher modulus upon the addition of MWCNT with good dispersion.

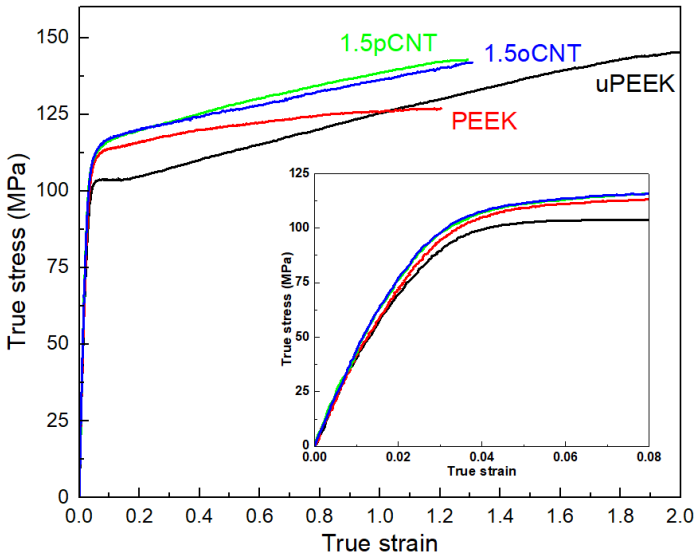

Figure 3-7 Representative true stress - true strain plots of PEEK and nanocomposites. Inserted one is the enlargement of the initial stage

Table 3-5 Summary of true stress true strain properties of neat PEEK and nanocomposites and their crystallinities. E is Young's Modulus, σ_t is tensile strength and ε_t is true strain at break.

Samples	$X_{c,\ normalized}$	E **/GPa**	σ_t **/MPa**	ε_t
uPEEK	37.5%	3.7 ± 0.1	153 ± 15	2.53 ± 0.24
PEEK	40.1%	4.1 ± 0.1	137 ± 19	1.43 ± 0.15
0.5pCNT	37.6%	4.2 ± 0.1	149 ± 15	1.42 ± 0.18
1.0pCNT	37.2%	4.3 ± 0.1	143 ± 14	1.34 ± 0.19
1.5pCNT	36.8%	4.5 ± 0.1	147 ± 11	1.42 ± 0.15
0.5oCNT	36.6%	4.3 ± 0.1	144 ± 13	1.40 ± 0.16
1.0oCNT	36.9%	4.4 ± 0.1	142 ± 15	1.29 ± 0.14
1.5oCNT	37.5%	4.5 ± 0.1	141 ± 10	1.06 ± 0.20

It has been reported that annealing will increase the modulus and yielding stress but decrease the true tensile strength of PEEK.[86] Similarly here, the unannealed PEEK exhibits a

much higher true tensile strength than that of annealed PEEK. This may be due to the embrittlement resulting from the annealing process. However, if all annealed, PEEK/MWCNT nanocomposites exhibit slightly higher true tensile strengths compared to that of PEEK (Table 3-5). The true tensile strengths of PEEK/MWCNT nanocomposites with different MWCNT loadings appear to be similar to each other considering the standard deviations. It should be noted that the tensile strength is highly correlated to the defects present in the test specimen.

For a comprehensive understanding of the tensile failure behaviors of PEEK/MWCNT nanocomposites, the fracture surfaces of tensile specimens were investigated by SEM. Figure 3-8 shows the typical fractographs of neat PEEK and PEEK/MWCNT nanocomposites from micro to nano scale. Across both length scales, no obvious agglomerations of MWCNT can be found, further confirming the good dispersion of MWCNT in PEEK matrix. Both neat PEEK and PEEK/MWCNT nanocomposites show similar tensile fracture characteristics. Figure 3-8 shows wide-spread micro-scale patches on the tensile fracture surfaces, suggesting lacking of large critical defect to cause premature fracture. Further investigation of PEEK/MWCNT nanocomposites under higher magnification shows that MWCNT are well dispersed in the PEEK matrix with short ends of MWCNT homogeneously distributed . It also reveals that most MWCNT are well correlated with PEEK patches with some MWCNT having their short ends exposed. And the exposed MWCNT ends are very short in length, suggesting that the fracture of MWCNT is likely to have occurred. Meanwhile, no obvious pull-out of MWCNT is found, indicating that a strong interfacial adhesion between MWCNT and PEEK matrix has been achieved. This is unexpected since there is no covalent bonding between PEEK and MWCNT in this work and the interfacial interaction between PEEK and MWCNT was claimed to be weak according to some literature.[87, 88] However, our finding suggests that PEEK and MWCNT have

certain affinity to each other. This may be attributed to the π-π interaction between PEEK and MWCNT.[89, 90]

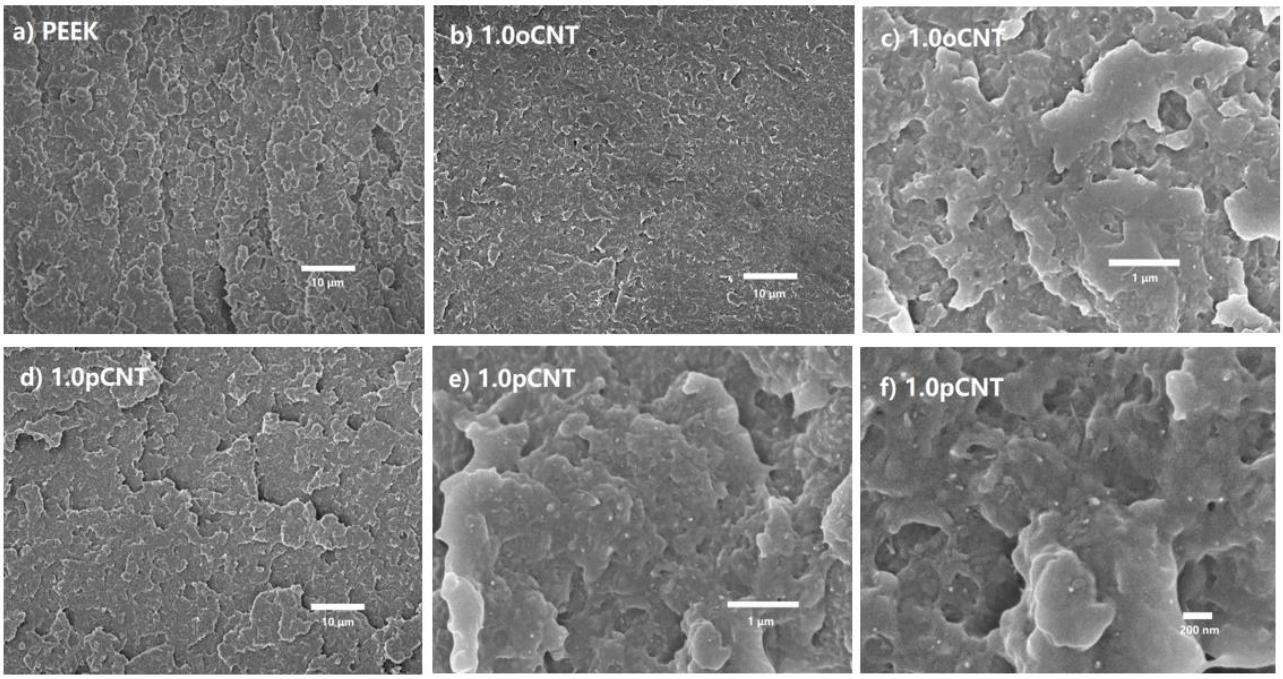

Figure 3-8 Representative SEM images of tensile fracture surfaces: neat PEEK (a), 1.0oCNT (b, c) and1.0pCNT (d-f).

3.3.6. CTE

Besides thermal and tensile properties, CTE is another important material parameter, especially for structural applications where dimensional stability is critical upon exposure to large temperature changes. The linear expansion as a function of temperature is plotted in Figure 3-9 and slopes of curves at 30 °C – 110 °C and 165 °C – 200 °C are used to calculate α_L below and above T_g, respectively (Table 3-6). Annealing appears to affect little on the CTE of neat PEEK below T_g while it can reduce CTE of neat PEEK by 10% at $T > T_g$. Compared to neat PEEK, nanocomposites exhibit moderate reductions (< 7%) of CTE below T_g. Above T_g, addition of MWCNT may contribute to a reduction of CTE by as high as 28% at only 1.5 wt.% loading. This is important because many PEEK components are machined at room temperature

but used at high temperatures, which may induce significant thermal stress and cause premature failure. A reduction of CTE at both moderate and high temperatures is beneficial to its applications across a wide temperature range.

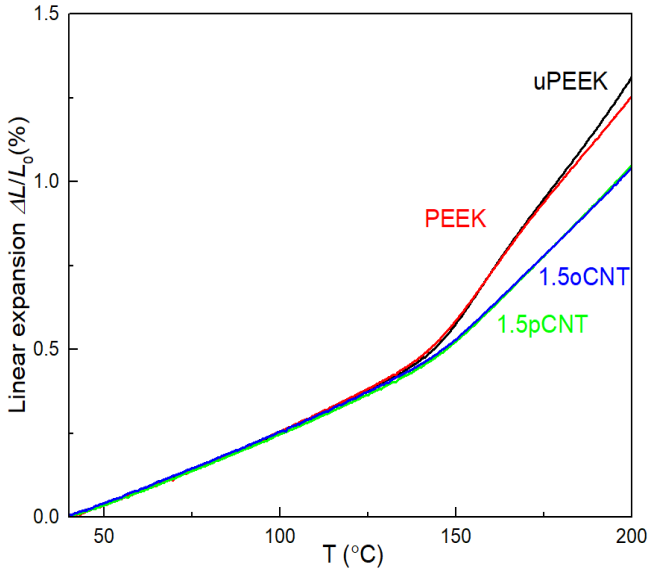

Figure 3-9 Representative linear thermal expansion of PEEK, 1.5pCNT and 1.5oCNT.

Table 3-6 Coefficients of linear thermal expansion below and above T_g.

Samples	α_L /(ppm/°C) (30-110 °C)	α_L /(ppm/°C) (165-200
uPEEK	48.9 ± 0.3	142.9 ± 0.4
PEEK	48.7 ± 0.2	130.6 ± 0.5
0.5pCNT	48.3 ± 0.1	114.7 ± 0.2
1.0pCNT	47.5 ± 0.2	112.8 ± 0.1
1.5pCNT	45.5 ± 0.1	106.8 ± 0.2
0.5oCNT	48.6 ± 0.2	113.3 ± 0.2
1.0oCNT	47.6 ± 0.1	112.7 ± 0.1
1.5oCNT	45.6 ± 0.2	103.5 ± 0.2

3.3.7. Dispersion mechanism

It is surprising that by simply mixing PEEK/DCA and MWCNT/NMP solutions together, a good dispersion of MWCNT in PEEK can be easily achieved after removal of solvents. To explain this phenomenon, a PEEK wrapping of MWCNT mechanism is proposed (Figure 3-10). Before mixing, PEEK is dissolved in DCA solvent as polymer coils at room temperature.[80, 81] And MWCNT are well dispersed in NMP.[91] It is hypothesized that when mixed with PEEK/DCA solution, the individually dispersed MWCNT will immediately encounter and interact with PEEK polymer coils, allowing them to wrap around each other. Meanwhile, the solvent mixture of DCA and NMP becomes a poor solvent for PEEK/MWCNT and causes the nanocomposite to precipitate out. It should be noted that the choice of solvent for the initial dispersion of MWCNT is critical as it determines how well MWCNT will be dispersed and wrapped by PEEK. If MWCNT are agglomerated in the solvent at the beginning and mixed with PEEK/DCA, then PEEK coils will wrap around these MWCNT aggregates, making it difficult for subsequent redispersion of MWCNT in PEEK after solvent removal. Therefore, NMP solvent

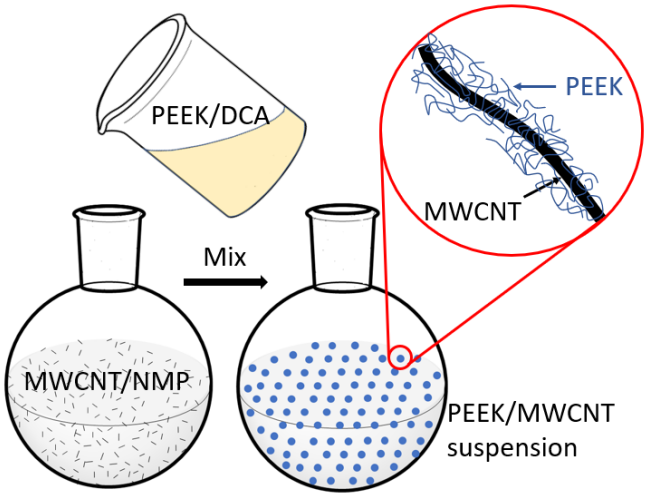

Figure 3-10 A schematic of PEEK wrapping of MWCNT mechanism.

was chosen in this work for dispersing MWCNT to ensure its good dispersion before mixing it with PEEK/DCA.[91]

Note that using solution approaches to prepare PEEK/MWCNT nanocomposites is still a challenge since it requires a suitable solvent capable of well-dispersing MWCNT and dissolving PEEK without destroying their chemical structure. That is why the solution approach for preparation of successful PEEK nanocomposites has rarely been reported.[92] To our best knowledge, the present work has demonstrated a simple but efficient solution mixing approach to prepare PEEK/MWCNT nanocomposites with good dispersion for the first time. This approach results in such a good dispersion of MWCNT in PEEK, contributing to a much higher effectiveness on Young's modulus reinforcement at low MWCNT loadings. The excellent thermal stability and the greatly reduced CTE make the PEEK/MWCNT nanocomposites prepared in the present work attractive to many applications, especially at high temperatures. It should be noted that the approach described in this study has achieved a success of good dispersion of MWCNT in PEEK up to 1.5 wt.% loading. Agglomeration of MWCNT would appear when a higher concentration of MWCNT is incorporated. Future work will focus on refining preparation of well-dispersed PEEK/MWCNT nanocomposites at higher MWCNT loadings.

3.4. Conclusion

PEEK/MWCNT nanocomposites are prepared through simple mixing of PEEK/DCA and MWCNT/NMP solutions. The dispersion states have been extensively characterized by TOM, TEM and SEM at micro and nano scales to support that a uniform distribution and individual dispersion of MWCNT have been achieved. The homogeneous dispersion of individual

MWCNT in the PEEK matrix is achieved *via* PEEK wrapping of MWCNT. Although well-dispersed MWCNT impede the crystallization of PEEK and decrease the T_c and X_c due to the confinement effect, it still shows much higher Young's modulus reinforcement effect. This is mainly attributed to the good dispersion of MWCNT and sufficiently strong interfacial interaction between PEEK and MWCNT, with retained thermal stability. Furthermore, at $T > T_g$, CTE shows a reduction of 28% while the storage modulus ($G'_{230\,°C}$) shows an increase of ~70%, which are important for high temperature applications of PEEK. It is believed that the solution mixing approach presented in this work is scalable for fabricating well-dispersed PEEK/MWCNT nanocomposites. A similar strategy may also be applicable to prepare other well-dispersed polymer nanocomposite systems.

This chapter described a novel and easy solution mixing approach to achieve good dispersion of MWCNT in PEEK. However, the mechanical reinforcement, though quite efficient, is not very high due to low loadings of MWCNT. Therefore, to achieve mechanical properties, more MWCNT should be added to reinforce PEEK while maintain their good dispersion state. In the next chapter, a modification based on this novel solution mixing approach will be applied to help prepare a high concentration PEEK/MWCNT system.

4. HIGH CONCENTRATION PEEK/MWCNT NANOCOMPOSITE SYSTEM

4.1. Introduction

High-performance semicrystalline poly(ether-ether-ketone) (PEEK) has excellent mechanical properties, thermal stability, and chemical resistance, enabling its applications in a very broad range of engineering fields. One example is using it to make downhole back-up seals since in the aggressive downhole environment, seals made of elastomers or fluoropolymers will lose their mechanical integrity while semicrystalline PEEK can still maintain acceptable mechanical properties at high temperature.[38, 40] Mechanical reinforcement of PEEK can help expand its applications not only in the oil and gas industry but also in other high-end markets like the biomedical field. For instance, to be used as orthopedic implants, the Young's modulus of the implant needs to match that of human bone (10-20 GPa).[13] However, neat PEEK resin possesses a Young's modulus of 3.7 GPa, failing to meet this requirement. Therefore, mechanical reinforcement of PEEK is very critical for the value-addition of PEEK-based materials and for the expansion of PEEK's applications in many high-end markets.

Our previous work presented a novel solution mixing approach to prepare well-dispersed PEEK/MWCNT nanocomposites.[7] These nanocomposites appear to be highly efficient in the mechanical reinforcement of PEEK. With addition of only 1.5 wt.% MWCNT, the Young's modulus can be increased by 22% from 3.7 GPa to 4.5 GPa. Such an improvement is attributed to the good dispersion state of MWCNT in PEEK matrix and the adequately strong interaction between MWCNT and PEEK *via* π-π interaction. Through this novel approach, MWCNT can be individually dispersed and uniformly distributed in the PEEK matrix. Though the morphological and mechanical properties are very encouraging, this approach was only able to achieve a

loading of 1.5 wt.% MWCNT at that time. While obvious aggregations of MWCNT can be observed when it goes to higher concentrations.

In this chapter, a modification of the previous solution mixing approach is proposed and utilized to prepare well-dispersed PEEK/MWCNT nanocomposite with a higher MWCNT loading (10 wt.%). From the morphological aspect, the 10 wt.% PEEK/MWCNT nanocomposite exhibits a good distribution and dispersion of MWCNT in the PEEK matrix. The consequent modulus enhancement appears to be highly effective. In addition to the morphological and mechanical investigations, its thermal stability, thermal expansion, and crystallization behaviors will also be studied.

4.2. Experimental

4.2.1. Materials

All raw materials remain the same with those used in the section 3.2.1.

4.2.2. Preparation of nanocomposites

Only o-MWCNT is used here to prepare the 10 wt.% PEEK/o-MWCNT nanocomposite. Procedures are the same with section 3.2.2 and 3.2.3 while the major difference is that solution concentrations are different. In current case, PEEK/DCA (0.15 wt.%, 100g) and o-MWCNT/NMP solution (0.25 mg/mL, 64 mL) solutions were used to prepare the high concentration nanocomposite. Solution concentrations are more diluted than those in low concentration nanocomposite preparation process. All other processing conditions are kept the same with section 3.2.2. And following the naming rule in Table 3-1, this 10 wt.% PEEK/o-MWCNT nanocomposite annealed at 260 ℃ for 1 hour is named “10oCNT”.

4.2.3. Characterization

All characterization methods remain the same with section 3.2.4 and will not be repeated here.

4.3. Results and discussion

4.3.1. Dispersion

Dispersion state of the nanocomposite was evaluated using TEM, shown in Figure 4-1. Figure 1a shows no obvious agglomerations of MWCNT at microscale. And MWCNT are evenly distributed in the PEEK matrix. A further investigation at a higher magnification confirms the homogeneous dispersion of MWCNT at nanoscale (Figure 4-1). The outer diamaters of MWCNT can be clearly measured and they are all smaller than 10 nm. This suggests that MWCNT are individually dispersed since the measured value of outer diameter of MWCNT matches that provided by the vendor (6-9 nm).

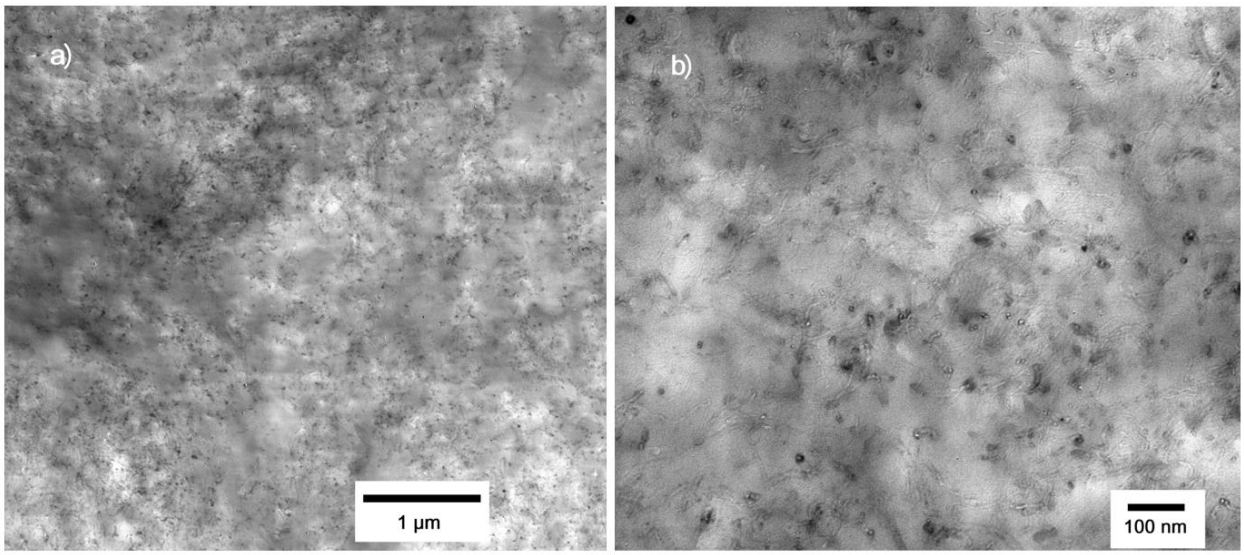

Figure 4-1 Representative TEM images of 10oCNT at micro and nano scales.

TEM results strongly confirm a uniform distribution and individual dispersion of MWCNT in PEEK matrix at micro and nano scales, respectively. A combination of micro- and

nano-scale investigation on the morphology is very critical as it can provide more inclusive information about the dispersion state from a more comprehensive perspective.

4.3.2. Thermal stability

Thermal stability is one of the most important properties as PEEK-based materials are used at high temperature in many applications. On the other hand, the processing temperature of PEEK sometimes can be as high as about 400 ℃, also requiring it to be quite thermally stable. TGA result suggests that the thermal stability of 10oCNT is slightly reduced due to the thermal degradtion of o-MWCNT (Figure 4-2). However, it should be noted that below 400 ℃, a common processing temperature for PEEK, the weight loss of nanocomposite is still negligible. Therefore, the thermal stability of PEEK/MWCNT is still retained and other characterizations that will be discussed later also proves that this negligible weight loss imposes little influence on their mechanical properties.

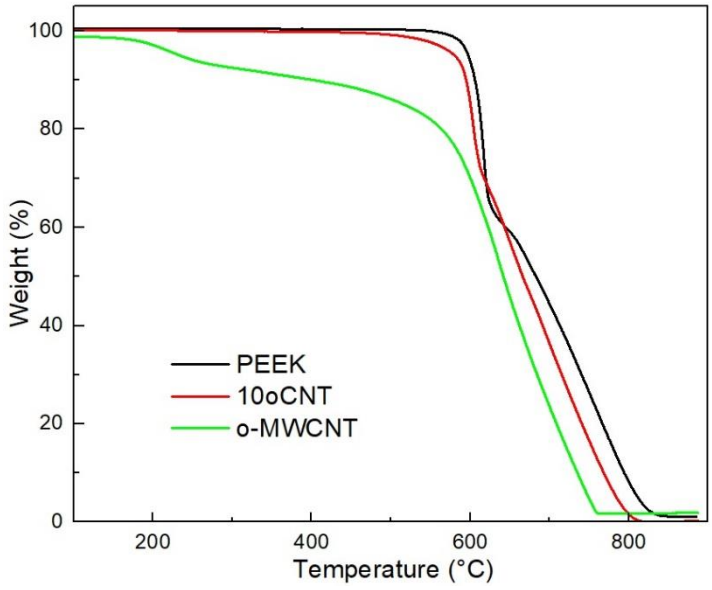

Figure 4-2 TGA plots in air of neat PEEK, o-MWCNT and 10oCNT.

4.3.3. Crystallinity and crystallization behaviors

The nanocomposite was annealed at 260 to ℃ for 1 hour to maximize its crystallinity. After annealing and normalization by the loading of MWCNT, the degree of crystallinity of PEEK component is about 37.9%, similar with that of unannealed PEEK ($X_c \approx 37.4\%$) but still lower than that of annealed PEEK ($X_c \approx 40\%$).

The non-isothermal crystallization behaviors of neat PEEK and PEEK/MWCNT nanocomposite were also studied. Similar with our previous results (section 3.3.3), the addition of 10 wt.% MWCNT decreases both the peak crystallization temperature (T_c) and the degree of crystallinity (X_c), compared to the neat PEEK. It can be mainly attributed to the predominant confinement effect of well-dispersed MWCNT.

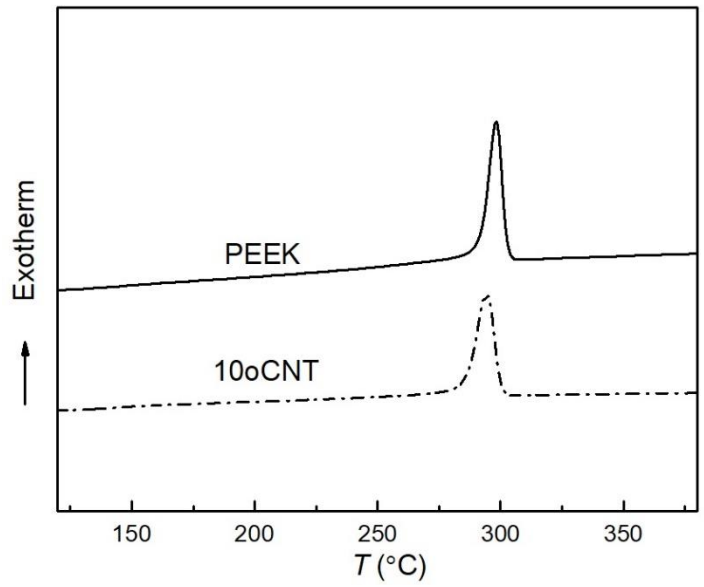

Figure 4-3 DSC cooling scans of neat PEEK and 10oCNT.

Table 4-1 Peak melting temperature (T_m), peak crystallization temperature (T_c), onset of crystallization (T_o) and degree of crystallinity (X_c).

Samples	1st heating scan		1st cooling scan		
	T_m /°C	$X_{c,\ normalized}$/%	T_o /°C	T_c /°C	$X_{c,\ normalized}$/%
uPEEK	345 ± 1	37.4 ± 0.2	306 ± 1	298 ± 1	40.0 ± 0.2
PEEK	345 ± 1	40.0 ± 0.2	306 ± 1	297 ± 1	40.2 ± 0.3
10oCNT	344 ± 1	37.9 ± 0.3	303 ± 2	293 ± 1	37.3 ± 0.2

4.3.4. Tensile properties

True stress-true strain plots were presented in Figure 4-4 and Table 4-2. The most notable one is that 10oCNT nanocomposite exhibits a much higher Young's modulus than that of neat PEEK. Its Young's modulus is increased from 3.7 GPa to 7.3 GPa, almost doubled. On the other hand, it is not surprising that PEEK/MWCNT nanocomposite becomes much more brittle with addition of 10 wt.% MWCNT. Its elongation to break is only about 0.1, much shorter than that of neat PEEK.

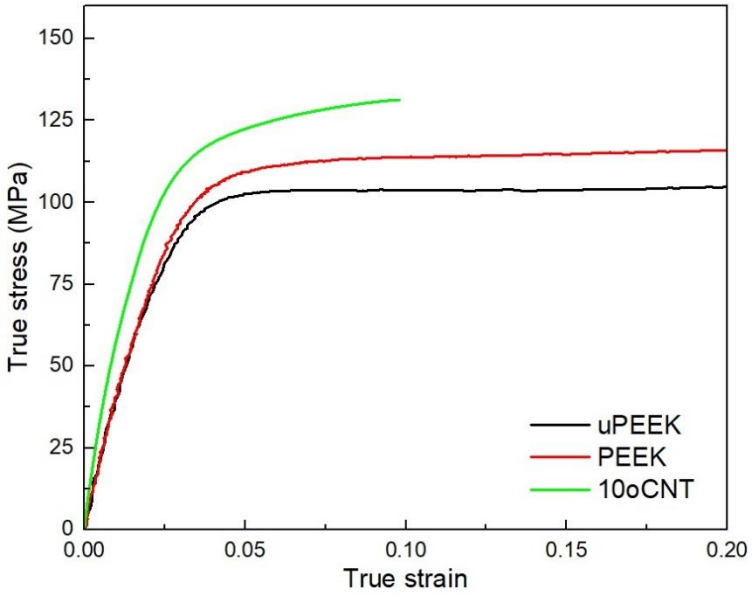

Figure 4-4 True stress-true strain plots of annealed and annealed PEEK and 10oCNT.

Table 4-2 Summary of true stress true strain properties.

Samples	$X_{c,\ normalized}$	E /GPa	σ_t /MPa	ε_t
uPEEK	37.5%	3.7 ± 0.1	153 ± 15	2.53 ± 0.24
PEEK	40.1%	4.1 ± 0.1	137 ± 19	1.43 ± 0.15
10oCNT	37.9%	7.3 ± 0.4	131 ± 12	0.098 ± 0.012

The fracture surfaces of failed tensile specimens were also analyzed (Figure 4-5). No large critical defects that could cause premature fracture can be observed. And an investigation of the fracture surface at a high magnification further confirms the individual dispersion of MWCNT in PEEK matrix. It is notable that no obvious holes or pull-out of MWCNT can be observed. And many short ends of MWCNT are presented on the fracture surface, indicating that fracture of MWCNT is likely to occur, rather than pulling out of MWCNT. This further suggests that the interfacial interaction between MWCNT and PEEK is adequately strong, consistent with our previous results.[7] The origin of this strong interaction between MWCNT and PEEK may come from the π-π interaction as both MWCNT surfaces and PEEK polymer backbones have abundant aromatic structures.

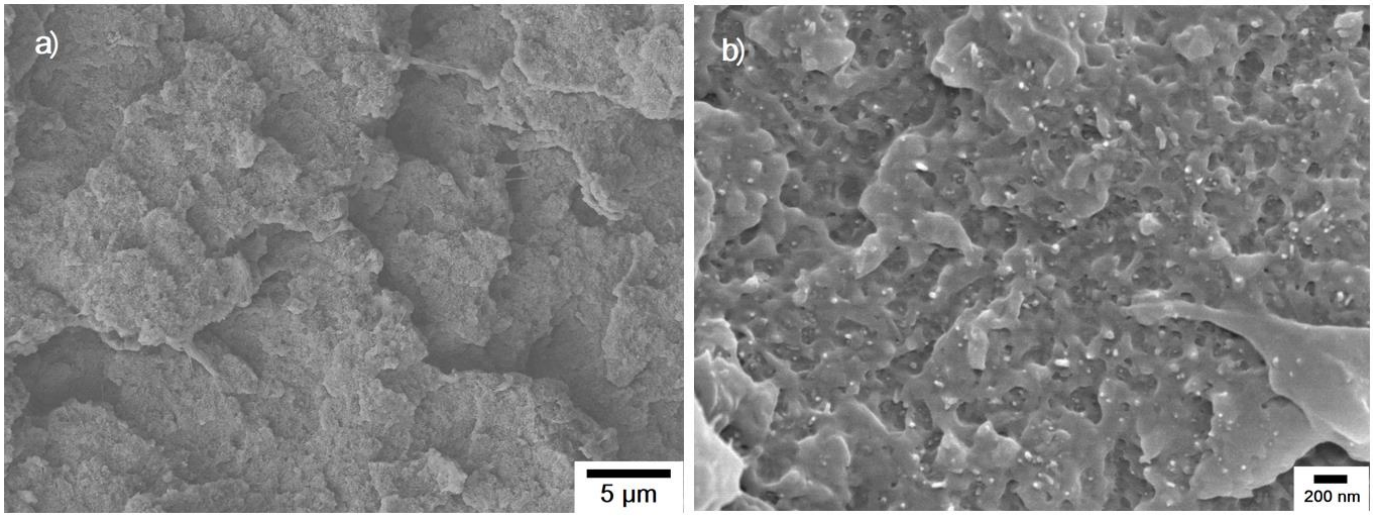

Figure 4-5 Typical SEM images of tensile fracture surfaces of 10oCNT.

PEEK/MWCNT nanocomposites have been extensively studied by many researchers so far.[67, 73, 93-97] To compare the effectiveness on mechanical properties reinforcement of this work and other researchers' findings, the increase of Young's modulus with MWCNT loadings normalized by that of neat PEEK was summarized and visualized in Figure 4-6. The details of the different sample preparation methods are provided in Table 4-3. It can be seen that the PEEK/MWCNT nanocomposites prepared by this novel solution mixing approach shows a much higher effectiveness on Young's modulus reinforcement. It has been reported that MWCNT dispersion state and interfacial bonding between PEEK and MWCNT can influence Young's modulus substantially.[98, 99] This highly efficient modulus enhancement is mainly attributed to the homogeneous distribution of individually dispersed MWCNT in PEEK, as evidenced by TOM, TEM and SEM at both micro and nano scales, and adequately strong interfacial adhesion between PEEK and MWCNT, which is supported by the absence of pull-out of MWCNT.

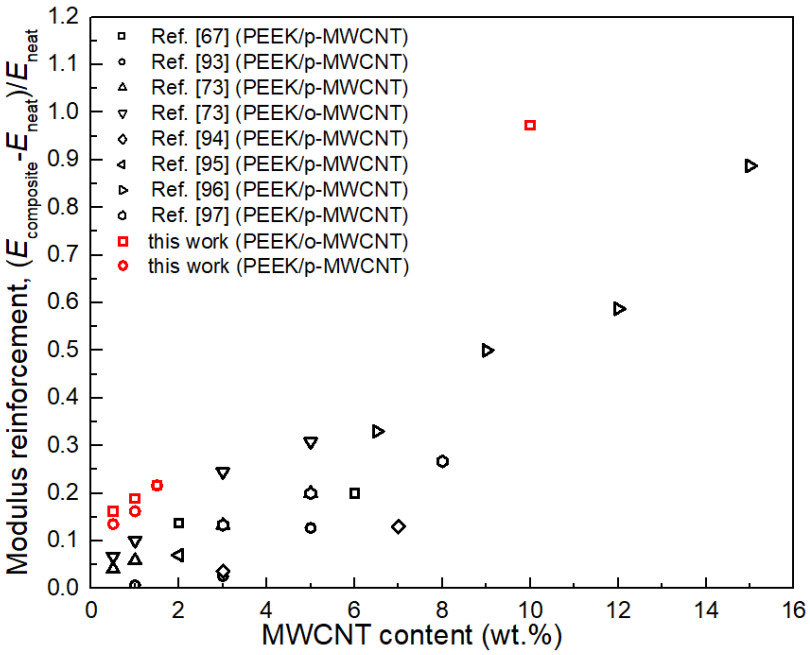

Figure 4-6 Comparison of effectiveness on modulus reinforcement of PEEK by adding various amounts of MWCNTs from results of various researchers.

Table 4-3 Materials and details of PEEK/MWCNT composites preparation.

Reference	PEEK Grade	MWCNT characteristics	Interfacial modification	Mixing approach	Processing	Dispersion quality
This work	Victrex 150G	Grade: SWeNT SMW 100; Length=5 μm; O.D.=6-9 nm.	PEEK/p-MWCNT PEEK/o-MWCNT	Solution mixing	Injection molding	Good (OM, TEM, SEM)
Ref. [67]	Victrex 151G	Grade: Nanocyl-7000; Length=1.5 μm; O.D.=9.5 nm.	PEEK/p-MWCNT	Melt blending	Injection molding	Moderate; small agglomeration (SEM and TEM)
Ref. [93]	Evonik 2000P	Grade: Graphistrength C100; Length=0.1-10 μm; O.D.=10-15 nm.	PEEK/p-MWCNT	Melt blending	Injection molding	Not provided
Ref. [93]	Jilin Univ. PEEK	Length=10-30 μm; O.D.=10-20 nm.	PEEK/p-MWCNT PEEK/o-MWCNT	Solution premixing and Melt blending	Injection molding	o-CNT good dispersion; p-CNT agglomeration (SEM)
Ref. [94]	Jilin Univ. PEEK	Length=10-30 μm; O.D.=10-20 nm.	PEEK/PES/MWCNT	Powder premixing and melt blending	Injection molding	Moderate (SEM)
Ref. [95]	Evonik 2000P	Graphistrength C100;	PEEK/p-MWCNT	Melt blending	Injection molding	Moderate (SEM)
Ref. [96]	Victrex 151G	Length=a few micrometer; O.D.=20-100 nm.	PEEK/p-MWCNT	Melt blending	Injection molding	Moderate (SEM, TEM)
Ref. [97]	Victrex 450G	Not provided	PEEK/p-MWCNT	Melt mixed with 10 wt.% mater batch.	Extrusion as filament.	Not provided

4.3.5. DMA

DMA was also utilized to evaluate the modulus change with increasing temperature, especially at high temperature (Figure 4-7 and Table 4-4). The high temperature storage

modulus, $G'_{230°C}$, of 10oCNT is increased by 229% from 0.13 GPa to 0.44 GPa, compared to the neat PEEK with similar degree of crystallinity. While at ambient temperature, $G'_{30°C}$, is increased by 117% from 1.22 GPa to 2.65 GPa. The difference in the modulus enhancement at mild temperature (below T_g) and high temperature (above T_g) is attributed to that MWCNT restricts more on the segmental motion of PEEK polymer chain while for molecular motions at a shorter length scale (namely lower temperature), its restrictive impact becomes less significant.

Table 4-4 Summary of T_g and storage modulus at 30 °C and 230 °C.

Samples	T_g /°C	$G'_{30\,°C}$ /×10^9Pa	$G'_{230\,°C}$ /×10^8Pa
uPEEK	158.9	1.22	1.33
PEEK	160.3	1.26	1.90
10oCNT	160.6	2.65	4.37

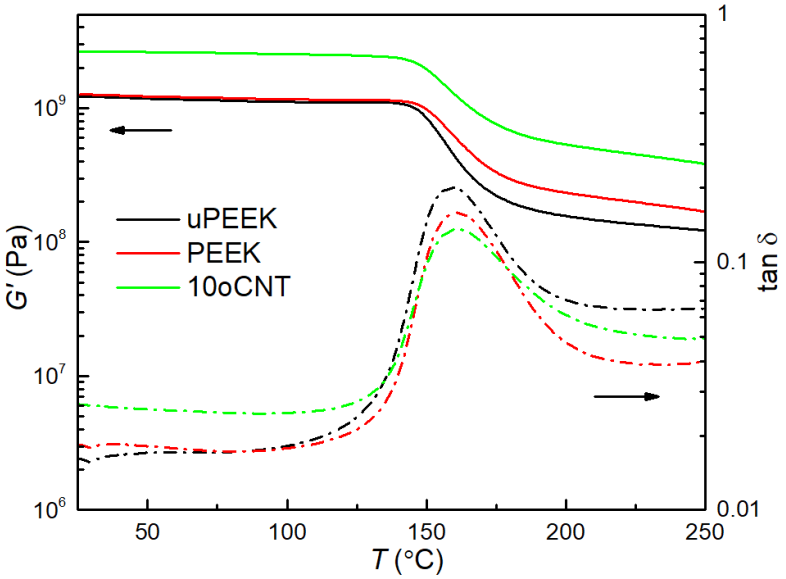

Figure 4-7 DMA plots of PEEK and 10oCNT.

4.3.6. CTE

Besides thermal and tensile properties, CTE is another important material parameter, especially for structural applications where dimensional stability is critical upon exposure to

large temperature changes. The linear expansion as a function of temperature is plotted in Fig. 9 and slopes of curves at 30 °C – 110 °C and 165 °C – 200 °C are used to calculate α_L below and above T_g, respectively (Table 5). Annealing appears to affect little on the CTE of neat PEEK below T_g while it can reduce CTE of neat PEEK by 10% at $T > T_g$. Compared to neat PEEK, nanocomposites exhibit moderate reductions (< 7%) of CTE below T_g. Above T_g, addition of MWCNT may contribute to a reduction of CTE by as high as 28% at only 1.5 wt.% loading. This is important because many PEEK components are machined at room temperature but used at high temperatures, which may induce significant thermal stress and cause premature failure. A reduction of CTE at both moderate and high temperatures is beneficial to its applications across a wide temperature range.

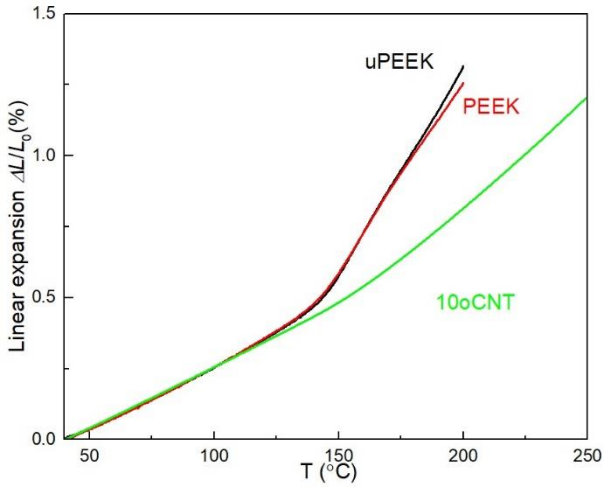

Figure 4-8 Linear thermal expansion of PEEK and 10oCNT.

Table 4-5 Coefficients of linear thermal expansion below and above T_g.

Samples	α_L /(ppm/°C) (30-110 °C)	α_L /(ppm/°C) (165-200 °C)
uPEEK	48.9 ± 0.3	142.9 ± 0.4
PEEK	48.7 ± 0.2	130.6 ± 0.5
10oCNT	41.9 ± 0.3	80.5 ± 0.4

4.4. Conclusion

By modification of the previous solution mixing approach, namely using diluted PEEK/DCA and MWCNT/NMP solutions, well-dispersed PEEK/MWCNT nanocomposite with a loading of 10 wt.% MWCNT is successfully prepared. Though o-MWCNT shows a degraded thermal stability, the thermal stability of 10oCNT is not significantly affected. And 10oCNT shows a much higher mechanical enhancement. Its Young's modulus is almost doubled, increased to 7.3 GPa while its storage modulus at high temperature, $G'_{230°C}$, is increased by 228%. Besides, the CTE is also significantly reduced, improving its dimensional stability.

The excellent properties of 10oCNT indicate that it should be a good candidate for high temperature use. In the next chapter, its high -temperature stress relaxation behaviors will be studied using a physics-based Ngai coupling model. And a comparison of 10oCNT and PEEK/PBI will be made to differentiate their mechanical properties at mild and high temperatures to guide their applications for different fields.

5. STRESS RELAXATION BEHAVIORS OF PEEK-BASED SYSTEMS[*]

5.1. Introduction

Previous results suggest that both blending with PBI particles and incorporating MWCNT into PEEK will enhance the mechanical properties of PEEK at room temperature, which is beneficial for its structural applications such as sealing and load-bearing component.[40] However, the mechanical properties of PEEK-based materials will exhibit time-temperature dependence due to its viscoelastic nature, raising great concerns over the validity of predicting long-term performance based on short-term property measurements. PEEK will relax with time under external strain, possibly causing catastrophic failure upon indefinite usage. For example, for PEEK-based seals, the maintenance of its modulus is very important for a seal to serve effectively. It is thus of great interest to develop testing methods and standards for reliable predictions of long-term viscoelastic behavior of PEEK under different service conditions and to ensure its long-term safe usage.

The conventional TTS principle is usually utilized to build master curves for describing the long-term viscoelastic behavior of polymers where short-term tests are conducted at higher temperatures if TTS can be safely applied within this temperature window. For the TTS protocol to be valid, the collective molecular scale motions responsible for the viscoelastic behavior need to correspond to the same activation energy value within the temperature window for TTS. This can pose a potential problem given that a higher temperature testing may lead to morphological

[*] Part of this chapter is reprinted with permission from "Effect of annealing on the viscoelastic behavior of poly(ether-ether-ketone)" by Jiang, Z. Y.; Liu, P.; Sue, H. J.; Bremner, T., *Polymer* **2019,** *160*, 231-237. Copyright 2019 by Elsevier Ltd.

changes, such as partial melting of lamellae or even chemical degradation, which may limit the prediction window that TTS can be applied. The goal of this work is to determine the range of conditions that the TTS is valid for PEEK-based materials, namely PEEK/PBI blend and PEEK/MWCNT nanocomposite, and to apply the physics-based Ngai coupling model to predict their long-term viscoelastic behavior.

The spring-dashpot model is often used for modeling the viscoelastic behavior of polymers. This model has a huge flexibility in its equation form depending on the numbers of spring or dashpot elements used and the way the springs and dashpots are arranged in series or in parallel. Usually, the more spring-dashpot elements are used, the better the modeling fit will become. However, this will also significantly increase the complexity of the modeling. Generally, a four-element spring-dashpot model is used. Yang et al. used the four-element spring-dashpot model to predict the long-term tensile viscoelastic behavior of nylon 66 nanocomposites and attempts were made by the authors to correlate the modeling parameters to the structural characteristics of the nylon 66 nanocomposites.[100, 101] On the other hand, power-law equations were also used by S. W. Bradley et al. to study the viscoelastic behavior of thermosets and its composites.[102] However, these models have inherent limitations as they are empirical in nature. Most importantly, they are incapable of predicting the linear viscoelastic behavior of polymers outside the experimental condition that the tests were carried out. Although empirical models are useful for the ease of analysis, they become invalid when the testing condition and the material exposure to environment are varied. Therefore, these models can only be regarded as descriptive, rather than being predictive. A physics-based model that can predict the long-term viscoelastic behavior for engineering polymers is desired.

The coupling model proposed by Ngai from Naval Research Laboratory in the late 1970s has been used by Feng et al. to predict the long-term viscoelastic behavior of epoxy resins.[103-105] This model takes into account the physical coupling interaction between polymer chain segments and their non-covalent bonded surrounding species. This molecular scale coupling process slows down the relaxation of polymer chains, which is dependent on the strength of the intermolecular interactions between polymer chains and their surroundings. The forces that can contribute to the overall intermolecular interaction include polar forces, steric interferences, hydrogen bonding and other specific non-bonded forces.[106] According to the coupling model, the coupling parameter *n* reflects the overall strength of these intermolecular interactions. The value of *n* is between 0 and 1. A higher value of *n* indicates a stronger intermolecular interaction and thus a higher degree of constraints imposed by the surroundings on polymer chains. Therefore, the Ngai's coupling model correlates the coupling parameter *n* to the molecular mobility of polymers and polymers with a higher value of *n* would show a more retarded relaxation behavior.

The description of the stress relaxation based on Ngai's coupling model is as follows:[103, 107]

$$G(t) = G_e + (G_0 - G_e)exp\left[-(\frac{t}{\tau^*})^{1-n}\right]$$

where $G(t)$ is the modulus as a function of time; G_e and G_0 are equilibrium shear modulus and initial shear modulus at time zero, respectively; τ^* is the effective relaxation time; n is the coupling parameter.

Comparing to other empirical and descriptive models, the significance of the Ngai's coupling model is the clear physical meaning of the model parameters and its capability to predict the viscoelastic behavior, e.g., stress relaxation. The long-term stress relaxation of

polymers can be modeled using the equation. The coupling model parameters, i.e., n and τ^*, can be obtained by various means, including dynamical mechanical frequency sweep, stress relaxation, creep, dielectric relaxation and neutron scattering measurements.[106, 108, 109] However, it should be noted that the n value may be dependent on the nature of the experimental probe.[110] Other physical terms can be obtained *via* shear test and DMA in torsional mode.[103] Once all these parameters are known, the viscoelastic behavior can be predicted by the coupling model if all assumptions involved are met, without carrying out any creep or stress relaxation tests, making the Ngai's coupling model attractive for the prediction of long-term creep and stress relaxation behavior of amorphous polymers.

It should be emphasized that this predictability of the coupling model has only been shown to be applicable to amorphous polymers until now; Its applicability to semicrystalline polymers, such as PEEK in the present work, has not been extensively reported.[108] Furthermore, it has been shown that the relaxation spectrum of semicrystalline polymers is not homogeneously masked by the crystallinity and can no longer follow the Kohlrausch-Williams-Watts (KWW) form, which the coupling model is based upon.[108] Therefore, acquisition of model parameters n and τ^* via the curve fitting of the relaxation spectrum appears to be inappropriate for semicrystalline polymers. On the other hand, Ngai and his coworker also found that semicrystalline polymers having a stronger coupling interaction would exhibit a more intense temperature dependence of segmental relaxation time, which indicates the potential usefulness of the coupling model for understanding the viscoelastic behavior of semicrystalline polymers, at least semi-quantitatively.[108] The coupling parameter n represents the combined effects of various structural and environmental factors, including chemical structure, crosslink density, aging and

so on, which can influence the relaxation process.[106, 107, 111] In this study, it is anticipated that blending with PBI and addition MWCNT will influence the viscoelastic behaviors of PEEK.

According to Yee et al., the magnitude of the coupling parameter *n* of a glassy polymer can be approximated by the slope of log $E \sim \log t$ when the polymer is relaxed at a temperature far below T_g.[107] Another approach is to directly fit the relaxation curves with the coupling model, which is used in the present study. Considering the physical meaning of the coupling parameters, the Ngai's coupling model is still favored over other empirical models for gaining fundamental understanding on how blending with PBI and adding MWCNT will influence the viscoelastic behavior of PEEK, respectively. These influences on the stress relaxation behaviors of PEEK were investigated and the coupling model was used to reveal these effects from a molecular coupling perspective.

Firstly, short-term stress relaxations were studied at different temperatures below T_g to obtain master curves *via* TTS principle for the long-term viscoelastic behavior prediction. To determine the differences from a molecular basis, Ngai's coupling model were employed to assess their molecular mobility. The usefulness of Ngai's coupling model for predicting long-term viscoelastic behavior of semi-crystalline polymers is discussed.

5.2. Experimental

5.2.1. Material and treatment

Materials used for this study include neat PEEK 150 G, PEEK/PBI polymer blend (50 wt.%) and PEEK/MWCNT nanocomposite (10 wt.%). For PEEK/PBI and PEEK/MWCNT, both were annealed at 260 ℃ for 1 hour to maximize its crystallinity and eventually, crystallinities of all three systems were kept the same, that is about 37%.

To investigate the influence of water absorption on the mechanical performance of these three systems, they were placed in a tube full of deionized water at 95 ℃ for certain days. The weight change of these samples was monitored, and the state of saturated water absorption was achieved until there was no significant weight change of them.

5.2.2. Characterization

5.2.2.1. DMA

DMA of all dry and wet systems were measured using ARES-G2 rheometer. Bulk samples (35 mm * 8 mm * 3 mm) were heated from -120 ℃ to 250 ℃ with a frequency of 1 Hz and a small strain of 0.1%.

5.2.2.2. Stress relaxation behavior

Short-term stress relaxation measurements were carried out using a TA Instruments ARES-G2 torsional rheometer and isothermal stress relaxation tests were done in torsional mode for 1 h at temperatures ranging from 30 °C to 150 °C. For stress relaxation studies, a constant strain of 0.5% was held and the corresponding modulus relaxation with time was recorded. The reason that such small strains were chosen is to ensure they are still in the linear viscoelastic regime. Short-term stress relaxation data at different temperatures were then both horizontally and vertically shifted to achieve the best fitting for master curves using Trios software provided by TA Instruments Inc. The horizontal shift factors are found to follow an Arrhenius-type relationship and thus used for the calculation of activation energy, E_a, which is an indicator of the energy barrier for polymer relaxation. The generated master curves were fitted based on Ngai's coupling model using EXCEL software.

Bulk samples (35 mm * 8 mm * 3 mm) were used in these isothermal short-term tests. Since the test is relatively short (1 hour) and samples are relatively thick, water loss of wet samples during testing is assumed to be negligible.

5.3. Results and discussion

5.3.1. DMA

DMA of neat PEEK, PEEK/PBI blend (50 wt.% PBI), and PEEK/MWCNT nanocomposite (10 wt.% MWCNT) were presented in Figure 5-1. These samples, as well as samples for stress relaxation tests, possess the same level of crystallinity to minimize the influence of crystallinity on their thermomechanical and viscoelastic properties. With the same level of crystallinity, the storage modulus of three systems at room temperature (23 ℃) can be ranked as follows: PEEK/MWCNT > PEEK/PBI > PEEK. This is not surprising, and it is consistent with the Young's modulus results from tensile testing where PEEK/MWCNT shows a much higher modulus improvement than PEEK/PBI. However, when it comes to a higher temperature (i.e., 230 ℃, above T_g of PEEK), their storage modulus is ranked: PEEK/PBI > PEEK/MWCNT > PEEK. This is due to the different weight or volume fractions of PBI and MWCNT in PEEK/PBI and PEEK/MWCNT systems. In PEEK/PBI, even at a high temperature (230 ℃) above the T_g of PEEK, there are still 50 vol.% stiff PBI particles since this temperature is still below the T_g of PBI (436 ℃). And these 50 vol.% stiff PBI particles, contributing to a relatively higher storage modulus at 230 ℃. For PEEK/MWCNT, although MWCNT also contribute to the enhancement of modulus, it only occupies 9.7 vol.% and more than 90 vol.% are PEEK matrix which becomes softened at high temperatures. Therefore, under the dry condition, 9.7 vol% MWCNT can enhance the modulus of PEEK at room temperature significantly. However, at high temperature (above the T_g of PEEK), its contribution is limited

by its relatively low volume concentration. And PEEK/PBI shows a higher storage modulus at high temperature regime due to its much higher loading of PBI (50 vol.%).

However, PBI has its drawbacks as it is very sensitive to water. The wet PBI will cause significant drop in its mechanical properties. It should be noted that in a full water-saturated system, PEEK/PBI can uptake much more water than PEEK/MWCNT and neat PEEK (Table 5-1). Here, the DMA of water-saturated systems are also presented in Figure 5-1. It can be

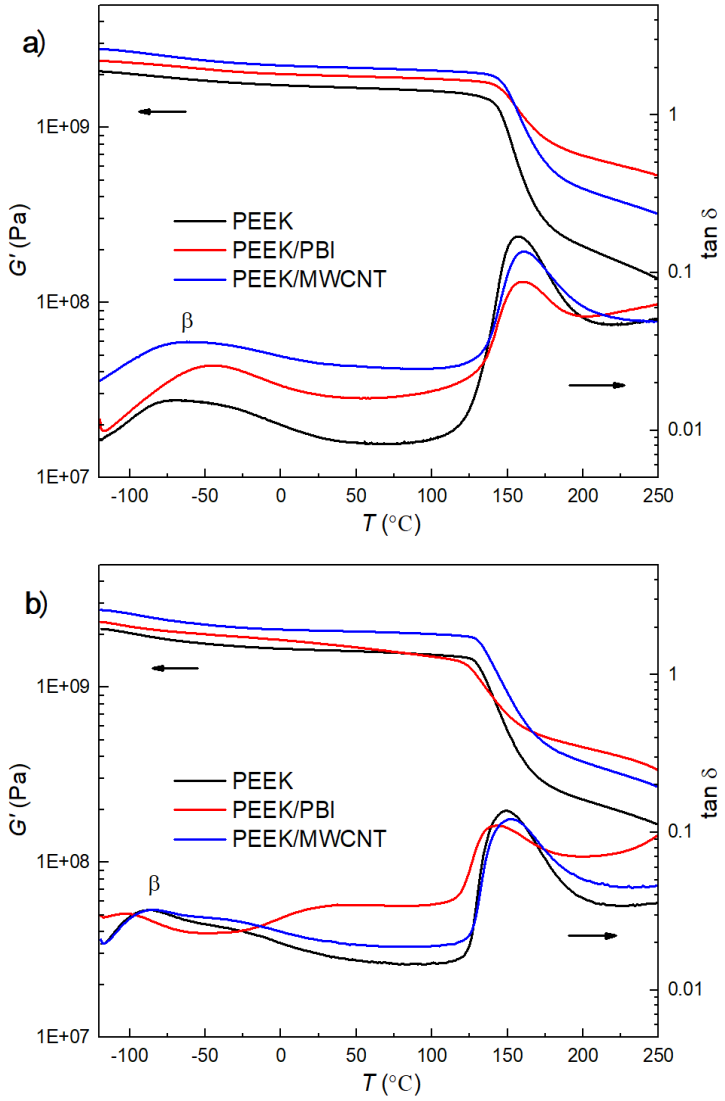

Figure 5-1 DMA of PEEK, PEEK/PBI and PEEK/MWCNT systems: a) dry condition; b) wet condition.

concluded that in all water-saturated systems, all show a decrease of T_g compared to the dry samples. Among them, PEEK/PBI's T_g drops from 160.4 ℃ to 143.4 ℃ while T_g of PEEK/MWCNT and neat PEEK only drop from 160.6 ℃ to 152.3 ℃ and from 157.1 ℃ to 148.5 ℃, respectively. The water-saturated PEEK/PBI exhibits the lowest T_g among three systems, showing how significantly the performance will be deteriorated when PEEK/PBI is exposed to water.

Table 5-1 Summary of DMA results of PEEK, PEEK/PBI and PEEK/MWCNT under dry and wet conditions.

	Properties	**PEEK**	**PEEK/PBI**	**PEEK/MWCNT**
Dry	T_β /℃	-70.3	-45.5	-61.1
	T_g /℃	157.1	160.4	160.6
	$G'_{23\,℃}$ /GPa	1.71	1.99	2.22
	$G'_{230\,℃}$ /GPa	0.18	0.59	0.37
Wet	T_β /℃	-86.5	-103.4	-84.0
	T_g /℃	148.5	143.4	152.3
	$G'_{23\,℃}$ /GPa	1.63	1.79	2.11
	$G'_{230\,℃}$ /GPa	0.18	0.39	0.31
	Water absorption /wt.%	0.5 ± 0.1	0.6 ± 0.1	6.5 ± 0.3

5.3.2. Stress relaxation under dry and wet conditions

In addition to thermomechanical properties, the stress relaxation behaviors of these three systems are also studied since it is very important for some applications such as sealing materials. The stress relaxation behaviors of them under dry and water-saturated conditions are

also studied for the evaluation of their performances under dry and wet scenarios. The master curves based on a reference temperature of 90 ℃ are shown in Figure 5-2 and they are also fitted using Ngai coupling model with fitting parameters listed in Table 5-2.

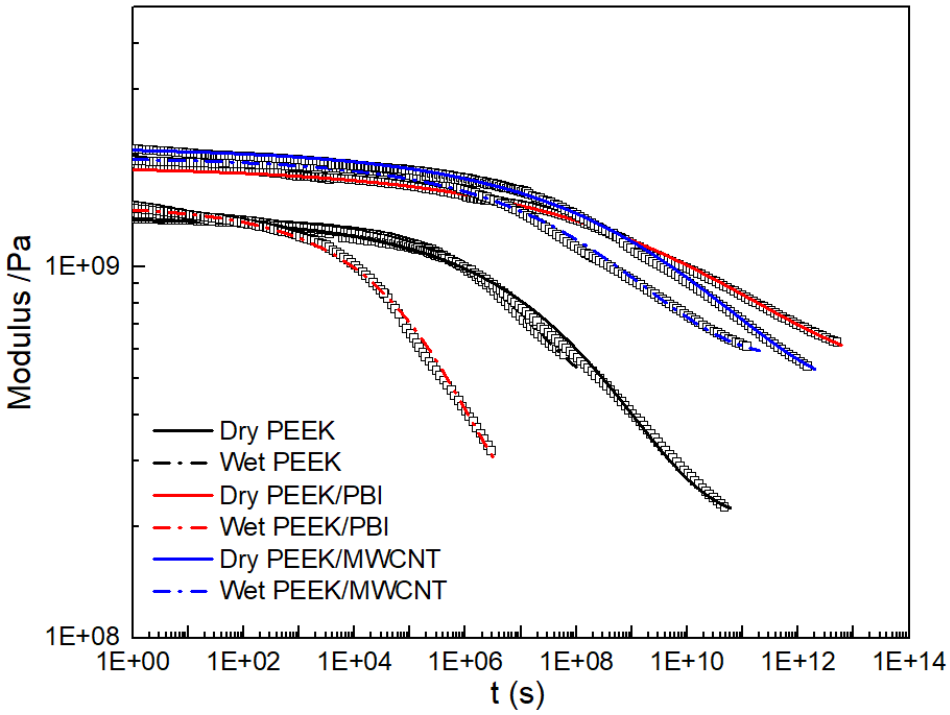

Figure 5-2 Master curves of short-term stress relaxations (hollow dots) fitted by Ngai coupling model (solid lines). The reference temperature is 90 ℃.

Under dry condition, incorporation of 50 wt.% PBI or 10 wt.% MWCNT can both retard the stress relaxation of PEEK. PEEK/PBI system shows a coupling parameter n=0.85 and characteristic relaxation time $\tau^*=9\times10^9$ s, both higher than those of PEEK/MWCNT and PEEK. It suggests that more PBI imposes more restrictions on the polymer chain motions. Incorporation of 10 wt.% also restricts the molecular motions, but to a less extent compared to PEEK/PBI system. When exposed to wet condition, PEEK and PEEK/MWCNT only exhibit slight decrease in their modulus retention capability due to their relatively low water absorption.

However, PEEK/PBI system shows a significant drop in its modulus retention capability under wet condition because of its much more water absorption (Table 5-1). The Ngai coupling parameter, *n*, and characteristic relaxation time, τ^*, of wet PEEK/PBI are decreased to 0.67 and 1.3×10^5 s, respectively, suggesting that a large amount of water absorption leads to much less restrictions on polymer motions and the modulus of wet PEEK/PBI will degrade very fast due to less constrained polymer chain mobility.

The activation energy, E_a, of stress relaxation also supports that dry PEEK/PBI system has the highest value of E_a due to strong restrictions imposed by 50 vol.% PBI. But once exposed to water, its activation energy is significantly dropped from 157 kJ/mol to 110 kJ/mol (Figure 5-3 and Table 5-2). This activation energy indicates the energy barrier for polymer chain relaxation.

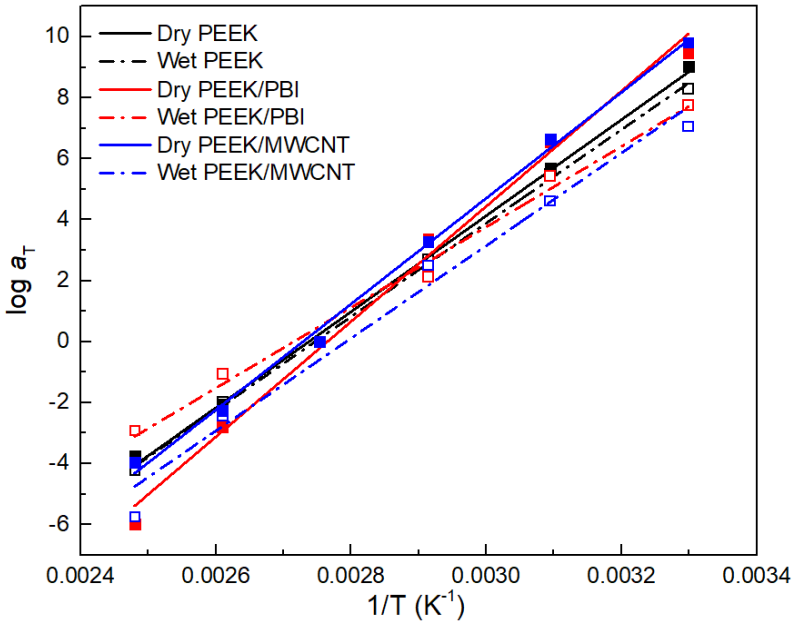

Figure 5-3 Linear fitting of horizontal shift factors of stress relaxation measurements under both dry and wet conditions.

Table 5-2 Curve fitting parameters based on Ngai coupling model and activation energy based on the TTS of short-term stress relaxation measurements.

Sample and treatment		G_0 /GPa	G_e /GPa	n	τ /s	E_a /(kJ/mol)
PEEK	Dry	1.37	0.45	0.78	7.0E7	131
	Wet	1.35	0.21	0.68	7.5E6	128
PEEK /PBI	Dry	1.87	0.52	0.85	9.0E9	157
	Wet	1.46	0.21	0.67	1.3E5	110
PEEK /MWNCT	Dry	2.10	0.57	0.83	3.0E9	145
	Wet	1.97	0.45	0.79	2.5E8	126

5.4. Conclusion

Incorporation of PBI and MWCNT into PEEK can improve the modulus retention capability of PEEK, which is very important for sealing materials. PEEK/PBI system shows relatively more restrictions on polymer chain motions compared to PEEK/MWCNT system due to its much high loading of PBI (50 vol.%). This is supported by the Ngai coupling model fitting which shows that the value of PEEK/PBI's coupling parameter, *n*, is slightly higher than that of PEEK/MWCNT. However, due to vulnerability of PBI to water, PEEK/PBI system can absorb 6.5 wt.% water when exposed to wet condition. The wet PEEK/PBI shows a significant drop in its modulus retention capability and its modulus degrades very fast under hot and wet condition. On the other hand, the modulus retention capability of PEEK/MWCNT is slightly affected under wet condition, enabling its applications as sealing component under hot and wet condition. Compared to PEEK/PBI, the advantage of PEEK/MWCNT is that it is resistant to moisture and other chemicals while the high modulus is maintained.

6. CONCLUSION

Mechanical reinforcement of PEEK is very useful for expanding its applications and value-addition. In this dissertation, firstly, commercially available model PEEK/PBI polymer blend systems were studied. It was found that for immiscible PEEK/PBI blends, melt pre-mixing is critical to achieve an acceptable level of interfacial mixing. Compared with powder pre-mixed system, the melt pre-mixed PEEK/PBI system shows a thicker interface and better interfacial mixing, causing the modulus to increase to 5.3 GPa. However, according to the "rule of mixer", further improvement of modulus is limited due to the relatively low Young's modulus of PBI (7.1 GPa). And the water absorption of PBI will cause the mechanical and viscoelastic properties of PEEK/PBI to drop significantly when it is used under wet condition, limiting the application of PEEK/PBI. To overcome these drawbacks, we developed a novel and simple solution mixing approach to prepare well-dispersed PEEK/MWCNT nanocomposites. This approach can achieve a high concentration of 10 wt.% MWCNT and maintain the good dispersion of MWCNT in PEEK at the same time. The PEEK/MWCNT nanocomposites prepared by this approach exhibit uniform distribution and individual dispersion of MWCNT. On the other hand, a sufficiently strong interaction between PEEK and MWCNT is achieved. The combination of good dispersion state and strong interfacial interaction contributes to the significant mechanical enhancement. In 10 wt.% PEEK/MWCNT system, Young's modulus and tensile strength are improved to 7.3 GPa and 128 MPa, respectively, outperforming PEEK/PBI system. More importantly, PEEK/MWCNT system exhibits resistance to water so that it can be safely used in the scenario where water is presented.

To conclude, the significance of this work lies in that PEEK/MWCNT nanocomposites prepared by a novel solution mixing approach show very high efficiency on mechanical

reinforcement. With addition of only 10 wt.% MWCNT, its Young's modulus and tensile strength outperforms those of 50 wt.% PEEK/PBI system at room temperature under dry condition. More importantly, the PEEK/MWCNT system is resistant to water, expanding its applications to some hot and wet scenarios where PEEK/PBI suffers significant mechanical property deterioration.

REFERENCE

1. Marathe, U.; Padhan, M.; Bijwe, J., Carbon nanotubes- A powerful nano-filler for enhancing the performance properties of polyetherketoneketone composites and adhesives. *Compos Sci Technol* **2021,** *210*.

2. Shukla, D.; Negi, Y. S.; Sen Uppadhyaya, J.; Kumar, V., Synthesis and Modification of Poly(ether ether ketone) and their Properties: A Review. *Polym Rev* **2012,** *52* (2), 189-228.

3. Salazkin, S. N.; Shaposhnikova, V. V., Poly(arylene ether ketones): Thermostable, Heat Resistant, and Chemostable Thermoplastics and Prospects for Designing Various Materials on Their Basis. *Polym Sci Ser C+* **2020,** *62* (2), 111-123.

4. Colquhoun, H. M.; Zhu, Z. X.; Dudman, C. C., Enthalpy-driven ring-opening polymerization of highly strained macrocyclic biaryl-ether-ketones. *Macromolecules* **2005,** *38* (25), 10421-10428.

5. Chan, K. P.; Wang, Y. F.; Hay, A. S.; Hronowski, X. P. L.; Cotter, R. J., Synthesis and Characterization of Novel Cyclic (Aryl Ether Ketone)S, Cyclic (Aryl Ether Phthalazine)S, and Cyclic (Aryl Ether Isoquinoline)S. *Macromolecules* **1995,** *28* (20), 6705-6717.

6. Mullins, M. J.; Woo, E. P., The Synthesis and Properties of Poly[Aromatic Ketones]. *J Macromol Sci R M C* **1987,** *C27* (2), 313-341.

7. Jiang, Z. Y.; Chen, Q. H.; Zhu, Z. W.; Tsai, C. Y.; Zhao, M. Z.; Sue, H. J.; Chang, A.; Bremner, T.; DiSano, L. P., Well-dispersed poly(ether-ether-ketone)/multi-walled carbon nanotube nanocomposites prepared via a simple solution mixing approach. *Polym Int* **2021,** *70* (8), 1090-1098.

8. Jiang, Z. Y.; Liu, P.; Chen, Q. H.; Sue, H. J.; Bremner, T.; DiSano, L. P., The influence of processing conditions on the mechanical properties of poly(aryl-ether-ketone)/polybenzimidazole blends. *J Appl Polym Sci* **2020,** *137* (33).

9. Jiang, Z. Y.; Liu, P.; Sue, H. J.; Bremner, T., Effect of annealing on the viscoelastic behavior of poly(ether-ether-ketone). *Polymer* **2019,** *160*, 231-237.

10. Zoidis, P.; Papathanasiou, L., Modified PEEK resin-bonded fixed dental prosthesis as an interim restoration after implant placement. *J Prosthet Dent* **2016,** *116* (5), 637-641.

11. Schwitalla, A. D.; Spintig, T.; Kallage, I.; Muller, W. D., Flexural behavior of PEEK materials for dental application. *Dent Mater* **2015,** *31* (11), 1377-1384.

12. Li, C. S.; Vannabouathong, C.; Sprague, S.; Bhandari, M., The Use of Carbon-Fiber-Reinforced (CFR) PEEK Material in Orthopedic Implants: A Systematic Review. *Clin Med Insights-Ar* **2015,** *8*, 33-45.

13. Rho, J. Y.; Ashman, R. B.; Turner, C. H., Youngs Modulus of Trabecular and Cortical Bone Material - Ultrasonic and Microtensile Measurements. *J Biomech* **1993,** *26* (2), 111-119.

14. Laux, K. A.; Jean-Fulcrand, A.; Sue, H. J.; Bremner, T.; Wong, J. S. S., The influence of surface properties on sliding contact temperature and friction for polyetheretherketone (PEEK). *Polymer* **2016,** *103*, 397-404.

15. Sasuga, T.; Hagiwara, M., Radiation Deterioration of Several Aromatic Polymers under Oxidative Conditions. *Polymer* **1987,** *28* (11), 1915-1921.

16. Jockisch, K. A.; Brown, S. A.; Bauer, T. W.; Merritt, K., Biological Response to Chopped-Carbon-Fiber-Reinforced Peek. *J Biomed Mater Res* **1992,** *26* (2), 133-146.

17. Sagomonyants, K. B.; Jarman-Smith, M. L.; Devine, J. N.; Aronow, M. S.; Gronowicz, G. A., The in vitro response of human osteoblasts to polyetheretherketone (PEEK) substrates compared to commercially pure titanium. *Biomaterials* **2008,** *29* (11), 1563-1572.

18. Lin, T. W.; Corvelli, A. A.; Frondoza, C. G.; Roberts, J. C.; Hungerford, D. S., Glass peek composite promotes proliferation and osteocalcin production of human osteoblastic cells. *J Biomed Mater Res* **1997,** *36* (2), 137-144.

19. Petrovic, L.; Pohle, D.; Munstedt, H.; Rechtenwald, T.; Schlegel, K. A.; Rupprecht, S., Effect of beta TCP filled polyetheretherketone on osteoblast cell proliferation in vitro. *J Biomed Sci* **2006,** *13* (1), 41-46.

20. Abu Bakar, M. S.; Cheang, P.; Khor, K. A., Mechanical properties of injection molded hydroxyapatite-polyetheretherketone biocomposites. *Compos Sci Technol* **2003,** *63* (3-4), 421-425.

21. Kuo, M. C.; Tsai, C. M.; Huang, J. C.; Chen, M., PEEK composites reinforced by nano-sized SiO2 and Al2O3 particulates. *Mater Chem Phys* **2005,** *90* (1), 185-195.

22. Wu, X. M.; Liu, X. C.; Wei, J.; Ma, J.; Deng, F.; Wei, S. C., Nano-TiO2/PEEK bioactive composite as a bone substitute material: in vitro and in vivo studies. *Int J Nanomed* **2012,** *7*, 1215-1225.

23. Wang, D. H.; Baek, J. B.; Tan, L. S., Grafting of vapor-grown carbon nanofibers (VGCNF) with a hyperbranched poly (ether-ketone). *Mat Sci Eng B-Solid* **2006,** *132* (1-2), 103-107.

24. Kurtz, S. M.; Devine, J. N., PEEK biomaterials in trauma, orthopedic, and spinal implants. *Biomaterials* **2007,** *28* (32), 4845-4869.

25. Han, C. M.; Lee, E. J.; Kim, H. E.; Koh, Y. H.; Kim, K. N.; Ha, Y.; Kuh, S. U., The electron beam deposition of titanium on polyetheretherketone (PEEK) and the resulting enhanced biological properties. *Biomaterials* **2010,** *31* (13), 3465-3470.

26. Wang, L. X.; He, S.; Wu, X. M.; Liang, S. S.; Mu, Z. L.; Wei, J.; Deng, F.; Deng, Y.; Wei, S. C., Polyetheretherketone/nano-fluorohydroxyapatite composite with antimicrobial activity and osseointegration properties. *Biomaterials* **2014,** *35* (25), 6758-6775.

27. Panayotov, I. V.; Orti, V.; Cuisinier, F.; Yachouh, J., Polyetheretherketone (PEEK) for medical applications. *J Mater Sci-Mater M* **2016,** *27* (7).

28. Theiler, G.; Gradt, T., MoS2-filled PEEK composite as a self-lubricating material for aerospace applications. **2010**.

29. Theiler, G.; Harsha, A. P.; Gradt, T., On the Sliding Wear Behavior of PAEK Composites in Vacuum Environment. *J Tribol-T Asme* **2019,** *141* (4).

30. Liu, Z. L.; Wang, L.; Hou, X. B.; Wu, J., Investigation on dielectrical and space charge characteristics of peek insulation used in aerospace high-voltage system. *Ieej T Electr Electr* **2020,** *15* (2), 172-178.

31. Iannone, M.; D'Amore, A., Processing of PEEK/PEI Blends for High Performance Composites in Aerospace. *9th International Conference on Structural Analysis of Advanced Materials (Icsaam 2019)* **2019,** *2196*.

32. Small, G., Outstanding physical properties make PEEK ideal for sealing applications. *Sealing Technology* **2014,** *2014* (4), 9-12.

33. One-component silicone is resistant to high temperatures. *Sealing Technology* **2014,** *2014* (4), 2-3.

34. Liu, P.; Mullins, M.; Bremner, T.; Browne, J. A.; Sue, H. J., Hygrothermal behavior of polybenzimidazole. *Polymer* **2016,** *93*, 88-98.

35. Sharma, S.; Padenko, E.; Bijwe, J.; Wetzel, B.; Friedrich, K., Erosive and sliding wear of polybenzimidazole at elevated temperatures. *J Mater Sci* **2016,** *51* (1), 262-270.

36. Jean-Fulcrand, A.; Masen, M. A.; Bremner, T.; Wong, J. S. S., High temperature tribological properties of polybenzimidazole (PBI). *Polymer* **2017,** *128*, 159-168.

37. Deimede, V.; Voyiatzis, G. A.; Kallitsis, J. K.; Qingfeng, L.; Bjerrum, N. J., Miscibility behavior of polybenzimidazole/sulfonated polysulfone blends for use in fuel cell applications. *Macromolecules* **2000,** *33* (20), 7609-7617.

38. Jean-Fulcrand, A.; Maser, M. A.; Bremner, T.; Wong, J. S. S., Effect of temperature on tribological performance of polyetheretherketone-polybenzimidazole blend. *Tribol Int* **2019,** *129*, 5-15.

39. Leung, L.; Williams, D. J.; Karasz, F. E.; Macknight, W. J., Miscible Blends of Aromatic Polybenzimidazoles and Aromatic Polyimides. *Polym Bull* **1986,** *16* (5), 457-464.

40. Liu, P.; Mullins, M.; Bremner, T.; Benner, N.; Sue, H. J., Interfacial Phenomena and Mechanical Behavior of Polyetheretherketone/Polybenzimidazole Blend under Hygrothermal Environment. *J Phys Chem B* **2017,** *121* (21), 5396-5406.

41. Hermes, H. E.; Higgins, J. S., Effects of processing conditions and copolymer molecular weight an the mechanical properties and morphology of compatibilized polymer blends. *Polym Eng Sci* **1998,** *38* (5), 847-856.

42. Liu, H. Z.; Song, W. J.; Chen, F.; Guo, L.; Zhang, J. W., Interaction of Microstructure and Interfacial Adhesion on Impact Performance of Polylactide (PLA) Ternary Blends. *Macromolecules* **2011,** *44* (6), 1513-1522.

43. Seo, Y.; Kim, B.; Kwak, S.; Kim, K. U.; Kim, J., Morphology and properties of compatibilized ternary blends (nylon 6/a thermotropic liquid crystalline polymer/a functionalized polypropylene) processed under different conditions. *Polymer* **1999,** *40* (16), 4441-4450.

44. Charoensirisomboon, P.; Chiba, T.; Torikai, K.; Saito, H.; Ougizawa, T.; Inoue, T.; Weber, M., Morphology-interface-toughness relationship in polyamide/polysulfone blends by reactive processing. *Polymer* **1999,** *40* (25), 6965-6975.

45. Willis, J. M.; Favis, B. D.; Lunt, J., Reactive Processing of Polystyrene-Co-Maleic Anhydride Elastomer Blends - Processing-Morphology-Property Relationships. *Polym Eng Sci* **1990,** *30* (17), 1073-1084.

46. Liu, H. Z.; Chen, F.; Liu, B.; Estep, G.; Zhang, J. W., Super Toughened Poly(lactic acid) Ternary Blends by Simultaneous Dynamic Vulcanization and Interfacial Compatibilization. *Macromolecules* **2010,** *43* (14), 6058-6066.

47. Zhang, C. L.; Feng, L. F.; Gu, X. P.; Hoppe, S.; Hu, G. H., Efficiency of graft copolymers as compatibilizers for immiscible polymer blends. *Polymer* **2007,** *48* (20), 5940-5949.

48. Cecere, A.; Greco, R.; Ragosta, G.; Scarinzi, G.; Taglialatela, A., Rubber Toughened Polybutylene Terephthalate - Influence of Processing on Morphology and Impact Properties. *Polymer* **1990,** *31* (7), 1239-1244.

49. Chaudhry, B. I.; Hage, E.; Pessan, L. A., Effects of processing conditions on the phase morphology of PC/ABS polymer blends. *J Appl Polym Sci* **1998,** *67* (9), 1605-1613.

50. Cimmino, S.; Coppola, F.; Dorazio, L.; Greco, R.; Maglio, G.; Malinconico, M.; Mancarella, C.; Martuscelli, E.; Ragosta, G., Ternary Nylon-6 Rubber Modified Rubber Blends

- Effect of the Mixing Procedure on Morphology, Mechanical and Impact Properties. *Polymer* **1986,** *27* (12), 1874-1884.

51. Ohlsson, B.; Hassander, H.; Tornell, B., Effect of the mixing procedure on the morphology and properties of compatibilized polypropylene/polyamide blends. *Polymer* **1998,** *39* (20), 4715-4721.

52. Li, H. G.; Chiba, T.; Higashida, N.; Yang, Y.; Inoue, T., Polymer-polymer interface in polypropylene/polyamide blends by reactive processing. *Polymer* **1997,** *38* (15), 3921-3925.

53. Seo, J.; Gohn, A. M.; Dubin, O.; Takahashi, H.; Hasegawa, H.; Sato, R.; Rhoades, A. M.; Schaake, R. P.; Colby, R. H., Isothermal crystallization of poly (ether ether ketone) with different molecular weights over a wide temperature range. *Polymer Crystallization* **2019,** *2* (1), e10055.

54. Dominguez, S.; Derail, C.; Leonardi, F.; Pascal, J.; Brule, B., Study of the thermal properties of miscible blends between poly(ether ketone ketone) (PEKK) and polyimide. *Eur Polym J* **2015,** *62*, 179-185.

55. Wang, W.; Schultz, J. M.; Hsiao, B. S., Dynamic study of crystallization- and melting-induced phase separation in PEEK/PEKK blends. *Macromolecules* **1997,** *30* (16), 4544-4550.

56. Jin, L.; Ball, J.; Bremner, T.; Sue, H. J., Crystallization behavior and morphological characterization of poly(ether ether ketone). *Polymer* **2014,** *55* (20), 5255-5265.

57. Krikorian, V.; Pochan, D. J., Unusual crystallization behavior of organoclay reinforced poly(L-lactic acid) nanocomposites. *Macromolecules* **2004,** *37* (17), 6480-6491.

58. Blundell, D. J.; Newton, A. B., Variations in the Crystal-Lattice of Peek and Related Para-Substituted Aromatic Polymers .2. Effect of Sequence and Proportion of Ether and Ketone Links. *Polymer* **1991,** *32* (2), 308-313.

59. Ho, R. M.; Cheng, S. Z. D.; Hsiao, B. S.; Gardner, K. H., Crystal Morphology and Phase Identifications in Poly(Aryl Ether Ketone)S and Their Copolymers .1. Polymorphism in Pekk. *Macromolecules* **1994,** *27* (8), 2136-2140.

60. Talbott, M. F.; Springer, G. S.; Berglund, L. A., The Effects of Crystallinity on the Mechanical-Properties of Peek Polymer and Graphite Fiber Reinforced Peek. *J Compos Mater* **1987,** *21* (11), 1056-1081.

61. Hansen, C. M., Solubility parameters: A user's handbook. CRC Press Boca Raton: 2007.

62. Database, P. Poly(ether ether ketone). http://polymerdatabase.com/polymers/polyetheretherketone.html.

63. Database, P. Poly(ether ketone ketone). https://polymerdatabase.com/polymers/polyetherketoneketone.html.

64. Shi, G. M.; Chen, H. M.; Jean, Y. C.; Chung, T. S., Sorption, swelling, and free volume of polybenzimidazole (PBI) and PBI/zeolitic imidazolate framework (ZIF-8) nano-composite membranes for pervaporation. *Polymer* **2013,** *54* (2), 774-783.

65. Yuan, Y.; Goodson, J.; Fan, R., HP/HT Hot-wet resistance of thermoplastic PEEK and its composites. In *Composite Materials and Joining Technologies for Composites, Volume 7*, Springer: 2013; pp 161-177.

66. Yuan, Y.; Goodson, J., HP/HT Hot-Wet Thermomechanical Behavior of Fiber-Reinforced High-Temperature Polymer Composites. In *Experimental Mechanics of Composite, Hybrid, and Multifunctional Materials, Volume 6*, Springer: 2014; pp 125-147.

67. Bangarusampath, D. S.; Ruckdaschel, H.; Altstadt, V.; Sandler, J. K. W.; Garray, D.; Shaffer, M. S. P., Rheology and properties of melt-processed poly(ether ether ketone)/multi-wall carbon nanotube composites. *Polymer* **2009,** *50* (24), 5803-5811.

68. Diez-Pascual, A. M.; Naffakh, M.; Gomez, M. A.; Marco, C.; Ellis, G.; Martinez, M. T.; Anson, A.; Gonzalez-Dominguez, J. M.; Martinez-Rubi, Y.; Simard, B., Development and characterization of PEEK/carbon nanotube composites. *Carbon* **2009,** *47* (13), 3079-3090.

69. Garcia-Gonzalez, D.; Rodriguez-Millan, M.; Rusinek, A.; Arias, A., Investigation of mechanical impact behavior of short carbon-fiber-reinforced PEEK composites. *Compos Struct* **2015,** *133*, 1116-1126.

70. Shrivastava, A., 4 - Additives for Plastics. In *Introduction to Plastics Engineering*, Shrivastava, A., Ed. William Andrew Publishing: 2018; pp 111-141.

71. Gulgunje, P. V.; Newcomb, B. A.; Gupta, K.; Chae, H. G.; Tsotsis, T. K.; Kumar, S., Low-density and high-modulus carbon fibers from polyacrylonitrile with honeycomb structure. *Carbon* **2015,** *95*, 710-714.

72. Ogasawara, T.; Tsuda, T.; Takeda, N., Stress-strain behavior of multi-walled carbon nanotube/PEEK composites. *Compos Sci Technol* **2011,** *71* (2), 73-78.

73. Rong, C. R.; Ma, G.; Zhang, S. L.; Song, L.; Chen, Z.; Wang, G. B.; Ajayan, P. M., Effect of carbon nanotubes on the mechanical properties and crystallization behavior of poly(ether ether ketone). *Compos Sci Technol* **2010,** *70* (2), 380-386.

74. Diez-Pascual, A. M.; Naffakh, M.; Gonzalez-Dominguez, J. M.; Anson, A.; Martinez-Rubi, Y.; Martinez, M. T.; Simard, B.; Gomez, M. A., High performance PEEK/carbon nanotube composites compatibilized with polysulfones-I. Structure and thermal properties. *Carbon* **2010,** *48* (12), 3485-3499.

75. Diez-Pascual, A. M.; Naffakh, M.; Gonzalez-Dominguez, J. M.; Anson, A.; Martinez-Rubi, Y.; Martinez, M. T.; Simard, B.; Gomez, M. A., High performance PEEK/carbon

nanotube composites compatibilized with polysulfones-II. Mechanical and electrical properties. *Carbon* **2010,** *48* (12), 3500-3511.

76. Lin, L.; Wu, X.; Han, Y. T.; Zhang, H. B.; Jiang, Z. H.; Chen, Z., Novel soluble carbazole-based poly(aryl ethers): Preparation, properties, and application for dispersing multiwalled carbon nanotubes. *J Appl Polym Sci* **2018,** *135* (20).

77. Lin, L.; Han, Y. T.; Zhao, X. H.; Wang, Y. W.; Zhang, H. B.; Jiang, Z. H.; Chen, Z., Effectively improving the performance of MWNT/PEEK composite by choosing PAK-Cz as the solubilizer. *High Perform Polym* **2019,** *31* (8), 875-884.

78. Diez-Pascual, A. M.; Martinez, G.; Martinez, M. T.; Gomez, M. A., Novel nanocomposites reinforced with hydroxylated poly(ether ether ketone)-grafted carbon nanotubes. *J Mater Chem* **2010,** *20* (38), 8247-8256.

79. Boo, W. J.; Sun, L. Y.; Liu, J.; Clearfield, A.; Sue, H. J.; Mullins, M. J.; Pham, H., Morphology and mechanical behavior of exfoliated epoxy/alpha-zirconium phosphate nanocomposites. *Compos Sci Technol* **2007,** *67* (2), 262-269.

80. Talley, S. J.; Yuan, X. J.; Moore, R. B., Thermoreversible Gelation of Poly(ether ether ketone). *Acs Macro Lett* **2017,** *6* (3), 262-266.

81. Talley, S. J.; AndersonSchoepe, C. L.; Berger, C. J.; Leary, K. A.; Snyder, S. A.; Moore, R. B., Mechanically robust and superhydrophobic aerogels of poly(ether ether ketone). *Polymer* **2017,** *126*, 437-445.

82. Jiang, Z. Y.; Liu, P.; Chen, Q. H.; Sue, H. J.; Bremner, T.; DiSano, L. P., The influence of processing conditions on the mechanical properties of poly(aryl-ether-ketone)/polybenzimidazole blends. *J Appl Polym Sci* **2020**.

83. Gohn, A. M.; Seo, J.; Colby, R. H.; Schaake, R. P.; Androsch, R.; Rhoades, A. M., Crystal nucleation in poly(ether ether ketone)/carbon nanotube nanocomposites at high and low supercooling of the melt. *Polymer* **2020,** *199*.

84. Jin, J.; Song, M.; Pan, F., A DSC study of effect of carbon nanotubes on crystallisation behaviour of poly(ethylene oxide). *Thermochim Acta* **2007,** *456* (1), 25-31.

85. Perez, R. A.; Lopez, J. V.; Hoskins, J. N.; Zhang, B. Y.; Grayson, S. M.; Casas, M. T.; Puiggali, J.; Muller, A. J., Nucleation and Antinucleation Effects of Functionalized Carbon Nanotubes on Cyclic and Linear Poly(epsilon-caprolactones). *Macromolecules* **2014,** *47* (11), 3553-3566.

86. Jar, P. Y.; Kausch, H. H.; Cantwell, W. J.; Davies, P.; Richard, H., The Effect of Annealing on the Short and Long-Term Behavior of Peek. *Polym Bull* **1990,** *24* (6), 657-664.

87. Tsuda, T.; Ogasawara, T.; Deng, F.; Takeda, N., Direct measurements of interfacial shear strength of multi-walled carbon nanotube/PEEK composite using a nano-pullout method. *Compos Sci Technol* **2011,** *71* (10), 1295-1300.

88. Wang, B.; Zhang, K.; Zhou, C. H.; Ren, M. F.; Gu, Y. T.; Li, T., Engineering the mechanical properties of CNT/PEEK nanocomposites. *Rsc Adv* **2019,** *9* (23), 12836-12845.

89. Hamester, M. R. R.; Dalmolin, C.; Becker, D., Role of pi-pi interactions and chain flexibility in dispersion and dynamic-mechanical properties of nanocomposites with multiple wall carbon nanotubes. *J Appl Polym Sci* **2019,** *136* (45).

90. Yang, D. Q.; Rochette, J. F.; Sacher, E., Spectroscopic evidence for pi-pi interaction between poly(diallyl dimethylammonium) chloride and multiwalled carbon nanotubes. *J Phys Chem B* **2005,** *109* (10), 4481-4484.

91. Furtado, C. A.; Kim, U. J.; Gutierrez, H. R.; Pan, L.; Dickey, E. C.; Eklund, P. C., Debundling and dissolution of single-walled carbon nanotubes in amide solvents. *J Am Chem Soc* **2004,** *126* (19), 6095-6105.

92. Modi, S. H.; Dikovics, K. B.; Gevgilili, H.; Mago, G.; Bartolucci, S. F.; Fisher, F. T.; Kalyon, D. M., Nanocomposites of poly(ether ether ketone) with carbon nanofibers: Effects of dispersion and thermo-oxidative degradation on development of linear viscoelasticity and crystallinity. *Polymer* **2010,** *51* (22), 5236-5244.

93. Boyer, F.; Olivier, P.; Pons, F.; Cadaux, P. In *Mechanical and electrical behavior of a peek/carbon nanotubes composite*, ECCM15-15th European conference on composite materials, Venice, Italy, 2012.

94. Wang, H. S.; Wang, G. B.; Li, W. L.; Wang, Q. T.; Wei, W.; Jiang, Z. H.; Zhang, S. L., A material with high electromagnetic radiation shielding effectiveness fabricated using multi-walled carbon nanotubes wrapped with poly(ether sulfone) in a poly(ether ether ketone) matrix. *J Mater Chem* **2012,** *22* (39), 21232-21237.

95. Pavlenko, E.; Boyer, F.; Puech, P.; Olivier, P.; Sapelkin, A.; King, S.; Heenan, R.; Pons, F.; Gauthier, B.; Cadaux, P. H.; Bacsa, W., Origin of mechanical modifications in poly (ether ether ketone)/carbon nanotube composite. *J Appl Phys* **2014,** *115* (23).

96. Deng, F.; Ogasawara, T.; Takeda, N., Tensile properties at different temperature and observation of micro deformation of carbon nanotubes-poly(ether ether ketone) composites. *Compos Sci Technol* **2007,** *67* (14), 2959-2964.

97. Rinaldi, M.; Ghidini, T.; Nanni, F., Fused filament fabrication of polyetheretherketone/multiwalled carbon nanotube nanocomposites: the effect of thermally

conductive nanometric filler on the printability and related properties. *Polym Int* **2021,** *70* (8), 1080-1089.

98. Aghadavoudi, F.; Golestanian, H.; Beni, Y. T., Investigating the effects of CNT aspect ratio and agglomeration on elastic constants of crosslinked polymer nanocomposite using multiscale modeling. *Polym Composite* **2018,** *39* (12), 4513-4523.

99. Shi, D. L.; Feng, X. Q.; Huang, Y. G. Y.; Hwang, K. C.; Gao, H. J., The effect of nanotube waviness and agglomeration on the elastic property of carbon nanotube-reinforced composites. *J Eng Mater-T Asme* **2004,** *126* (3), 250-257.

100. Yang, J. L.; Zhang, Z.; Schlarb, A. K.; Friedrich, K., On the characterization of tensile creep resistance of polyamide 66 nanocomposites. Part I. Experimental results and general discussions. *Polymer* **2006,** *47* (8), 2791-2801.

101. Yang, J. L.; Zhang, Z.; Schlarb, A. K.; Friedrich, K., On the characterization of tensile creep resistance of polyamide 66 nanocomposites. Part II: Modeling and prediction of long-term performance. *Polymer* **2006,** *47* (19), 6745-6758.

102. Bradley, S. W.; Puckett, P. M.; Bradley, W. L.; Sue, H. J., Viscoelastic creep characteristics of neat thermosets and thermosets reinforced with E-glass. *J Compos Tech Res* **1998,** *20* (1), 51-58.

103. Feng, C. W.; Keong, C. W.; Hsueh, Y. P.; Wang, Y. Y.; Sue, H. J., Modeling of long-term creep behavior of structural epoxy adhesives. *Int J Adhes Adhes* **2005,** *25* (5), 427-436.

104. Ngai, K. L.; White, C. T., FREQUENCY-DEPENDENCE OF DIELECTRIC LOSS IN CONDENSED MATTER. *Phys Rev B* **1979,** *20* (6), 2475-2486.

105. Ngai, K. L.; Jonscher, A. K.; White, C. T., ORIGIN OF THE UNIVERSAL DIELECTRIC RESPONSE IN CONDENSED MATTER. *NATURE* **1979,** *277* (5693), 185-189.

106. Ngai, K. L.; Roland, C. M., CHEMICAL-STRUCTURE AND INTERMOLECULAR COOPERATIVITY - DIELECTRIC-RELAXATION RESULTS. *Macromolecules* **1993,** *26* (25), 6824-6830.

107. Yee, A. F.; Bankert, R. J.; Ngai, K. L.; Rendell, R. W., STRAIN AND TEMPERATURE ACCELERATED RELAXATION IN POLYCARBONATE. *J Polym Sci Pol Phys* **1988,** *26* (12), 2463-2483.

108. Ngai, K. L.; Roland, C. M., INTERMOLECULAR COOPERATIVITY AND THE TEMPERATURE-DEPENDENCE OF SEGMENTAL RELAXATION IN SEMICRYSTALLINE POLYMERS. *Macromolecules* **1993,** *26* (11), 2688-2690.

109. Roland, C. M.; Ngai, K. L., SEGMENTAL RELAXATION AND MOLECULAR-STRUCTURE IN POLYBUTADIENES AND POLYISOPRENE. *Macromolecules* **1991,** *24* (19), 5315-5319.

110. Ngai, K. L.; Mashimo, S.; Fytas, G., INTERCOMPARISONS OF DIELECTRIC-RELAXATION, DYNAMIC LIGHT-SCATTERING, AND VISCOELASTIC PROPERTIES OF THE LOCAL SEGMENTAL MOTION IN AMORPHOUS POLYMERS. *Macromolecules* **1988,** *21* (10), 3030-3038.

111. Plazek, D. J.; Ngai, K. L.; Rendell, R. W., AN APPLICATION OF A UNIFIED RELAXATION MODEL TO THE AGING OF POLYSTYRENE BELOW ITS GLASS TEMPERATURE. *Polym Eng Sci* **1984,** *24* (14), 1111-1116.